THESIS


ESTIMATING CONTRIBUTIONS OF PRIMARY BIOMASS COMBUSTION TO

FINE PARTICULATE MATTER AT SITES IN THE WESTERN UNITED STATES




Submitted by

Amanda S. Holden

Department of Atmospheric Science




In partial fulfillment of the requirements

For the Degree of Master of Science

Colorado State University

Fort Collins, CO

Fall, 2008

COLORADO STATE UNIVERSITY

September 26, 2008

WE HEREBY RECOMMEND THAT THE THESIS PREPARED UNDER OUR
SUPERVISION BY AMANDA HOLDEN ENTITLED ESTIMATING
CONTRIBUTIONS OF PRIMARY BIOMASS COMBUSTION TO FINE
PARTICULATE MATTER AT SITES IN THE WESTERN UNITED STATES
BE ACCEPTED AS FULFILLING IN PART REQUIREMENTS FOR THE DEGREE
OF MASTER OF SCIENCE.

Committee on Graduate work

Dr. Charles S. Henry (Outside Committee Member)

Dr. Sonia M. Kreidenweis (Committee Member)

Dr. Jeffrey L. Collett, Jr. (Adviser)

Dr. Richard H. Johnson (Department Head)

ABSTRACT OF THESIS

ESTIMATING CONTRIBUTIONS OF PRIMARY BIOMASS COMBUSTION TO

FINE PARTICULATE MATTER AT SITES IN THE WESTERN UNITED STATES

Biomass combustion occurs throughout the world and has many implications for human health, air quality and visibility, and climate change.  To better understand the impacts of biomass combustion in the western United States, six-day integrated fine particle samples were collected during the winter and summer seasons of 2004-2006 at seven IMPROVE sampling sites using Hi-Vol samplers.  These sites included both urban and rural locations.  Filter samples were analyzed for organic and elemental carbon, levoglucosan, and a suite of particulate ions.  Levoglucosan, a thermal degradation product of cellulose, is a widely used tracer for primary biomass combustion. Measurements of levoglucosan and other carbohydrates were made using a new approach involving aqueous filter extraction followed by direct analysis using High Performance Anion Exchange Chromatography.  In this method carbohydrates are separated on a Dionex Carbopac PA-10 column and detected using pulsed amperometry.

Source profiles for primary biomass combustion were applied to each of these samples to estimate the contributions of carbon from both residential wood burning (during the winter seasons) and wildland fires (during the summer seasons).  Wildland fire source profiles were determined from FLAME (Fire Lab at Missoula Experiment) campaigns at the USFS/USDA Fire Science Lab in Missoula, MT, during which fine particle samples were collected from source burns of approximately 30 fuel types. Residential wood combustion source profiles were collected from the literature.

Primary biomass combustion contributions to contemporary PM$_{2.5}$ carbon, determined separately from carbon isotope measurements at Lawrence Livermore National Laboratory, ranged from 0.4% to more than 100%. Contributions of primary biomass combustion were higher at rural sites, while urban sites showed greater contributions of fossil carbon. Primary biomass combustion contributed a larger fraction of total carbon in the summer at southern sites, while northern sites had larger contributions during the colder winter months.

Amanda S. Holden
Department of Atmospheric Science
Colorado State University
Fort Collins, CO 80523
Fall 2008

ACKNOWLEDGEMENTS

TABLE OF CONTENTS

# LIST OF TABLES

# LIST OF FIGURES

# LIST OF ACRONYMS

| | |
|---|---|
| AMS | Accelerator mass spectrometry |
| BSTFA | N,O-bis-(trimethylsilyl)trifluoroacetamide |
| CCN | Cloud condensation nuclei |
| CSU | Colorado State University |
| DI | Deionized (water) |
| EC | Elemental carbon |
| ED | Electrochemical detection |
| $F_C$ | Contemporary carbon fraction |
| $F_F$ | Fossil carbon fraction |
| FID | Flame ionization detection |
| FLAME | Fire Lab at Missoula Experiment |
| $F_M$ | Modern carbon fraction |
| GC-MS | Gas chromatography-mass spectrometry |
| HANC | Grand Canyon, AZ |
| HDPE | High-density polyethylene |
| HPAEC | High performance anion-exchange chromatography |
| HPLC | High performance liquid chromatography |
| HYSPLIT | HYbrid Single-Particle Lagrangian Integrated Trajectory |
| IC | Ion chromatography |
| IMPROVE | Interagency Monitoring of Protected Visual Environments |
| IPA | Isopropanol/isopropyl alcohol |
| LOD | Limit of detection |
| MCE | Modified combustion efficiency |
| MORA | Mount Rainier, WA |
| NCDC | National Climatic Data Center |
| NDIR | Non-dispersive infrared |
| NIOSH | National Institute for Occupational Safety and Health |
| NOAA | National Oceanic and Atmospheric Administration |
| ns-K | Non-soil potassium |
| NW | Northwest (U.S.) |
| OC | Organic carbon |
| PAD | Pulsed amperometric detection |
| PHOE | Phoenix, AZ |
| PMF | Positive matrix factorization |
| PTFE | Poly(tetrafluoroethene) |
| PUSO | Puget Sound, WA |
| RM | Rocky Mountains |
| ROMO | Rocky Mountain National Park, CO |
| SAGO | San Gorgonio Wilderness, CA |
| SOA | Secondary organic aerosols |
| SW | Southwest (U.S.) |
| TC | Total carbon |
| TCMS | Trimethylchlorosilane |

| | |
|---|---|
| TONT | Tonto National Monument, AZ |
| TOT | Thermal optical transmission |
| TSP | Total suspended particulates |
| URG | University Research Glassware |
| USDA | United States Department of Agriculture |
| USFS | United States Forest Service |
| VOC | Volatile organic compounds |
| YACS | Yosemite Aerosol Characterization Study |

# Chapter 1 Introduction

## 1.1 Background and Motivation

### 1.1.1 Contribution of Fires to Atmospheric Aerosols and Environmental Effects

Biomass combustion occurs throughout the world in a variety of methods. Biomass is burned for land clearing, for land type conversion, for the removal of vegetation, for clearing agricultural waste, and as fuel in stoves and fire places (Crutzen and Andreae, 1990). In addition, biomass is burned during prescribed and wild fires. It is estimated that in the United States approximately 37% of direct fine particulate emissions are from combustion, including open biomass burning (Nizich et al., 2000).

Biomass burning has been found to be a large source of organic matter emissions. Yokelson et al. (2007) state that, along with biogenic emissions, biomass combustion produces the largest emissions of volatile organic compounds (VOC) and fine particulate carbon throughout the troposphere. Figure 1.1 shows the fraction of fine particulate matter ($PM_{2.5}$, particles with an aerodynamic diameter of 2.5 μm or less) attributed to organic carbon in the United States. There are obvious maxima in these fractional contributions in the western half of the country, where the climate is also drier and more wild fires occur. Most measurements of organic carbon mass in the western U.S. fall between approximately 0.5 and 2.0 μgC/m$^3$, with higher values near urban areas (*e.g.*, 4.65 μgC/m$^3$ in Phoenix, 4.06 μgC/m$^3$ in Puget Sound) (Malm et al., 2004). These

masses are higher on average in the eastern part of the country, but higher concentrations of fine particulate matter, due in part to high sulfate mass, result in lower organic carbon fractions at these sites (Malm et al., 2004).
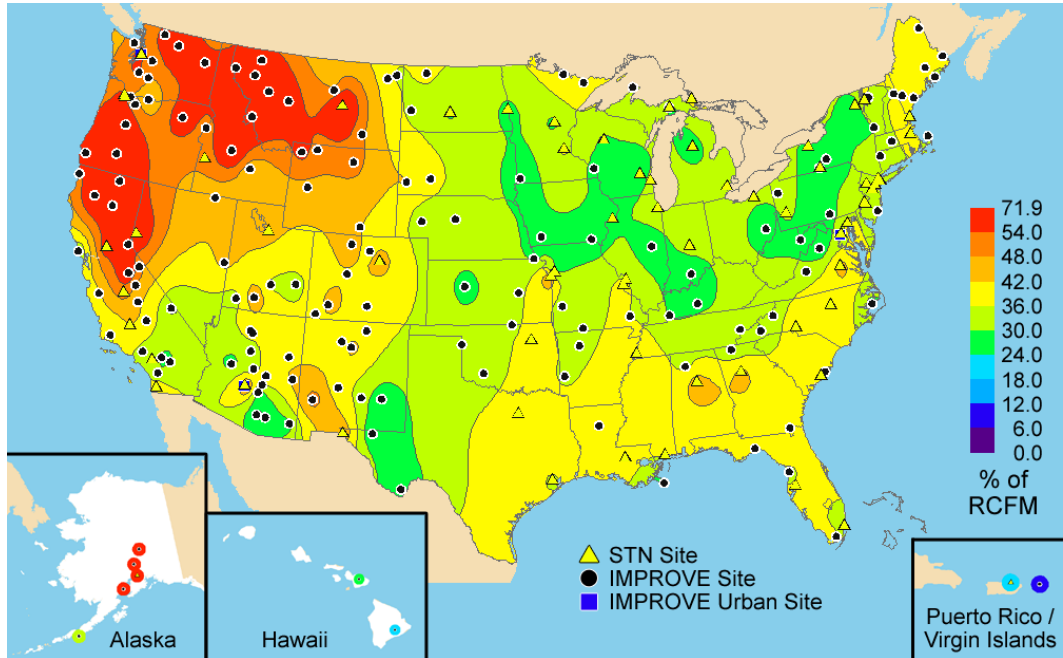


**Figure 1.1** *Organic carbon as a percent of fine particulate mass (PM$_{2.5}$)* (Schichtel et al., 2007)**.**

The high emissions of organic matter from biomass combustion have many detrimental environmental and health effects. Aerosols in general can have direct and indirect effects on the global radiative balance (Gao et al., 2003). Aerosols have a direct influence by scattering and absorbing solar radiation, which affects the amount of radiation that reaches the Earth's surface (Gao et al., 2003). Particles in biomass smoke plumes are mostly in the submicron range, <1 μm diameter (Herckes et al., 2006). These particles fall within the accumulation mode, which contains atmospheric particles ranging in diameter from approximately 0.08 μm to 1 μm (Finlayson-Pitts and J.N. Pitts, 2000; Seinfeld and Pandis, 2006). Because these particles are smaller than 2.5 μm, data for fine particulate matter (PM$_{2.5}$) can be assumed to contain information about the majority of

biomass smoke particles.  Particles of this size can be hygroscopic and be incorporated into clouds, but are too small to be efficiently removed through dry deposition (Finlayson-Pitts and J.N. Pitts, 2000; Seinfeld and Pandis, 2006; Whitby and Cantrell, 1976).  These factors each contribute to the longer atmospheric lifetimes seen in accumulation mode particles (Finlayson-Pitts and J.N. Pitts, 2000; Seinfeld and Pandis, 2006; Whitby and Cantrell, 1976).

In addition to their extended lifetimes, the size of these particles allows them to efficiently scatter solar radiation.  Accumulation mode particles undergo Mie scattering and have the highest scattering per unit volume of the various aerosol size modes (Finlayson-Pitts and J.N. Pitts, 2000).  Biomass smoke plumes also contain elemental carbon (EC), which is highly absorbing in the visible spectrum (Crutzen and Andreae, 1990).  The atmosphere is then heated by the absorbed radiation with less radiation reaching the surface, causing an overall effect of meteorological stability (Crutzen and Andreae, 1990).  Aerosol extinction, the combined effects of scattering and absorption, leads to decreased visibility.  As there are many national parks and natural areas in the western United States, the impact of biomass combustion on visibility there is of great concern (Malm et al., 2004).

Aerosols also indirectly influence the radiation budget by changing the microphysical and optical properties of clouds (Crutzen and Andreae, 1990; Gao et al., 2003).  Particles emitted from biomass combustion have been found to act as good cloud condensation nuclei (CCN), particles on which water vapor condenses to form clouds (Crutzen and Andreae, 1990; Ruellan et al., 1999).  Hobbs et al. (1996) found CCN concentrations 1000 times greater in biomass smoke than in background air.  When cloud

droplets form on numerous small smoke particles they have a greater surface area, which allows them to reflect more incoming solar radiation (Crutzen and Andreae, 1990). These clouds are less likely to produce rain and can create a cooling effect on the land below (Crutzen and Andreae, 1990). Kaufman and Fraser (1997) found that in the presence of biomass combustion, cloud reflectance increases and cloud droplet size decreases.

The aerosols and gases emitted from biomass burning can also affect atmospheric chemistry (Crutzen and Andreae, 1990; Liousse et al., 1995). Biomass combustion emits nitrogen oxides and hydrocarbons that can react to form tropospheric ozone, a gas that has adverse effects on plant and animal health (Crutzen and Andreae, 1990). Nitrous acid (HONO) radicals can also be emitted in biomass smoke and photolyze to form hydroxyl (OH) radicals (Crutzen and Andreae, 1990). The presence of OH radicals increases the atmospheric photochemical activity and can oxidize many species, including CO (carbon monoxide) to $CO_2$ (carbon dioxide) (Crutzen and Andreae, 1990). Biomass smoke can also be transported globally, affecting atmospheric chemistry and climate in areas far from the combustion source (Crutzen and Andreae, 1990).

### 1.1.2 Biomass Combustion Chemistry

Biomass, being plant material, is largely made up of cellulose. Cellulose and hemi-cellulose, in fact make up 50-70% of dry biomass, with the remainder consisting of lignin (15-35%), minerals (up to 10%), and smaller amounts of proteins, amino acids, and other plant metabolites (Andreae and Merlet, 2001). The compounds that are found in biomass smoke therefore include many combustion products of cellulose.

There are three main breakdown pathways for cellulose, depending on the temperature of the combustion, which were described by Shafizadeh (1982). The first pathway occurs at lower temperatures, between approximately 150 and 190 °C. At these temperatures, cellulose breaks down to form gases and low molecular weight volatile compounds. During the second pathway, at temperatures from 300-500 °C, cellulose breaks down to form anhydrosugars, randomly linked oligosaccharides, and decomposition products of glucose. The anhydrosugars, including levoglucosan (1,6-anhydro-β-D-glucopyranose), form during a process called transglycosylation (Engling et al., 2006a; Shafizadeh, 1982). The glycosidic group in cellulose is cleaved and replaced with one of the compound's hydroxyl groups via intramolecular substitution (Shafizadeh, 1982). This process of transglycosylation is shown in Figure 1.2. The high temperatures involved in this pathway allow the cellulose molecule to become more flexible, reducing its molecular weight and breaking hydrogen bonds, essentially activating it for transglycosylation (Shafizadeh, 1982). The third pyrolysis pathway occurs at temperatures greater than 500°C and is known as "flash pyrolysis" (Shafizadeh, 1982). This process involves a series of fission, dehydration, disproportionation, decarboxylation, and decarbonylation reactions, which produce water, char, carbon dioxide and carbon monoxide (Shafizadeh, 1982).

A combination of these three competing pathways occurs during cellulose combustion in wild and prescribed fires and is described below (Andreae and Merlet, 2001; Shafizadeh, 1982; Simoneit et al., 1999). The process of combustion begins with an initial thermal decomposition, where biomass goes through hydrolysis, oxidation, dehydration, and pyrolysis as temperature increases. This first step is essentially the first

pathway described previously by Shafizadeh, where volatile compounds are produced. Eventually the ignition temperature is reached, which allows exothermic reactions to begin. The first phase of the actual fire is the flaming phase, named for the presence of flames. In this phase $CO_2$, $H_2O$, $NO_x$ (oxides of nitrogen), $N_2$, and $SO_2$ (sulfur dioxide) are produced, along with char and high concentrations of EC. The fire then begins to smolder, often at lower temperatures than the flaming phase. During this phase the char reacts with oxygen to produce CO and many other partially oxidized species. It is in this smoldering phase that anhydrosugars are produced according to the second pathway described by Shafizadeh, transglycosylation. The less vigorous nature and greater amounts of available oxygen keep levoglucosan and other anhydrosugars from breaking down into organic acids or losing oxygen to form simple molecules such as $SO_2$, $NO_x$, and $CO_2$ (Gao et al., 2003).
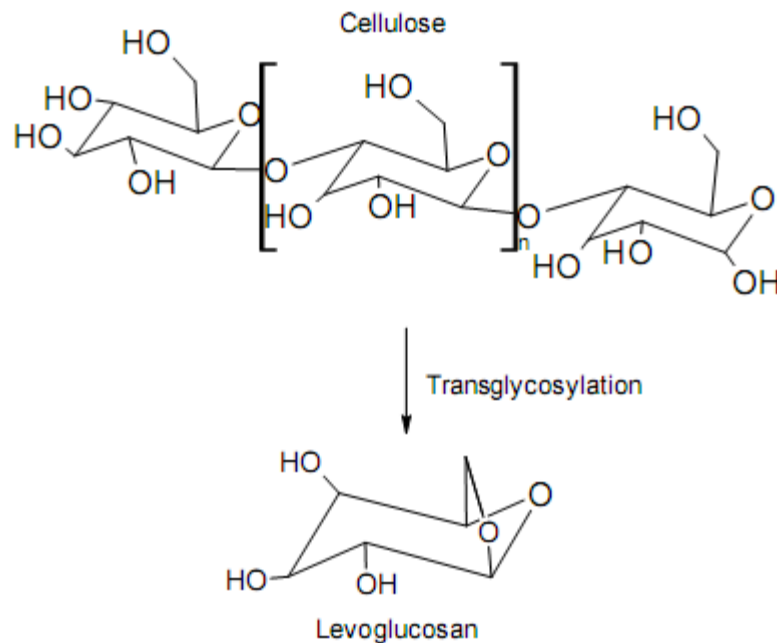


**Figure 1.2** *Mechanism of levoglucosan production via combustion of cellulose. Levoglucosan is formed through transglycosylation, a process in which the glycosidic linkages in cellulose are cleaved and replaced by free hydroxyl (OH) groups. Modified from Shafizadeh, 1982.*

**1.2 Current Analysis of Primary Biomass Burning**

*1.2.1 Carbon Isotope Analysis*

Carbon isotope analysis has become an important method for estimating the fraction of carbon due to contemporary carbon emission sources. Radiocarbon, $^{14}C$, is found in all living things: it oxidizes to $CO_2$ and is taken up by plants, which in turn become food for larger organisms (Bench and Herckes, 2004). "Fossil" carbon ($F_f$) is emitted from the use of fossil fuels (*i.e.,* coal, oil), materials which have been underground much longer than the half-life of $^{14}C$, which is 5,730 years (Bench and Herckes, 2004). Any $^{14}C$ in these sources would have decayed long before its use and subsequent emission into the atmosphere (Bench and Herckes, 2004). "Contemporary" carbon ($F_C$) comes from primarily biogenic sources (*e.g.*, emissions from plant growth and decomposition, and natural and anthropogenic combustion of plant matter), and has higher $^{14}C/C$ ratios (Bench and Herckes, 2004). Burning older biomass releases smaller quantities of $^{14}C$ into the atmosphere than with younger biomass, due to the increased time for $^{14}C$ to decay. This results in a gradient of $^{14}C/C$ ratios, with the larger ratios being emitted from the burning of younger biomass, and ratios decreasing with increasing biomass age.

Nuclear testing during the 1950s and 1960s also introduced $^{14}C$, doubling atmospheric radiocarbon concentrations in the Northern Hemisphere (Levin et al., 1985). The current measurable concentrations of $^{14}C$ are therefore different from contemporary carbon and are termed "modern" carbon (Stuiver and Polach, 1977). Modern carbon, $F_M$, is calculated as the $^{14}C/C$ ratio of a current sample divided by the $^{14}C/C$ ratio from 1950 (Schichtel et al., 2008). Since the late 1960s, $^{14}C$ levels have been decreasing due to

uptake by organisms and atmospheric mixing (Bench and Herckes, 2004). Values of $F_M$ have been reported to have decreased from 1.11 to 1.05 between 1999 and 2006 (Levin and Kromer, 2004). To correct for $^{14}C$ from atmospheric nuclear testing, contemporary carbon is calculated from modern carbon using the following equation (Schichtel et al., 2008):

$$F_C = \frac{F_M}{(1.08 \pm 0.06)}$$

The concentration of fossil carbon is then calculated as the remainder of the total carbon measured: $F_f = 1 - F_C$ (Schichtel et al., 2008). Quantifying the split between fossil and contemporary carbon in ambient samples gives an estimate of the upper limit of carbon emissions due to biomass burning.

*1.2.2 Source Profiles*

A chemical tracer, or source marker, is a compound that can be identified in ambient samples as originating from a specific source type. The specificity of levoglucosan to combustion of cellulose-containing materials makes it an excellent tracer for biomass combustion (Locker, 1988; Simoneit et al., 1999). Its intramolecular glycosidic linkage (the ring within a molecule of levoglucosan) also gives the molecule increased stability, allowing it to remain intact after extended transport in a biomass smoke plume (Hays et al., 2002). Other studies have also demonstrated the stability of levoglucosan; results from these studies are discussed in the following chapter (Fraser and Lakshmanan, 2000; Sullivan, 2008).

Levoglucosan has been used as a chemical tracer in many studies to estimate the contributions of both open and residential biomass combustion in controlled burns and

laboratory studies to fine particulate matter (Engling et al., 2006b; Gao et al., 2003; Gorin et al., 2006; Hays et al., 2002; Mazzoleni et al., 2007; Puxbaum et al., 2007; Ward and Smith, 2005). These data have been used to create source profiles for primary biomass combustion. The source profiles are values, usually a ratio of levoglucosan to OC, which have been measured during biomass combustion of a specific fuel, combination of fuels, or of a fire in a particular ecosystem. Source profiles can be applied to ambient data, in this case levoglucosan and OC concentrations, to estimate contributions of primary biomass combustion to fine particulate matter. While many source profiles have been published for residential wood combustion (*e.g.*, (Fine et al., 2001; Fine et al., 2002; Fine et al., 2004a; Fine et al., 2004b; Hedberg et al., 2002; Johansson et al., 2003; Kjallstrand and Olsson, 2004; Mazzoleni et al., 2007; McDonald et al., 2000; Rogge et al., 1998; Schauer et al., 2001; Simoneit et al., 1993), few exist for biomass combustion in wild and prescribed fires (Chow et al., 2004; Hays et al., 2002; Hays et al., 2005; Iinuma et al., 2007; Lee et al., 2005; Mazzoleni et al., 2007; Oros and Simoneit, 2001a; Oros and Simoneit, 2001b; Zheng et al., 2002).

Components of biomass combustion smoke can react further to form secondary organic aerosols (SOA), which can constitute a large portion of an aged smoke plume. Using levoglucosan, a primary component of biomass smoke, as a source marker will therefore describe a lower limit to the particulate matter from biomass smoke, as it does not account for these secondary aerosols. This underestimation would become more apparent in aged or transported smoke, since there would be more time for chemical reactions that produce SOA, as well as mixing with other pollution plumes, such as those from urban areas (Engling et al., 2006b).

*1.2.3 HPAEC-PAD Carbohydrate Analysis*

Anhydrosugars have been analyzed historically using a combination of gas chromatography and mass spectrometry (GC-MS) (Engling et al., 2006b; Fine et al., 2001; Fine et al., 2002; Fine et al., 2004a; Fine et al., 2004b; Fraser and Lakshmanan, 2000; Hays et al., 2002; Mazzoleni et al., 2007; Schauer et al., 2001; Simoneit et al., 1999). To analyze polar compounds, such as sugars, researchers must perform many preparatory steps before successful analysis with GC-MS. A common method for preparing quartz fiber filter samples for analysis of carbohydrate species by GC-MS involves first spiking the samples with deuterated internal standards (Fine et al., 2001; Fine et al., 2002; Fine et al., 2004a; Fine et al., 2004b). The filters are then sonicated twice in hexane, followed by three more sonications in a benzene/isopropanol mixture. Finally, extracts are filtered, combined, and reduced to a volume of 1 mL using nitrogen blow-down. Other studies have employed even more complicated methods for preparing filter samples for analysis. For example, the method described by Mazzoleni et al. (2007) involves concentrating the filter extracts by rotary evaporation and nitrogen blow down. The extracts are then derivatized at 70 °C for 2 hours using various derivatizing agents, including pyridine, acetonitrile, N,O-bis-(trimethylsilyl) trifluoroacetamide (BSTFA) with 1% trimethylchlorosilane (TCMS). In Engling et al. (2006b), sample extracts are divided into 3 groups, one of which is methylated with diazomethane, and a second group silylated with BSTFA and TCMS. These preparatory steps increase the amount of time needed per analysis and increase the potential for sample loss (Engling et al., 2006a).

In recent years a new method has been developed to replace the analysis of anhydrosugars by GC-MS. HPAEC-PAD, or high-performance anion exchange

chromatography with pulsed amperometric detection, allows analysis of anhydrosugars with less time and preparation per sample (Engling, 2006; Gao et al., 2003; Puxbaum et al., 2007). This method allows samples to be extracted in deionized (DI) water and analyzed directly without derivatization, removing the need for extensive sample preparation (Engling et al., 2006a). In a comparison of the HPAEC-PAD and GC-MS methods, similar ratios of levoglucosan to OC were found (Figure 1.3). Slightly higher concentrations of levoglucosan were seen with the HPAEC-PAD method, which could be due to losses during sample preparation for GC-MS analysis (Engling et al., 2006a). In addition, the detector response for HPAEC-PAD showed stability for at least 10 days, allowing calibrations to be performed on a less frequent basis (Engling et al., 2006a). The analytical limit of detection for this method was found to be better than 0.002 ng/μL with a signal/noise ratio of 3 (Engling et al., 2006a). The simplicity of this method also allows for more routine analysis of larger numbers of samples.

*1.2.4 Results from Previous Studies*

*1.2.4.1 Carbon Isotope Study*

As mentioned previously, measurements of $^{14}C/C$ ratios have been collected during various studies in an effort to quantify the amount of ambient contemporary carbon. An earlier study by Bench and Herckes (2004) measured these ratios at Turtleback Dome, inside Yosemite National Park. $PM_{2.5}$ filter samples were collected using a hi-volume sampler with an impactor plate. Daily samples were collected from July through September, 2004. These samples were analyzed via accelerator mass spectrometry (AMS) and values were reported as concentrations of fossil and contemporary carbon. The results showed fairly constant concentrations of fossil carbon,

11

averaging $0.7 \pm 0.1$ $\mu gC/m^3$, with contemporary carbon showing much more variability, ranging in concentration from approximately 2-9 $\mu gC/m^3$. Thus, the variation in total carbon was controlled by the concentration of contemporary carbon. Presence of smoke suggested impacts of nearby and regional forest fires on the high concentrations of contemporary carbon.
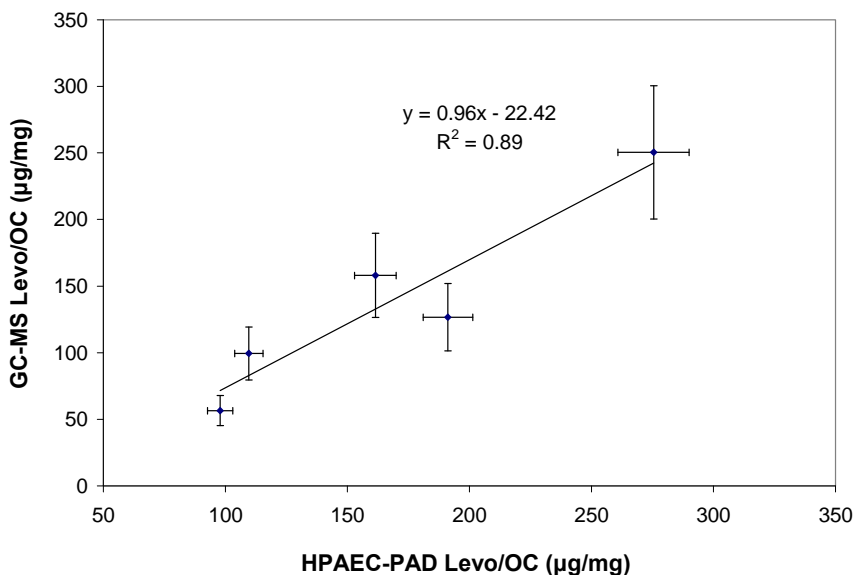


**Figure 1.3** *Comparison of levoglucosan/OC ratios measured by GC-MS and HPAEC-PAD methods. Error bars represent measurement uncertainties for both the GC-MS (20%) and HPAEC-PAD (5.3%) methods. Modified from (Engling et al., 2006a).*

An additional study was conducted during the summer and winter seasons of 2004-2006 using similar methodology (Bench et al., 2007). Here, data were collected weekly at nine IMPROVE (Interagency Monitoring of Protected Visual Environments) network sites: one rural, two urban, five within a national park, and one within a wildlife preserve. Six-day $PM_{2.5}$ filter samples were collected using hi-volume samplers and analyzed using AMS. The researchers found that at the urban sites in Puget Sound, Washington and Phoenix, Arizona, there were the highest average concentrations of total carbon and fossil carbon of the study. At these sites the fossil carbon made up about 50%

of the total carbon. Seasonal trends were also seen at these sites, with higher

concentrations of total and contemporary carbon during the winter. At the Phoenix site,

higher concentrations of fossil carbon were also seen in the winter. Much different

results were seen at the non-urban sites (the rural, national park, and wildlife preserve

sites). Opposite to the urban sites, at the many non-urban sites lower concentrations of

total and contemporary carbon were seen in the winter. The sites that did not show this

trend saw no significant difference in the contemporary and total concentrations between

seasons. Also, at the Grand Canyon, Arizona and Rocky Mountain National Park,

Colorado sites, fossil carbon concentrations were essentially non-existent during the

winter seasons. Also opposite of the urban sites, at the non-urban sites the total carbon

was dominated by contemporary carbon. This is similar to what was seen in Bench and

Herckes (2004), where changes in fossil carbon had little effect on total carbon because

of the dominance of contemporary carbon.

Schichtel et al. (2008) conducted further analysis on data from the studies by

Bench et al. (2007) and Bench and Herckes (2004). Twelve of the IMPROVE sites were

chosen for this analysis: two urban, four near-urban, and six remote sites. The results of

these analyses showed that at the urban sites, concentrations of contemporary and fossil

carbon were about equal, each making up about half of the total carbon. However, these

concentrations were greater in the winter than in the summer. During the winter, the

contemporary carbon at the urban sites was about twice that seen at neighboring non-

urban sites. The urban sites also showed anywhere from 4-20 times more fossil carbon

than neighboring non-urban sites during both summer and winter. The contemporary

carbon was similar at each of the sites during the summer with the exception of

Yosemite, California, which had higher concentrations due to smoke from wildfires. However, much more variability in contemporary carbon was seen during the winter. Concentrations ranged from 0.5 $\mu gC/m^3$ at the Rocky Mountain National Park, Colorado and Grand Canyon, Arizona sites to 2.8 $\mu gC/m^3$ at Puget Sound, Washington and 5.8 $\mu gC/m^3$ at Phoenix, Arizona. Because of lower total carbon concentrations at the non-urban sites, contemporary carbon dominated total carbon, agreeing with previous analyses. Contemporary carbon made up approximately 70-97% of total carbon at near-urban sites and 82-100% of total carbon at remote sites.

### 1.2.4.2 Source Apportionment Studies

A number of source apportionment studies have been published, typically using source profiles to determine the contributions of various sources to ambient particulate matter. These studies provide estimates of biomass smoke contributions for a variety of geographic locations and fuel types, as well as data for both residential and open biomass combustion. One study by Zheng et al. (2002) looked at contributions of biomass combustion to $PM_{2.5}$ at sites in Alabama, Mississippi, Georgia, and Florida. The wood combustion source profile chosen, 365 mg levoglucosan and 2902 mg OC per kg wood burned, was applied to monthly $PM_{2.5}$ filters taken at each of the sites during 1999 and 2000. The source profile was created with typical emissions from hardwoods and softwoods found in the southeast United States. The researchers estimated that wood combustion on average in these sites contributed to 15 ± 12% of fine particle mass and 25-66% of fine OC. Their results showed seasonal patterns, with wood combustion contributing more to fine particle mass in the fall and winter than in the warmer months. Contributions were estimated to be 19-48% of $PM_{2.5}$ in winter and 5-28% in fall, while

during the spring and summer contributions were only 2-24% and 2-18%, respectively.

A second study in this region found similar results. Liu et al. (2005) took daily integrated

$PM_{2.5}$ filter samples between 2000 and 2002 at four sites in Alabama and Georgia; two of

these sites were in rural areas, the other two were in urban areas. The data from these

filters were analyzed using positive matrix factorization (PMF) to calculate a source

apportionment, instead of using pre-specified source profiles. Wood smoke contributed,

averaged over the 2-year sampling period, 9% and 13% of $PM_{2.5}$ at the two urban sites.

Values at the rural sites were much higher, indicating that in these areas, wood

combustion can constitute 20-29% of fine particles.

Other source apportionment studies have been conducted in the western United

States. Ward and Smith (2005) used 35 source profiles to calculate the $PM_{2.5}$ coming

from wood combustion in the Missoula Valley of Montana during 2000-2001. Their

source profiles included chemical markers for wood burning, such as acetovanillone,

guaiacol, 4-ethylguaiacol, levoglucosan, abietic acid, dehydroabietic acid, and vanillin

(Ward, 2007). Daily $PM_{2.5}$ filter samples were collected at an urban and rural site in the

valley and data, including concentrations of the various chemical markers, were input

into a CMB (chemical mass balance) receptor model to calculate contribution estimates

(Ward and Smith, 2005). The researchers used the model outputs to calculate seasonal

averages of wood combustion contributions to fine particulate matter. They found that

wood combustion was the greatest source of $PM_{2.5}$ during spring (42%), summer (70-

72%), and fall (38-39%). During the winter, wood combustion was the second highest

source of $PM_{2.5}$, contributing to 23% at the urban site and 26% at the rural site. The

results suggested that biomass combustion is the source of 41% of the yearly $PM_{2.5}$ wood

combustion during the spring and summer months was estimated to be from both residential (burning yard waste) and open (slash burning, prescribed and wild fires) biomass burning. During the cooler months of fall and winter, biomass smoke was assumed to be produced only from residential wood combustion in stoves and fire places. The study also looked at one episode during August 2000 where conditions were noticeably smoky due to nearby forest fires. The model estimated that during this period, the fires were providing approximately 81% of the ambient fine particles in the Missoula Valley.

The Yosemite Aerosol Characterization Study (YACS) estimated that biomass smoke contributed 0.51-65% of OC (21% on average) during the summer of 2002 in Yosemite National Park (Engling et al., 2006b). The results found that approximately 39% of the fine particles were made up of OC, suggesting that biomass smoke also contributed largely to $PM_{2.5}$. Nearby and regional forest fires were assumed to be the main source of biomass smoke during the study period. Gorin et al. (2006) also found high contributions of biomass combustion to $PM_{2.5}$ in California, this time from residential wood combustion during the winter of 2003-2004 in Fresno. Here wood combustion was estimated to contribute 41% of OC and 18% of fine particle mass on average.

While many of these studies focused on a city or region, Park et al. (2007) looked at source apportionment across the United States. Daily $PM_{2.5}$ filter samples from the IMPROVE network during 2001-2004 were analyzed. Unlike studies previously mentioned, which used levoglucosan or similar carbohydrate compounds as chemical tracers, Park et al. used non-soil potassium (ns-K) as a tracer for both open biomass and

biofuel combustion.  Ratios of TC/ns-K were used as the source profiles for this study. The results suggested that approximately 50% of the annual mean TC averaged across the country was due to biomass burning.  Approximately 30% of $PM_{2.5}$ in the western and 20% of $PM_{2.5}$ in the eastern parts of the country were due to biomass burning (fires and biofuel combustion).  The researchers also estimated that in the western part of the country approximately 40% of the TC and 24% of the $PM_{2.5}$ were due to fires. Approximately 25% of the TC and 10% of the $PM_{2.5}$ were due to fires in the eastern part of the country.

Source apportionment has also been applied to samples of ambient air in other countries around the world.  For example, Puxbaum et al. (2007) estimated the contributions of biomass smoke to fine particulate matter at six sites across western Europe between 2002 and 2004.  Weekly $PM_{2.5}$ filter samples were collected at each of the sites and analyzed with HPLC (high performance liquid chromatography) with ED (electrochemical detection)/PAD to measure carbohydrate species.  Levoglucosan was used as the biomass smoke marker, and OC due to biomass smoke was calculated as 7.35 times the concentration of levoglucosan.  Puxbaum et al. found in the literature that K/levoglucosan ratios below 0.2 were considered to be representative of emissions from fire places and ovens, while ratios near 0.5 were assumed to be more indicative of open biomass combustion, such as wildfires and agricultural burning.  These ratios were calculated from the study's data and it was found that during the summer, biomass combustion was from burning of agricultural waste and forest fires; winter biomass combustion was from residential combustion in ovens and fireplaces.  Biomass smoke was estimated to make up 1-6% of organic matter (averaged over the six sites) during the

summer.  During the winter, biomass smoke contributed approximately 20% of the organic matter in mountain sites and 47-68% in rural sites of low elevation.  Overall, the researchers concluded that biomass smoke was the largest source of organic matter in Europe during winter.

Another study by Wang et al. (2007) looked at biomass burning contributions to $PM_{2.5}$ in the city of Guangzhou, China.  Daily $PM_{2.5}$ filter samples were taken from an urban and a suburban site during October 2004 and analyzed by GC-MS.  The researchers found that the biomass burning contributions to $PM_{2.5}$ were similar between the two sites, with a 4-19% contribution at the urban site, and 3-16.8% at the suburban site.

## 1.3 Study Objectives

Previous studies have shown the need for a better understanding of the contributions of primary biomass combustion to ambient fine particulate matter. Although many researchers have been able to quantify these contributions from residential wood combustion (*i.e.,* in wood stoves and fireplaces), a considerably smaller amount of research has focused on open biomass combustion in prescribed and wild fires. The objectives of this study were therefore as follows:

- To create accurate source profiles for prescribed/wild fires using data from laboratory combustion experiments,

- To apply these source profiles, along with established profiles for residential wood burning, to ambient samples to determine the contribution of biomass combustion to fine particulate matter,

- To verify previous estimates of contemporary carbon made using $^{14}C$ measurements,

- To compare biomass combustion contributions at sites of differing climates and population densities and between seasons,

- And to look for signatures in the data that could differentiate between different types of biomass burned.

To accomplish these objectives, biomass combustion source profiles were created from laboratory burns of various plant fuels during the FLAME (Fire Lab at Missoula Experiment) campaigns. These source profiles and published source profiles of residential biomass combustion were applied to ambient samples of fine particulate matter from various IMPROVE (Interagency Monitoring of Protected Visual Environments) sites throughout the western United States to estimate biomass combustion contributions to $PM_{2.5}$. These sites represented environments of the Pacific Northwest, Rocky Mountains, and desert southwest U.S., and included both rural and urban areas. Chapter 2 describes the methods undertaken for collection and analysis of FLAME and IMPROVE samples, creation of source profiles, and estimation of biomass combustion contributions to fine particulate matter. A description of the quality assurance and quality control steps taken during this study is also given.

Results of the study are given in Chapter 3, beginning with a description of the FLAME data and source profiles. Next, the levoglucosan, OC/EC, and $K^+$ data for each IMPROVE site are shown. The estimates of biomass combustion contributions to $PM_{2.5}$ are then given for each of these sites and compared to carbon isotope, particle back

trajectory, and satellite smoke data. Comparisons of biomass combustion contributions to $PM_{2.5}$ between rural and urban IMPROVE sites, as well as between IMPROVE sites of different geographical regions and seasons are presented. Results are also compared to those from previously published studies. A portion of the samples were analyzed further using source profiles based on fuel type (*e.g.*, branches, needles, etc.). Ratios of species measured (*e.g.*, $K^+$/OC) were examined to determine their potential as source profiles for biomass combustion. The potential interference of arabitol was also assessed. Finally, conclusions from the study and recommendations for future work are given in Chapters 4 and 5.

## Chapter 2 Experimental Methods

### 2.1 FLAME Sampling

*2.1.1 Facility Description*

Source samples of fine particulate matter were collected during the FLAME (Fire

Lab at Missoula Experiment) campaign at the USFS (U.S. Forest Service)/USDA (U.S.

Department of Agriculture) Fire Science Lab in Missoula, Montana.  The lab contains a

combustion chamber that is 12.5 m x 12.5 m x 22 m in dimension (length x width x

height).  The chamber is pressurized with ambient air, pre-conditioned for temperature

and humidity.  Figure 2.1 shows a simplified diagram of the combustion chamber.

Within the chamber is a stack that starts approximately 2.1 m above the floor, and

continues up to the roof of the building.  The stack is 3.66 m in diameter at its opening

and tapers off to 1.6 m in diameter. A bed (80 x 210 cm) for burning fuels lies beneath

the stack.  Air can be vented through this stack, entraining emissions from fires burned in

the chamber.  A platform approximately 15.2 m above the floor surrounds the stack and

can support multiple sampling instruments.  Sampling ports, approximately 1.32 m above

the platform floor (approximately 17 m from chamber floor), allow for direct sampling of

air within the stack.
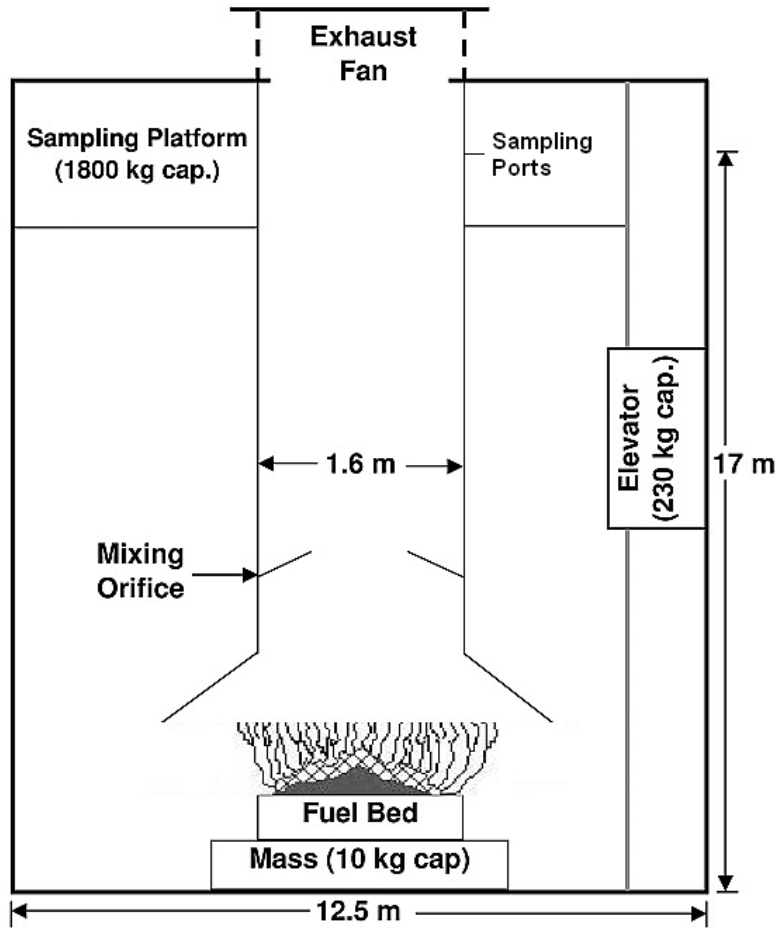
**Figure 2.1** *Diagram of combustion chamber at the USFS/USDA Fire Science Lab in Missoula, MT. Modified from (Christian et al., 2004).*

*2.1.2 Sampling and Handling*

Samples were collected during two campaigns: FLAME I, which took place during the summer of 2006 (May 25-28, May 30-June 1, and June 5-9), and FLAME II, which took place during the summer of 2007 (May 20-26, May 29-June 2, and June 4-6). During FLAME I, fuels were ignited by butane lighters and propane torches. In FLAME II, a different method was used, with a Variac warming a set of heating tapes that had been wetted with ethanol. The fuel sat on this bed and ignited as the tapes were heated. Stack and chamber burns were sampled for both years. During stack burns, fuels were burned directly below the stack on the chamber floor. The smoke flowed up through the

stack and was sampled via sampling ports above the platform. During the chamber burns, smoke was allowed to fill the entire burn chamber, and air was not exhausted through the stack. Stack burns were usually less than 25 minutes long, while chamber burns were at least 1.5-2 hours long. Hi-vol (hi-volume) sampler and URG (University Research Glassware) denuder/filter-pack samples were collected for both types of burns.

*2.1.2.1 Hi-vol*

Particulate samples were collected on Whatman Quartz Microfibre Filters (20.3 x 25.4 cm) using Thermo Fisher Scientific TSP (total suspended particulates) Hi-vol samplers (manufactured by General Metal Works, Village of Cleves, OH) with mass flow control and a $PM_{2.5}$ impactor plate. Quartz fiber filters were pre-baked at 550 °C for 12 hours to remove any artifacts that may have been deposited on the filter prior to the study. Filters were stored in aluminum sleeves before and during transport to the site. Tweezers were used to handle all filters, so that no contamination from skin oils and dirt could occur. Filter holders were cleaned with cotton swabs and IPA (isopropyl alcohol) between uses. The filter holders contained two different types of quartz fiber filters. The first was a "coarse" filter, which collected particles with an aerodynamic diameter greater than 2.5 μm. Then, $PM_{2.5}$ (particles with an aerodynamic diameter of 2.5 μm or smaller) was deposited on a 20.3 cm x 25.4 cm filter. The flow rate, in $ft^3$/min, was read off a flow chart that ran along with the sampler and was recorded for calculating the ambient concentrations of each filter sample. The hi-vol chart recorder was calibrated with a Thermo Fisher Scientific Hi-vol Sampler Calibration Kit before the start of the stack and chamber burns. The calibration kit was used to vary pressure on the sampler, which was then measured using a Magnehelic Pressure Gage. Pressure values were plotted against

flow rates from the chart recorder; linear relationships between these two sets of values were considered acceptable.

For the stack burns, one hi-vol sampler was placed at the platform near the top of the chamber. An aluminum manifold (6 inch diameter) was created to direct flow from the stack into the hi-vol sampler (see Figure 2.2). The manifold was wrapped in electrical insulating tape to limit air leaks. Each fuel was burned with two or three replicates and a hi-vol sample was taken across all burns for that fuel type. For the chamber burns, the hi-vol sampler was run on a platform approximately 4 feet in height on the opposite side of the chamber from the fire. The hi-vol sampler set-up for the chamber burns is shown in Figure 2.3. Once samples were collected, they were placed in aluminum sleeves and stored in a freezer.



**Figure 2.2** *Hi-vol sampler set-up during stack burns of the FLAME campaign. An aluminum manifold was attached to the side of the stack and directed air into the hi-vol sampler.*

**Figure 2.3** *Hi-vol sampler set-up during chamber burns of the FLAME campaign. The fuel bed was on the opposite side of the chamber, behind the camera view. Photo courtesy of C. Carrico.*

*2.1.2.2 URG*

A URG model URG-3000C Annular Denuder System was used to sample particulates and gases during the stack and chamber burns. Air was pumped via a computerized sampling pump (URG-3000-02BA) into a Teflon coated aluminum cyclone (URG-2000-30EN) with a diameter of 2.5 μm. Air then flowed into two, three channel annular denuders (URG-2000-30X242-3CSS) 242 mm in length where gaseous species were collected. Next, air passed through a 47 mm Teflon Filter Pack (URG-2000-30FG) containing a nylon filter (Nylasorb, 37 mm Pall Gelman, 1.0 μm pore size) and a citric acid coated cellulose filter (Whatman 47 mm filter papers). The nylon filter collected particulates in the sample, and then the cellulose filter collected any $NH_3$ that had volatilized. Finally, air flowed into the sampling pump, which gave readings of vacuum and air flow.

The filter pack/denuder/cyclone set-ups were held up by a tripod to a height appropriate for sampling (approximately 4-6 feet). During stack burns, the cyclone was connected directly into the stack sampling ports; ambient air was sampled from the room during chamber burns. During chamber burns, the URG system was approximately 7 m from the fire. Similar to sampling with the hi-vol samplers, URG samples were taken across all burns for that fuel type (anywhere from one to three replicates). An additional filter pack and set of denuders was kept on the tripod for the duration of each sampling day as a static blank. The ends of this set-up were capped so that ambient air could not get in. Figure 2.4 shows the URG set-up during stack burns, including a static blank.
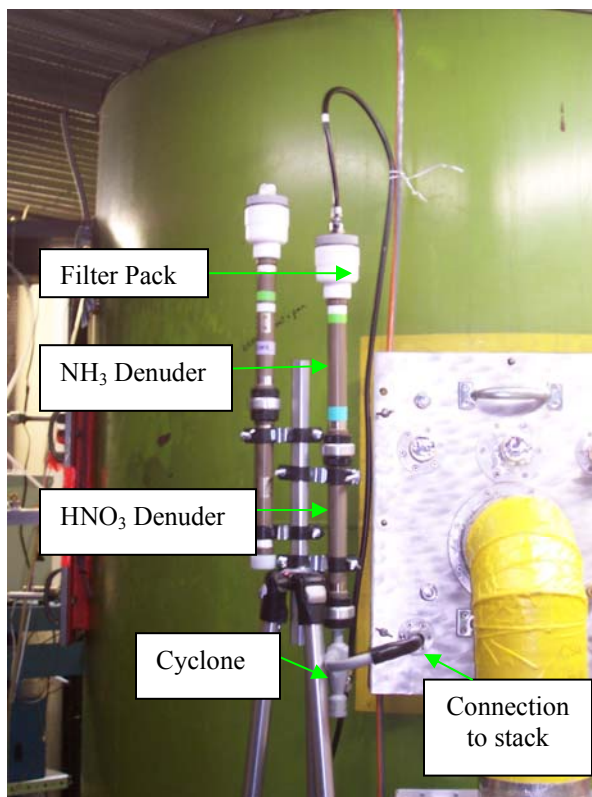


**Figure 2.4** *URG set-up during stack burns of the FLAME campaign. The $PM_{2.5}$ cyclone is connected via tubing to a sampling port on the stack. The filter pack is connected at the top with tubing to the URG sampling pump. The set-up during chamber burns was similar, except that the $PM_{2.5}$ cyclone was open to ambient air in the chamber.*

Cellulose filters were coated with citric acid and allowed to dry before transport to the Fire Science Lab. The cellulose filters were stored in individual Pall Gelman Petri dishes (50 mm x 9 mm), which were packed back in the Petri dish box for storage. All filters were handled with tweezers to prevent contamination. Following sampling, filters were removed from the filter pack and stored individually in 16 mL polystyrene test tubes in the freezer.

## 2.2 IMPROVE Sampling and Handling

Particulate matter was also sampled on quartz fiber filters as part of the IMPROVE Radiocarbon Study using hi-vol samplers in the same method as described above (Schichtel et al., 2008). Six-day integrated samples were taken during summer and winter 2004-2005 at 12 IMPROVE sites. Table 2.1 below gives the location and period of samples analyzed for the seven sites analyzed in this study. Note that the sampling period analyzed is not necessarily the entire sampling period at that site. The locations of the sites are also shown in a map in Figure 2.5. Two collocated sites were run in Phoenix during the winter of 2005. Previous analyses of these samples showed no significant difference in the split between contemporary and fossil carbon (Bench et al., 2007), so only one of the sites was analyzed here. Samples were stored in re-sealable zipper bags at room temperature at the Lawrence Livermore National Laboratory, and then shipped to Desert Research Institute where they were refrigerated. Filters were later shipped to CSU (Colorado State University), where they were stored in a laboratory freezer.

**Table 2.1** *Location of IMPROVE sites used in this study. Data from the IMPROVE Aerosol Database (Interagency Monitoring of Protected Visual Environments (IMPROVE), 2004).*

| Site Code | Site Name | Site Type | Latitude (dec. deg.) | Longitude (dec. deg.) | Elevation (m) | Samples Analyzed |
|---|---|---|---|---|---|---|
| HANC | Grand Canyon | Remote | 35.9731 | -111.984 | 2267 | Summer 2005 |
| MORA | Mount Rainier Nat'l Park | Remote | 46.7579 | -122.123 | 439 | Summer and Winter 2004 |
| PUSO | Puget Sound | Urban | 47.5696 | -122.312 | 97 | Summer and Winter 2004 |
| PHOE | Phoenix | Urban | 33.5038 | -112.096 | 342 | Summer and Winter 2005 |
| ROMO | Rocky Mountain Nat'l Park | Remote | 40.2783 | -105.546 | 2755 | Summer 2005 |
| SAGO | San Gorgonio Wilderness | Remote | 34.1924 | -116.9013 | 1705 | Summer 2005 |
| TONT | Tonto Nat'l Monument | Remote | 33.6494 | -111.109 | 775 | Summer and Winter 2005 |
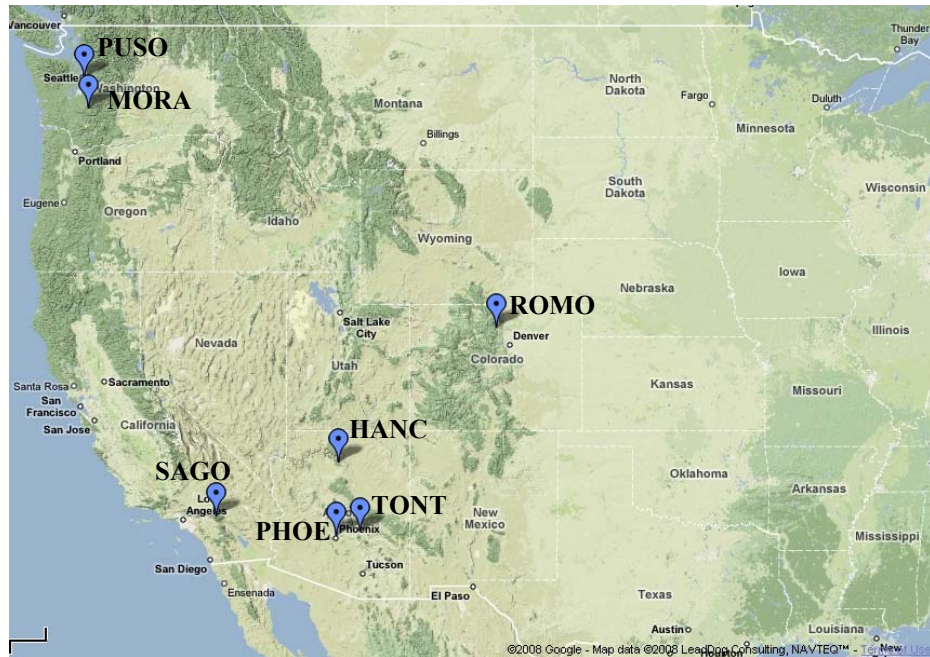


**Figure 2.5** *Map of the IMPROVE sites where PM$_{2.5}$ filters were taken from for this study. Sites are labeled with their abbreviations, which are listed in Table 2.1 above. Map was made using Google Maps (http://maps.google.com) and MapQuest (http://atlas.mapquest.com/maps/).*

**2.3 Sample Extraction**

*2.3.1 Hi-vol Filters*

      For FLAME filter samples, 2 punches (4.909 cm$^2$ each) were taken out of each filter. These punches were placed in 15mL Nalgene Amber Narrow-Mouth HDPE (High-density polyethylene) Bottles with 5 mL DI water. For IMPROVE filter samples, 10 punches (4.909 cm$^2$ each) were extracted in 20 mL DI water in 30mL Nalgene Amber Narrow-Mouth HDPE Bottles. More punches were used with the IMPROVE samples since they were ambient samples and assumed to be more dilute than the FLAME source samples.

      Bottles containing filter punches and DI water were sonicated with heat (60 °C) for 75 minutes, using a Branson 5210 Tabletop Ultrasonic Cleaner. The samples were allowed to cool to room temperature. Extracts were filtered using 0.2 μm PTFE (Poly(tetrafluoroethene)) membrane syringe filters. An aliquot of 600 μL of the filtered extract was then pipetted into Sun-Sri 0.5 mL polypropylene microsampling vials for analysis.

*2.3.2 URG Filters*

      Six mL of DI water were added to each test tube containing a URG filter, completely submerging the filter. The test tubes were sonicated without heat for 40 minutes and allowed to cool to room temperature. Sonicating does not break up nylon and cellulose filters, so no filtering of the extract was required. The extract was pipetted into 5 mL Nalgene Cryogenic vials; 600 μL was pipetted into microsampling vials for analysis. Excess extract was kept in a cold room.

**2.4 Analysis**

*2.4.1 High-Performance Anion Exchange Chromatography with Pulsed Amperometric Detection*

Hi-vol filters from the FLAME and IMPROVE studies were analyzed for levoglucosan and other carbohydrates using a High-Performance Anion Exchange Chromatography system with Pulsed Amperometric Detection (HPAEC-PAD). This method allows for analysis of carbohydrates without the long extraction and derivatization process associated with the common method of analysis via Gas Chromatography coupled with Mass Spectrometry (GC-MS). Our system is made up of a Dionex GP50 Gradient Pump, Dionex LC25 Chromatography Oven, Dionex CarboPac PA10 column, and a Thermo Separation Products AS3500 Autosampler. A Dionex ED50 Electrochemical detector worked in integrating amperometric mode to detect analytes. The detector contains a standard gold working electrode and a pH-Ag/AgCl (silver/silver chloride) reference electrode.

The separation method is 54 minutes long, using DI water (18.2 MΩ) and 200 mM NaOH (sodium hydroxide) as eluents and a flow rate of 0.5 mL/min. The eluents are continuously degassed with He (helium) gas. An injection of 50 μL of the sample is taken from the autosampler and injected onto the column. The method is then broken up into four sections. During the first 10 minutes there is isocratic elution with 18 mM NaOH to detect anhydrosugars. For the next 14 minutes, there is a linear gradient of NaOH from 18 to 60 mM to detect sugars (*e.g.,* glucose). The column is then cleaned with 180 mM NaOH for the next 14 minutes to remove any carbonate that might bind to the resin. The last 16 minutes are used as a re-equilibration step, with 18 mM NaOH, to

return the column to its initial conditions, preparing it for the next sample. Figure 2.6 shows the gradient of the eluents throughout the analysis.
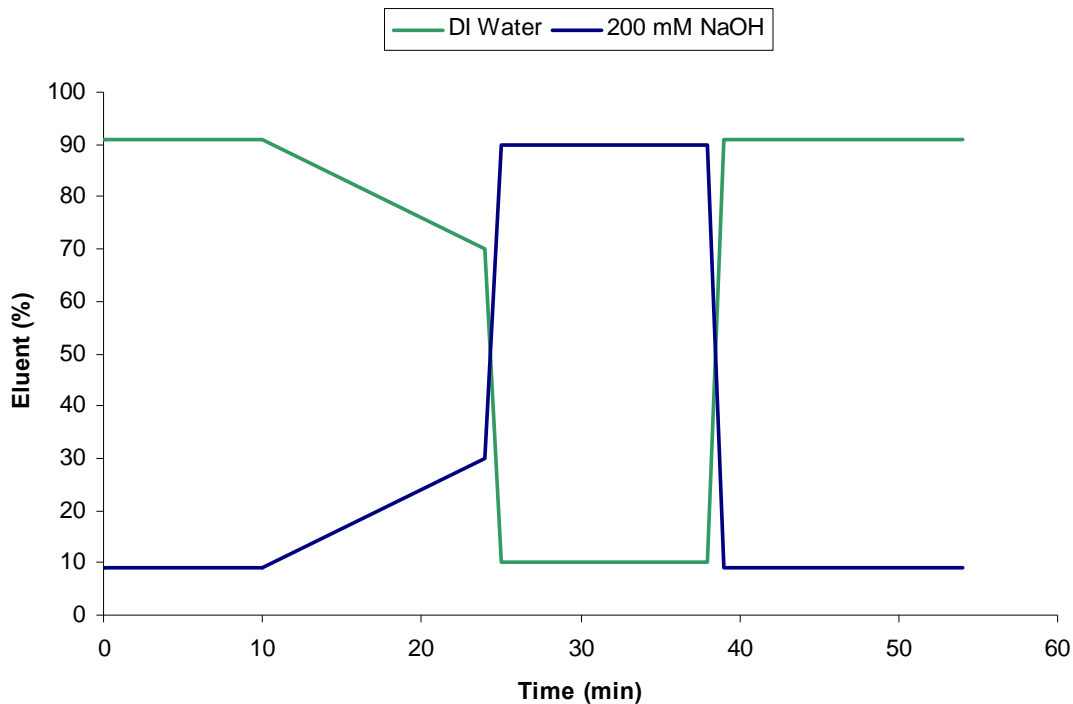


**Figure 2.6** *Eluent gradient during each sample run using the HPAEC-PAD method.*

Throughout the entire method, carbohydrates are electroanalytically oxidized on the surface of the working gold electrode via a positive potential. This potential is applied using a waveform of potential, alternating between anodic/oxidizing and cathodic/reducing polarizations, which act to clean the electrode for the next step (Lacourse and Johnson, 1993). A detection potential, $E_{det}$, is applied to the electrode and results in an output voltage signal, which is measured by the detector (Lacourse and Johnson, 1993). An oxidation potential, $E_{oxd}$ ($E_{oxd} \gg E_{det}$), is also applied to the electrode for a specific time period, called the oxidation time, or $t_{oxd}$ (Lacourse and Johnson, 1993). During the application of this potential, products that have adsorbed to

the electrode are desorbed through the formation of an oxide on the surface of the electrode (Lacourse and Johnson, 1993). Following this, a reduction potential, $E_{red}$ ($E_{red}$ << $E_{det}$), is applied for the reduction time, $t_{red}$ (Lacourse and Johnson, 1993). During this step, the oxide produced during $t_{oxd}$ is dissolved using a cathodic potential (Lacourse and Johnson, 1993). This alternation of potential is used because carbohydrates, like other polar aliphatic compounds, do not show a continuous response to a constant (dc, or direct current) potential applied to the electrode (Lacourse and Johnson, 1993).

To calibrate the instrument, a set of carbohydrate standards are run prior to each set of samples. Four injection volumes (10, 20, 30, and 40 μL) of two standard concentrations (240 and 2400 μg/L) are analyzed. Table 2.2 shows the mass of the carbohydrates for each standard. Note that five of the carbohydrates (levoglucosan, galactosan, galactose, glucose, and mannose) have the same mass, but the mass of mannosan differs slightly in both standards. Each of these standards is made from stock solutions of the six carbohydrates. The solids used to create the stock solutions were Fluka D(+)-Mannose (mannose, ~99%), Fluka D-(+)-Glucose anhydrous (glucose, ~99%), Fluka D(+)-Galactose (galactose, ~99.5%), Sigma 1,6-Anhydro-β-D-manno-pyranose (mannosan, ~98%), and Aldrich 1,6-Anhydro-β-D-glucose (levoglucosan, 99%). The galactosan used to make the stock solution was not available commercially and was provided by H. Puxbaum at the Vienna University of Technology, Vienna, Austria. These were added to DI water to create the stock solutions. The concentration in the stock solution, as well as the volume of that carbohydrate needed to make each standard, is shown below in Table 2.3. The appropriate volumes of each carbohydrate

32

stock are added to a clean 10 mL glass flask.  DI water is added to bring the total volume

to 10 mL.

**Table 2.2** *Mass of carbohydrates in the calibration standards and their varying injection volumes.  Note that levoglucosan, galactosan, galactose, glucose, and mannose are added in the same mass and are shown on the table under "Low" and "High".  The mass of mannosan used slightly differs from the other carbohydrates and is listed separately.*

|  | Carbohydrate Mass (µg) | | | |
|---|---|---|---|---|
| **Standard** | **10 µL** | **20 µL** | **30 µL** | **40 µL** |
| Low (240 µg/L) | 0.0024 | 0.0048 | 0.0072 | 0.0096 |
| High (2400 µg/L) | 0.024 | 0.048 | 0.072 | 0.096 |
| Mannosan Low | 0.0024 | 0.0049 | 0.0073 | 0.0097 |
| Mannosan High | 0.024 | 0.048 | 0.072 | 0.096 |

**Table 2.3** *Volume of carbohydrate stock solution added to create calibration standards.*

| Carbohydrate | Stock solution (µg/L) | Volume for low standard (µL) | Volume for high standard (µL) |
|---|---|---|---|
| Levoglucosan | 31,000 | 78 | 780 |
| Mannosan | 44,000 | 55 | 545 |
| Galactosan | 15,000 | 160 | 1,600 |
| Galactose | 47,000 | 51 | 510 |
| Glucose | 50,000 | 48 | 480 |
| Mannose | 48,000 | 50 | 500 |

The system gives a chromatogram for each sample.  The chromatograms are

analyzed using Dionex PeakNet Chromatography Workstation, version 5.21.  Figure 2.7

shows an example chromatogram.  The anhydrous sugars (levoglucosan, mannosan, and

galactosan) elute in the first 10 minutes of the method and the sugars (galactose, glucose,

and mannose) elute at about 25 minutes.  The software allows integration of individual

carbohydrate peaks.  Quadratic calibration curves created from the chromatograms of the

standards allow these peak areas to be converted into mass in µg.  These masses can then

be converted to ambient concentrations of the carbohydrates using information from the

sample, such as flow rate and time sampled.  See Appendix A for sample concentration

formulae.
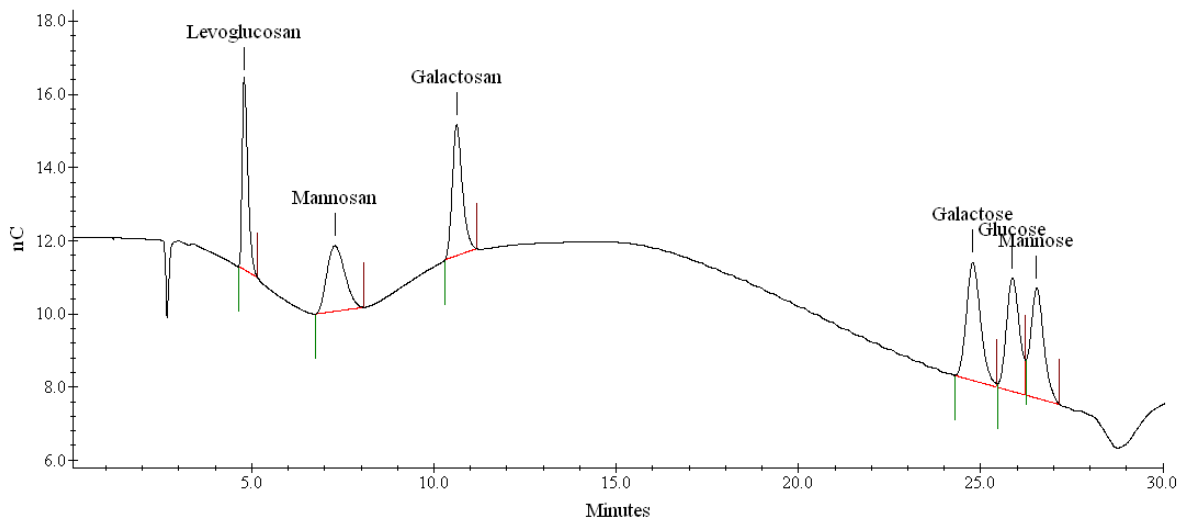
**Figure 2.7** *Chromatogram for a carbohydrate standard solution analyzed with the HPAEC-PAD method.*

## 2.4.2 Ion Chromatography

URG filter extracts were analyzed for ions using Ion Chromatography (IC). Two systems exist in our lab to analyze cations and anions separately. Both are Dionex systems with a Dionex CD20 Conductivity Detector, Dionex Isocratic Pump (the cation system uses a model IP20, the anion system uses an IP25), self-regenerating SRS-ULTRA suppressor, and SpectraSYSTEM AS3500 Autosampler. The cation system uses a Dionex IonPac CS12A-5 μm column (3 x 150 mm) and a 20 mM methanesulfonic acid (MSA) eluent. The anion system uses a Dionex IonPac AS14A column (4 x 250 mm) and an eluent of 1.8 mM sodium carbonate and 1.7 mM bicarbonate. Both systems use a method that takes about 15 minutes per sample, and use an injection volume of 25 μL. The cation IC has a flow rate of 0.5 mL/min and the anion IC has a flow rate of 1 mL/min.

A set of calibration standards was run on the IC at the beginning of each sample set. These standards were used to create a calibration curve, which was later used to

34

convert the samples' peak area to a concentration in μN.  There are eight standards for each of five cation and four anion species.  Table 2.4 below lists each standard and their relative concentrations.  One of the standards, usually Standard 4, was analyzed after every 10 samples injected, to check the stability of the system calibration.

**Table 2.4.** *Concentrations of ions in calibration standards used for the cation and anion IC systems.*

| Standard | Ion Concentration (μN) | | | | | | | | |
|---|---|---|---|---|---|---|---|---|---|
| | $Na^+$ | $NH_4^+$ | $K^+$ | $Mg^{2+}$ | $Ca^{2+}$ | $Cl^-$ | $NO_2^-$ | $NO_3^-$ | $SO_4^{2-}$ |
| Std 1 | 1 | 2 | 1 | 1 | 1 | 1 | 1 | 2 | 2 |
| Std 2 | 5 | 10 | 5 | 5 | 5 | 5 | 5 | 10 | 10 |
| Std 3 | 10 | 20 | 10 | 10 | 10 | 10 | 10 | 20 | 20 |
| Std 4 | 20 | 40 | 20 | 20 | 20 | 20 | 20 | 40 | 40 |
| Std 5 | 50 | 100 | 50 | 50 | 50 | 50 | 50 | 100 | 100 |
| Std 6 | 100 | 200 | 100 | 100 | 100 | 100 | 100 | 200 | 200 |
| Std 7 | 200 | 400 | 200 | 200 | 200 | 200 | 200 | 400 | 400 |
| Std 8 | 400 | 800 | 400 | 400 | 400 | 400 | 400 | 800 | 800 |

Once samples were run on the IC, their chromatograms were analyzed using Dionex PeakNet Chromatography Workstation, version 5.21.  Cellulose and hi-vol filters were only run on the cation IC; cellulose filters were analyzed for $NH_4^+$ (ammonium), hi-vol filters were analyzed for $K^+$ (potassium).  Nylon filters were run on both the anion and cation IC systems and their chromatograms are analyzed for $Na^+$ (sodium), $NH_4^+$, $K^+$, $Mg^{2+}$ (magnesium), $Ca^{2+}$ (calcium), $Cl^-$ (chloride), $NO_2^-$ (nitrite), $NO_3^-$ (nitrate), and $SO_4^{2-}$ (sulfate) ions.  Figure 2.8 shows sample chromatograms from the anion and cation IC systems for analysis of a nylon URG filter.  Similar to the carbohydrates, the concentration of each species, in this case in μN, can be converted to an ambient concentration using the samples flow rate and time sampled (see Appendix A).
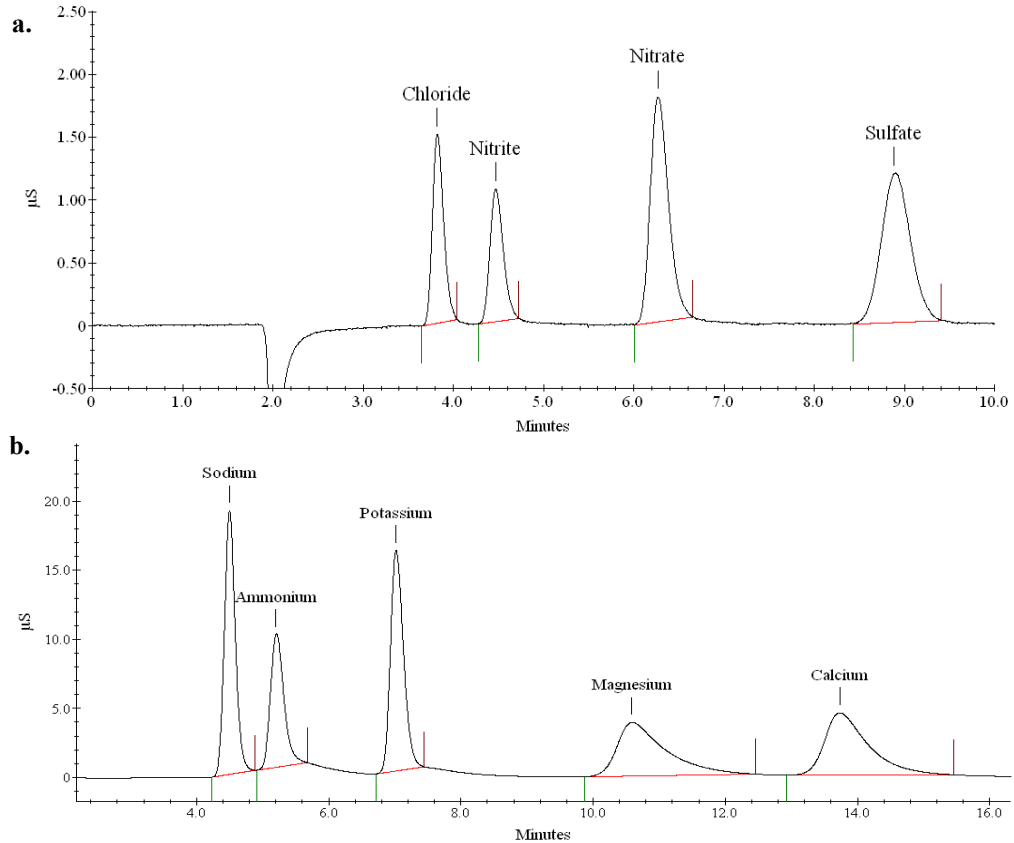
**Figure 2.8** *Chromatograms from analysis of standard solutions on the (a) anion and (b) cation IC systems.*

## 2.4.3 OC/EC Analysis

Hi-vol filters were also analyzed for OC and EC using a Sunset Labs OC/EC

Analyzer (Forest Grove, OR). A punch (1.4 cm$^2$) was taken from each filter and inserted

into the instrument sample oven via tweezers. Tweezers and puncher were cleaned with

methylene chloride between each filter and between sample replicates. The Sunset Labs

OC/EC Analyzer quantifies OC and EC by thermal/optical transmission (TOT),

following the NIOSH (National Institute for Occupational Safety and Health) method

5040, described below (Birch and Cary, 1996; Eller and Cassinelli, 1996). The analyzer

differs slightly from the NIOSH method in that NDIR (nondispersive infrared) detection

36

is used instead of FID (flame ionization detection).  NDIR detection measures analytes based on their absorption of infrared radiation.

The Sunset analyzer uses a pulsed diode He-Ne (helium-neon) laser and photodetector to measure the filter transmittance and to correct for char, which can form on the filter at temperatures above 300 °C and causes interference due to its strong absorption in the red/infrared region.  The instrument is calibrated by injecting a known amount of $CH_4$ (methane) gas, which occurs at the end of the sample method.  The $CH_4$ is measured and any necessary corrections are incorporated into the instrument software's calculations.  The first step of the analysis method involves volatilizing any OC from the filter in an environment of pure helium gas at approximately 870 °C.  The volatilized carbon is then catalytically oxidized to $CO_2$ at about 450 °C.  As the OC is being volatilized and oxidized, the filter transmittance decreases.  A mix of oxygen (10%) and helium gases is then used to combust the rest of the sample at temperatures of about 860 °C. At this point the transmittance begins to increase to the baseline, its level prior to initial heating.  The point at which the transmittance is equal to the baseline is determined to be the split between OC and EC, where carbon measured before the split is organic and carbon measured after the split is elemental.  The EC is also oxidized to $CO_2$ and measured by the detector.  Figure 2.9 gives an example of the temperature, $CO_2$, and transmittance seen in a sample analysis.  The instrument's accompanying software returns concentrations for each sample in terms of µg of C (carbon); that is, the mass of OC or EC for the punch of filter analyzed.  This mass of carbon is then converted to an ambient concentration through calculations described in Appendix A.
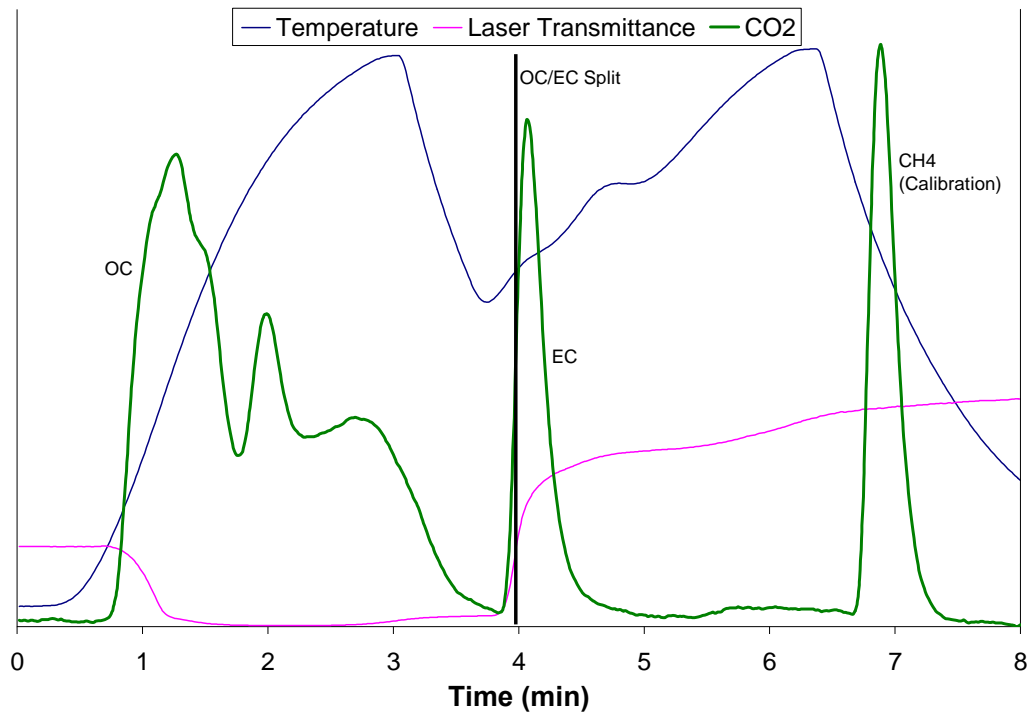
**Figure 2.9** *Temperature, laser transmittance, and $CO_2$ for a sample analyzed using the Sunset Labs OC/EC Analyzer. The thick black vertical line represents the split between OC and EC. All $CO_2$ before the split is OC; the first peak after the split is EC. The last peak is $CH_4$ from the instrument calibration.*

## 2.4.4 Carbon Isotope Analysis

PM$_{2.5}$ filters from the IMPROVE sites were analyzed for $^{14}$C/C (carbon isotope) ratios at the Lawrence Livermore National Laboratory using accelerator mass spectrometry (AMS). The fractions of fossil, modern, and contemporary carbon were reported, as well as the total carbon concentrations for each sample (Schichtel et al., 2008).

## 2.5 QA/QC

## 2.5.1 Sample Handling

To avoid contamination, all filters were handled with tweezers that were cleaned with methylene chloride (isopropanol during the FLAME campaign sampling) between

each use.  Punches used to cut portions of filters for HPAEC-PAD and OC/EC analysis were also cleaned with methylene chloride between each sample.  Filters were kept at temperatures no higher than 3 °C to keep reactions from occurring within samples and to deter microbial consumption of the samples.

*2.5.2 Blanks*

To estimate background contributions of particulate matter and the species measured here, multiple blanks were collected and analyzed during both the FLAME and IMPROVE studies.  Static blanks (taken during FLAME) were taken by setting up the hi-vol or URG as normal but without turning the pump on.  Dynamic blanks (taken during FLAME and IMPROVE) were similar except that the pump was run for a short period of time, usually between 2 and 10 minutes.  These blanks were analyzed along with the other samples for carbohydrates and ions, the concentrations of which were used in calculating limits of detection (LOD).  Two punches of a blank, unbaked, quartz fiber filter were also analyzed on the OC/EC instrument at the start of each day of analysis.  Because these fibers were not pre-baked, it is expected to see some carbon on them.  Blanks were considered acceptable if the punch concentration was less than 10 μg C for both OC and EC.

In addition to filter and denuder blanks, DI water blanks were also analyzed.  Microsampling vials containing DI water were analyzed as part of the calibration sequence for the HPAEC-PAD and IC systems.  One additional DI blank was analyzed for each sample group (containing up to 10 samples) in HPAEC-PAD analysis.  One DI blank was also analyzed for every 10 samples on the IC systems.

*2.5.3 Replicates*

Sample replicates were also run to ensure reproducibility of results. Every tenth sample was analyzed in replicate for IC analysis. Each sample was run in replicate for OC/EC analysis and the average value was used to calculate concentrations. If these replicates were not within ~10% of each other, an additional replicate was analyzed.

*2.5.4 LOD*

Limits of detection were calculated for each species analyzed in the various methods. The calculations for these LOD are shown in Appendix A. The LOD for OC and EC from the FLAME campaigns (using the Sunset Analyzer run in off-line mode) were calculated by Amy Sullivan.

*2.5.5 Carbohydrate Stability*

Previous work has shown that carbohydrates in FLAME $PM_{2.5}$ source samples remain stable over a period of days (Sullivan, 2008). This work involved analyzing samples for carbohydrates each hour up to 24 hours after sample filtration. The samples were also analyzed a week later for hourly measurements over 24 hours. The results show no significant difference in concentrations of the anhydrous sugars (levoglucosan, mannosan, galactosan) up to one week after sample filtration. Concentrations of galactose, glucose, and mannose showed less stability over time. Data from this work are shown in Appendix B. Since levoglucosan was used to create source profiles for the IMPROVE $PM_{2.5}$ filter samples, its stability is the most important.

An additional study by Fraser and Lakshmanan tested the stability of levoglucosan in an acidic environment (Fraser and Lakshmanan, 2000). The motivation

for this was the possible hydrolysis of levoglucosan to β-D-glucose by the presence of an acid, *e.g.*, in an acidic cloud. Their results showed that at a pH of 2, levoglucosan and β-D-glucose concentrations do not significantly change over a period of 10 days. Therefore any delays in analyzing samples due to time constraints or instrumental difficulties should not have biased the carbohydrate concentrations measured in the samples. However, observations during this study have shown that the carbohydrates in the calibration standards do degrade after approximately 7-8 days and standards are thus re-made on a weekly basis to avoid calibration errors.

## 2.6 Source Apportionment Calculations

Source profiles were created and applied to each IMPROVE sample to estimate the contribution of primary biomass combustion to ambient fine particulate matter. For summer samples, all biomass combustion was assumed to be from wild and prescribed fires, with no contributions from residential wood combustion. Source profiles were created with data from the FLAME experiments and applied to these samples. The HYSPLIT (HYbrid Single-Particle Lagrangian Integrated Trajectory) On-line Transport and Dispersion Model (http://www.arl.noaa.gov/ready/open/hysplit4.html) provided 48-hour back trajectories ending each sampling day. This data gave particle transport information, which showed the location of fires potentially influencing the IMPROVE samples. Fuels for the source profiles were picked from regions where these air masses originated, using available plant distribution data (USDA Natural Resources Conservation Service, 2008; USGS Earth Surface Processes, 2006). A sample back trajectory is shown below in Figure 2.10. Ratios of levoglucosan to total carbon (levoglucosan/TC, where TC = OC + EC) were calculated for appropriate fuels and then

averaged by fuel region to create regional source profiles of open (non-residential)

primary biomass combustion.
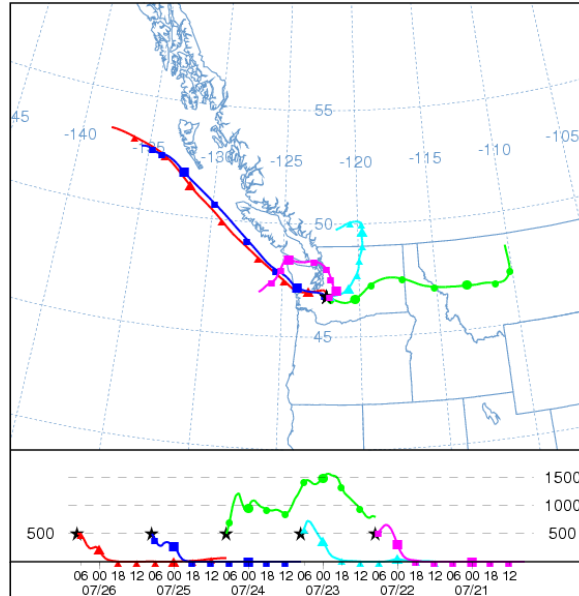


**Figure 2.10** *Sample back trajectory for the Mount Rainier (MORA) site. The location of the site is denoted by a black star. Each colored line represents a 48-hour back trajectory starting each sampling day. From the HYSPLIT On-line Transport and Dispersion Model (http://www.arl.noaa.gov/ready/open/hysplit4.html).*

Images of smoke plume presence were also examined for each summer

IMPROVE sample to estimate if there should be any biomass combustion influence.

This was done using the NOAA (National Oceanic and Atmospheric Administration)

National Geophysical Data Center's Satellite Fire Detections system

(http://map.ngdc.noaa.gov/website/firedetects/ viewer.htm). By combining these fire

maps with the back trajectories from the HYSPLIT model, a prediction could be made as

to whether any fire influence on particulate matter existed.

For winter samples, it was assumed that all contributions from primary biomass combustion were from residential wood burning.  It was also assumed that this residential burning occurred with fuel types found naturally in that state.  Source profiles were taken from the literature according to their distribution at each of the sites (USDA Natural Resources Conservation Service, 2008; USGS Earth Surface Processes, 2006).  Table 2.5 lists details for each source profile used for the winter samples.  Source profiles were averaged by fuel (*e.g.*, Douglas fir) and then by state to produce regional averages.

**Table 2.5** *Residential source profiles applied to winter IMPROVE samples. The state listed is the location where this type of fuel is typically burned in residential fire places and wood stoves.  The average for each state is listed, plus/minus one standard deviation.*

| Fuel | Levo/TC (gC/gC) | State | Reference |
|---|---|---|---|
| Douglas fir | 0.257 | AZ/WA | (Fine et al., 2004b) |
| Ponderosa pine | 0.066 | AZ/WA | (Fine et al., 2004b) |
| White spruce | 0.137 | AZ/WA | (Fine et al., 2004b) |
| Douglas fir | 0.372 | AZ/WA | (Fine et al., 2004a) |
| Douglas fir[1] | 0.296 | AZ/WA | (Fine et al., 2004a) |
| Cedar | 0.008 | WA | (Mazzoleni et al., 2007) |
| Cedar | 0.009 | WA | (Mazzoleni et al., 2007) |
| Hemlock | 0.091 | WA | (Fine et al., 2001) |
| Oak | 0.034 | WA | (Mazzoleni et al., 2007) |
| Oak | 0.222 | WA | (Schauer et al., 2001) |
| White pine | 0.037 | WA | (Fine et al., 2001) |
| White oak | 0.118 | WA | (Fine et al., 2004a) |
| White oak[1] | 0.091 | WA | (Fine et al., 2004a) |
| Quaking aspen | 0.185 | AZ/WA | (Fine et al., 2004b) |
| Black oak | 0.227 | WA | (Fine et al., 2004b) |
| White oak | 0.097 | WA | (Fine et al., 2004b) |
| Average | **0.174 ± 0.102** | **AZ** | |
| | **0.129 ± 0.091** | **WA** | |

[1]A catalyst was used during this experiment.

These source profiles (both groups described above) were then applied to their respective IMPROVE samples to give an estimate of carbon from primary biomass combustion (where levoglucosan is abbreviated "levo"):

$$\text{Biomass C } (\mu g/m^3) = \frac{levo_{sample}}{(levo/TC)_{source}}$$

The concentration of biomass carbon was also compared to fossil and contemporary

carbon concentrations for each sample.

Chapter 3 Results

This chapter presents the results from this study, beginning with limits of detection for each of the species measured during the FLAME experiments and at the IMPROVE sampling sites.  Data from the FLAME campaigns and the source profiles created from those data are then given.  Levoglucosan, OC/EC, and $K^+$ data are given for the IMPROVE site samples, followed by estimates of primary biomass combustion contributions to total carbon.  These estimates are compared to carbon isotope, particle back trajectory, and satellite smoke data.  Primary biomass combustion contributions are compared between the different IMPROVE sites and seasons sampled, as well as with data from previous studies.  A subset of the IMPROVE site samples were analyzed further using source profiles based on fuel type (*e.g.*, branches, needles).  Results of other further analyses are also shown, examining ratios of species (*e.g.*, $K^+$/OC) and the potential interference of arabitol during carbohydrate analyses.

**3.1 Limits of Detection**

*3.1.1 FLAME Experiments*

All data used in creating source profiles (levoglucosan and OC concentrations) were above their respective limits of detection, shown below in Table 3.1.  This table also contains the LOD for the other carbohydrates, as well as OC, EC, and $K^+$ measured on the hi-vol filters.  Table 3.2 gives the LOD for ions measured on the URG filters.  The

sugars have much lower LOD than the ions due to the high sensitivity of the

amperometric detection method used with the HPAEC-PAD instrument.

**Table 3.1** *Limits of detection for species measured on hi-volume PM$_{2.5}$ filters during the FLAME campaigns. LOD were converted to ambient concentrations (µg/m$^3$) by assuming an average sampling time of 20 minutes and flow rate of 1.13 m$^3$/min, according to calculations by A. Sullivan.*

| Species | LOD (µg/m$^3$) |
|---|---|
| Levoglucosan | 0.32 |
| Mannosan | 0.28 |
| Galactosan | 0.28 |
| Galactose | 0.24 |
| Glucose | 0.28 |
| Mannose | 0.24 |
| $K^+$ | 0.6 |
| OC | 6.0 |
| EC | 1.0 |

**Table 3.2** *Limits of detection for species measured on URG filters during the FLAME campaigns. All species are measured in their ionic forms. Data for URG LOD were from Lee, 2007. LOD were converted to ambient concentrations (µg/m$^3$) assuming an average sampling time of 20 minutes and flow rate of 10 L/min. $NH_4^+$\* denotes the $NH_4^+$ measured off the cellulose filter. No LOD data were available for $NO_2^-$.*

| Species | LOD (µg/m$^3$) |
|---|---|
| $Na^+$ | 1.9 |
| $NH_4^+$ | 2.2 |
| $K^+$ | 1.9 |
| $Mg^{2+}$ | 2.6 |
| $Ca^{2+}$ | 6.2 |
| $Cl^-$ | 1.9 |
| $NO_3^-$ | 7.6 |
| $SO_4^{2-}$ | 3.6 |
| $NH_4^{+*}$ | 2.7 |

*3.1.2 IMPROVE Sites*

Limits of detection for species measured in IMPROVE filter samples are given in

Table 3.3. Lower concentrations of species on blank filters allowed for lower LOD in the

IMPROVE samples than with the FLAME filter samples. Despite this, a large

percentage of samples showed values below species detection limits (Table 3.4). For

example, galactosan, glucose, mannose, and EC were below LOD in approximately 50%

46

or more of the IMPROVE filters sampled.  The high percentage of these sugars below

detection limits is not very detrimental to this study, as their concentrations are not

directly used in any calculations.  However, the low concentrations of EC measured leads

to a high uncertainty in these measurements.

**Table 3.3** *Limits of Detection for species measured on $PM_{2.5}$ filters from the IMPROVE sites.  LOD were converted to ambient concentrations ($\mu g/m^3$) by assuming an average sampling time of 6 days (8640 minutes) and flow rate of 1.13 $m^3/min$, according to calculations by A. Sullivan.*

| Species | LOD ($\mu g/m^3$) |
|---|---|
| Levoglucosan | 0.0006 |
| Mannosan | 0.0007 |
| Galactosan | 0.0005 |
| Galactose | $1.3000 \times 10^{-6}$ |
| Glucose | 0.007 |
| Mannose | 0.0002 |
| $K^+$ | 0.01 |
| OC | 0.7 |
| EC | 0.01 |

**Table 3.4** *Percent of IMPROVE filter samples equal to or above and below the LOD for each species.  All data from the IMPROVE samples are considered here.*

| Species | % Above LOD | % Below LOD |
|---|---|---|
| Levoglucosan | 100.0 | 0.0 |
| Mannosan | 93.0 | 7.0 |
| Galactosan | 47.0 | 53.0 |
| Galactose | 91.3 | 8.7 |
| Glucose | 50.4 | 49.6 |
| Mannose | 39.1 | 60.9 |
| $K^+$ | 98.3 | 1.7 |
| OC | 99.1 | 0.9 |
| EC | 39.1 | 60.9 |

## 3.2 FLAME Data

The FLAME campaigns consisted of 145 burns, 139 of which were burns of fuel

types or mixtures of fuel types.  The fuels burned covered a wide range of plant varieties

from the southeastern and western United States, as well as some fuels from Puerto Rico,

China, and Taiwan.  The variety of plants burned in these experiments produced a wide

range of results.  Concentrations of levoglucosan ranged from 0.08 to 54.9 $\mu gC/m^3$, with an average of $7.1 \pm 8.8$ $\mu gC/m^3$ ($\pm$ one standard deviation).  Carbon measurements also showed high variability, with OC ranging from 7.8 to 2562.0 $\mu gC/m^3$ ($268.2 \pm 379.2$ $\mu gC/m^3$, mean $\pm$ one standard deviation) and EC ranging from below detection limit to 425.2 $\mu gC/m^3$ ($24.5 \pm 55.0$ $\mu gC/m^3$, mean $\pm$ one standard deviation).  These wide ranges in concentrations of levoglucosan and organic and elemental carbon inevitably led to much variety in the ratio of levoglucosan to TC used in source profiles.  The average levoglucosan/TC ratio was approximately $0.027 \pm 0.015$ gC/gC ($\pm$ one standard deviation), with a range of 0.001 to 0.070 gC/gC.  Lower ratios were from burns of gallberry, Chinese sugar cane, palmetto, Montana grass, a rabbitbrush/sage mixture, juniper, Douglas fir, and chamise.  The higher ratios were from burns of longleaf pine, wiregrass, and white spruce.  Comprehensive data for each burn of the FLAME experiments are shown in Appendix C.

*3.2.1 Source Profile Information*

Project data were organized into regional groups and regional biomass burning source profiles were calculated according to the methods discussed in Chapter 2, using fuel types found in each region.  Three regional groups were created: Northwest U.S., Southwest U.S., and Rocky Mountains.  The Northwest group (NW) included the Mount Rainier National Park (MORA) and Puget Sound (PUSO) ambient aerosol monitoring sites.  The Southwest (SW) group consisted of the Grand Canyon (HANC), Phoenix (PHOE), San Gorgonio Wilderness (SAGO), and Tonto National Monument (TONT) sites.  The Rocky Mountain National Park (ROMO) site was the only site in the Rocky Mountain (RM) group.  The source profiles for individual FLAME tested fuels are listed

below in Table 3.5 as the ratio of levoglucosan to TC, along with information about the

corresponding region and fuel type. An average regional source profile is also listed in

this table for each of the three geographic regions. Source profiles were averaged by fuel

(*e.g.*, Ponderosa pine) and then by region, so that fuels were evenly weighted. The

average source profiles for each region were 0.026, 0.018, and 0.016 gC/gC for the

northwest, southwest, and Rocky Mountains regions, respectively. There is not much

difference between the averages of each of the regional source profile groups or their

standard deviations. This is most likely because there are many species of plants which

are found in the three regions examined here.

**Table 3.5** *FLAME source profiles (given as ratios of levoglucosan to TC) applied to summer IMPROVE samples. Codes: NW = Northwest U.S., SW = Southwest U.S., RM = Rocky Mountains (fuel region); df = duff, n = needles, b = branches, l = leaves, g = grasses, m = mixture of fuel types; D = dry, F = fresh. Averages for each regional group are listed as ± one standard deviation.*

| Fuel | Levo/TC (gC/gC) | Region | Fuel |
|---|---|---|---|
| Alaskan Duff | 0.046 | NW | df |
| Alaskan Duff | 0.057 | NW | df |
| Alaskan Duff | 0.039 | NW | df |
| Black Spruce | 0.028 | NW | n |
| Black Spruce | 0.034 | NW | n, D |
| Black Spruce | 0.035 | NW | n, F |
| Ceanothus | 0.022 | SW | l |
| Chamise | 0.007 | RM/SW | l |
| Chamise | 0.008 | RM/SW | l, D |
| Chamise | 0.047 | RM/SW | b, D |
| Chamise | 0.046 | RM/SW | b, F |
| Chamise | 0.011 | RM/SW | m, D |
| Chamise | 0.007 | RM/SW | m |
| Chamise | 0.028 | RM/SW | l, D |
| Chamise | 0.026 | RM/SW | l, F |
| Douglas Fir | 0.009 | NW/RM/SW | m, D |
| Douglas Fir | 0.019 | NW/RM/SW | m, D |
| Douglas Fir | 0.015 | NW/RM/SW | m, F |
| Juniper | 0.001 | RM/SW | l |
| Kudzu | 0.011 | NW/RM | l |
| Manzanita | 0.020 | NW/SW | l |
| Manzanita | 0.050 | NW/SW | b, F |

| Fuel | Levo/TC (gC/gC) | Region | Fuel |
|---|---|---|---|
| Manzanita | 0.014 | NW/SW | df, D |
| Manzanita | 0.022 | NW/SW | df, F |
| Montana Grass | 0.017 | NW/RM | g, D |
| Montana Grass | 0.009 | NW/RM | g, F |
| Phragmites | 0.033 | NW/RM/SW | g |
| Ponderosa Pine | 0.032 | NW/RM/SW | b, D |
| Ponderosa Pine | 0.019 | NW/RM/SW | b, D |
| Ponderosa Pine | 0.039 | NW/RM/SW | b, F |
| Ponderosa Pine | 0.038 | NW/RM/SW | b, F |
| Ponderosa Pine | 0.033 | NW/RM/SW | df |
| Ponderosa Pine | 0.029 | NW/RM/SW | m |
| Ponderosa Pine | 0.027 | NW/RM/SW | m |
| Ponderosa Pine | 0.036 | NW/RM/SW | m |
| Ponderosa Pine | 0.033 | NW/RM/SW | m |
| Ponderosa Pine | 0.031 | NW/RM/SW | m |
| Ponderosa Pine | 0.021 | NW/RM/SW | n |
| Ponderosa Pine | 0.016 | NW/RM/SW | n |
| Ponderosa Pine | 0.016 | NW/RM/SW | n, F |
| Ponderosa Pine | 0.013 | NW/RM/SW | n |
| Ponderosa Pine | 0.028 | NW/RM/SW | n |
| Ponderosa Pine | 0.015 | NW/RM/SW | n |
| Ponderosa Pine | 0.031 | NW/RM/SW | n |
| Ponderosa Pine | 0.041 | NW/RM/SW | n |
| Ponderosa Pine | 0.031 | NW/RM/SW | m, D |
| Ponderosa Pine | 0.015 | NW/RM/SW | m, D |
| Ponderosa Pine | 0.027 | NW/RM/SW | df |
| Rabbitbrush/Sage | 0.006 | NW/RM/SW | l |
| Sage | 0.013 | NW/RM/SW | l |
| Sage[1] | 0.011 | NW/RM/SW | l |
| Sage[1] | 0.012 | NW/RM/SW | l |
| White Spruce | 0.059 | NW | n |
| **Average** | **0.026 ± 0.017** | **NW** | |
| | **0.018 ± 0.011** | **SW** | |
| | **0.016 ± 0.010** | **RM** | |

[1]Part of a dilution experiment.

The ratio of levoglucosan to TC was used for these source profiles, but

levoglucosan/OC ratios could have also been used.  Figure 3.1 shows a comparison of

these two types of source profiles, levoglucosan/OC and levoglucosan/TC ratios.  It is

interesting to note that for the majority of the samples used to calculate source profiles,

the concentrations of OC and TC are very similar, and many times the same value. This shows that for the most part, the carbon from these source burns consisted mostly of organic carbon, with very small amounts (if any) of elemental carbon. Because of the similarity between the OC and TC for these samples, applying levoglucosan/OC as source profiles to the IMPROVE samples would have produced similar results. As described previously, using levoglucosan/TC source profiles makes it possible to estimate the contribution of primary biomass combustion to total carbon (fossil + contemporary carbon) concentrations.
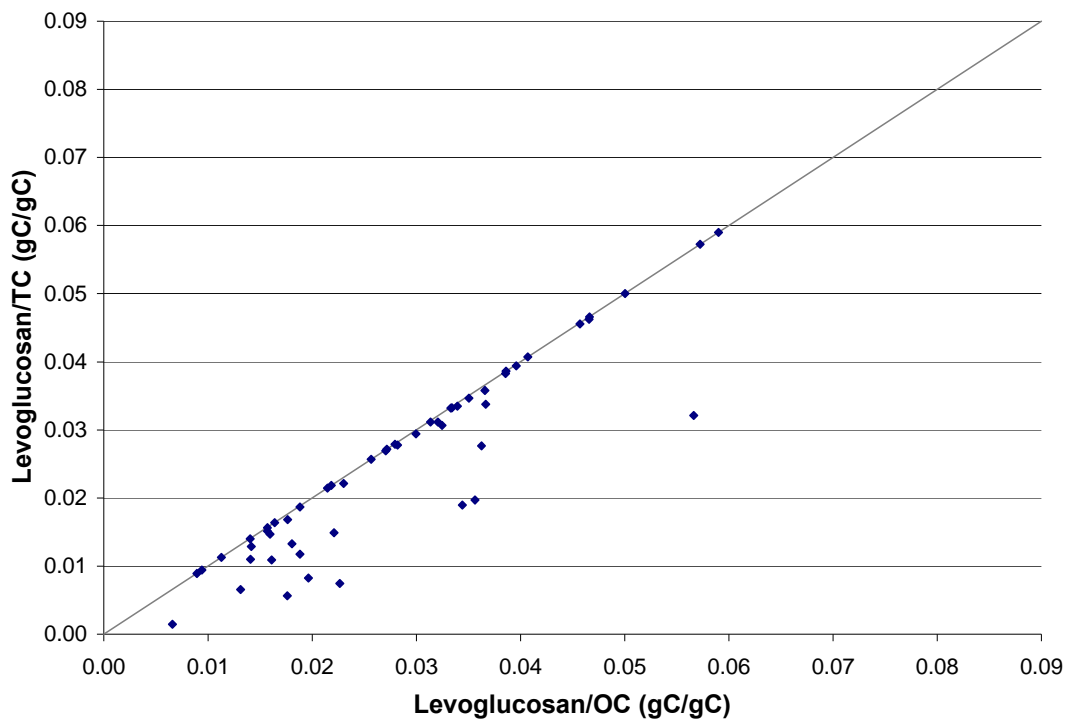


**Figure 3.1** *Comparison of source profiles from FLAME experiment data. Source profiles calculated as the ratio of levoglucosan/OC (organic carbon) are plotted against the ratio of levoglucosan/TC (total carbon) for each sample. The gray line represents a 1:1 relationship.*

### 3.2.2  Other Species Data

Additional species concentrations measured during the FLAME campaigns are listed below. Species measured from the hi-vol filters, including OC, EC, $K^+$, and

individual carbohydrates, are listed in Table 3.6. Table 3.7 gives concentrations of the various anions and cations measured from analysis of the URG filters. Only data from fuels that were used to create regional source profiles are listed. Though not all of these compounds were used in calculating source profiles, they can still provide important information about the various fuels burned. For example, each of the fuels burned emitted higher concentrations of anhydrosugars (levoglucosan, mannosan, and galactosan) than regular sugars (galactose, glucose, and mannose). This is most likely due to the fact that anhydrosugars are a major product of the transglycosylation of cellulose, while regular sugars are not (Shafizadeh, 1982). The anhydrosugars are essentially regular sugars that have had a water molecule removed; *e.g.*, levoglucosan is a glucose anhydride. During the combustion of cellulose, an internal ring forms on the levoglucosan molecule (see Chapter 1), leading to the loss of a molecule of water and the production of anhydrous sugars (Lakshmanan et al., 1969).

As stated previously, OC dominated TC for most of the burns used in creating source profiles. The few exceptions to this trend included burns of juniper, sage, and a mixture of rabbitbrush and sage, where EC made up about 78%, 34%, and 68% of the TC on average, respectively. These three fuels (or fuel mixtures) are all characteristic of the southwest U.S. and the drier environments often found there. The high EC could be due to the plants' biological makeup and/or their combustion efficiencies. Combustion of cellulose and hemicellulose produces more OC, while combustion of lignin produces more EC (Gelencsér, 2004). These plants could have higher concentrations of lignin, producing more EC when burned. The type of burn could have also affected the EC concentration. If the fire was more flaming, with less oxygen present, more EC would

have been emitted (Gelencsér, 2004).  McMeeking et al. (2008, submitted) shows that

this statement is in fact true.  Modified combustion efficiencies (MCE) were calculated

for each of the FLAME burns, with higher MCE values corresponding to more flaming

combustion.  Juniper, rabbitbrush/sage, and sage all had high MCE values (0.959, 0.942,

and 0.885, respectively), showing that there was mostly flaming combustion occurring

during these burns and explaining the high ratios of EC/TC.

It is also interesting to compare the concentrations of potassium measured on the

hi-vol and URG filters.  Many of the burns produced no significant $K^+$ on the hi-vol

filters though considerable amounts of $K^+$ were measured on the corresponding URG

filters (see Figure 3.2).  Quartz fiber filters, like those for the hi-vol samples, are

generally not used to measure inorganic species, such as $K^+$, because of their high

background concentrations.  However, because only hi-vol samples were collected for the

IMPROVE sites, $K^+$ was measured on the hi-vol FLAME filters as well, to be consistent.
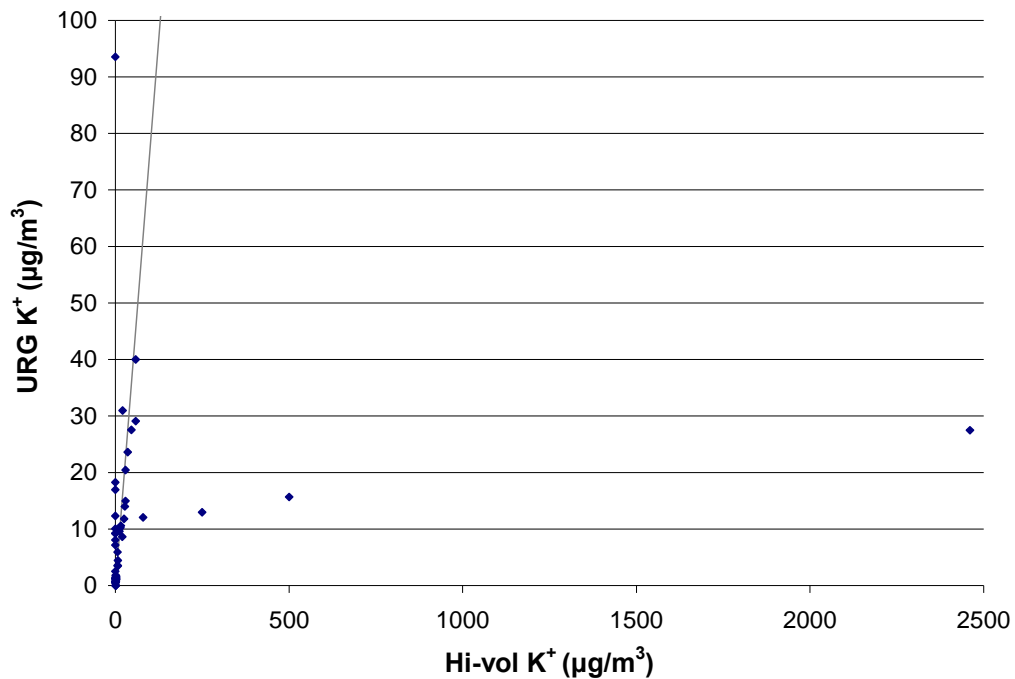


**Figure 3.2** *Comparison of $K^+$ measured from Hi-vol and URG filters.  The gray line represents a 1:1 relationship between the data.*

**Table 3.6** *Additional species concentrations from the FLAME hi-vol (PM$_{2.5}$) samples. Concentrations are averaged over species and are in units of μg/m$^3$.*

| Fuel | OC | EC | K$^+$ | Mannosan | Galactosan | Galactose | Glucose | Mannose |
|------|------|------|------|------|------|------|------|------|
| Alaskan Duff | 129.6 | 0.3 | 1.2 | 11.92 | 5.64 | 0.034 | 0.080 | 0.032 |
| Black Spruce | 248.7 | 18.2 | 0.5 | 5.63 | 2.04 | 0.053 | 0.12 | 0.056 |
| Ceanothus | 147.7 | 5.8 | 20.1 | 0.34 | 0.65 | 0.013 | 0.067 | 0.00 |
| Chamise | 127.4 | 26.3 | 21.8 | 0.56 | 1.05 | 0.022 | 0.091 | 0.015 |
| Douglas Fir | 80.8 | 9.3 | 2.8 | 0.78 | 0.43 | 0.0067 | 0.036 | 0.019 |
| Juniper | 52.7 | 182.1 | 14.6 | 0.23 | 0.16 | 0.000 | 0.023 | 0.00 |
| Kudzu | 711.3 | 0.0 | 0.0 | 7.57 | 1.72 | 0.000 | 0.23 | 0.00 |
| Manzanita | 261.0 | 12.5 | 9.0 | 1.17 | 3.24 | 0.033 | 0.14 | 0.026 |
| Montana Grass | 222.6 | 5.4 | 43.9 | 0.57 | 0.62 | 0.000 | 0.064 | 0.00 |
| Phragmites | 224.1 | 1.3 | 0.0 | 0.92 | 1.59 | 0.000 | 0.33 | 0.14 |
| Ponderosa Pine | 595.5 | 22.8 | 158.6 | 19.64 | 9.14 | 0.039 | 0.16 | 0.059 |
| Rabbitbrush/Sage | 53.0 | 111.7 | 58.5 | 0.40 | 0.21 | 0.025 | 0.037 | 0.00 |
| Sage | 104.4 | 53.5 | 0.0 | 0.56 | 0.26 | 0.000 | 0.053 | 0.00 |
| White Spruce | 55.1 | 0.0 | 0.0 | 1.35 | 0.43 | 0.015 | 0.071 | 0.024 |

**Table 3.7** *Additional species concentrations from the FLAME URG nylon filter samples. Concentrations are averaged over species and are in units of $\mu g/m^3$.*

| Fuel | $Cl^-$ | $NO_2^-$ | $NO_3^-$ | $SO_4^{2-}$ | $Na^+$ | $NH_4^+$ | $K^+$ | $Mg^{2+}$ | $Ca^{2+}$ |
|---|---|---|---|---|---|---|---|---|---|
| Alaskan Duff | 0.4 | 0.0 | 0.7 | 0.5 | 1.1 | 0.9 | 1.5 | 0.2 | 0.4 |
| Black Spruce | 4.3 | 0.0 | 0.3 | 0.4 | 3.9 | 2.7 | 6.2 | 1.9 | 2.1 |
| Ceanothus | 8.1 | 0.0 | 1.0 | 4.6 | 0.7 | 0.0 | 8.6 | 0.0 | 0.5 |
| Chamise | 7.3 | 0.6 | 2.0 | 7.5 | 3.3 | 0.6 | 15.4 | 1.0 | 1.3 |
| Douglas Fir | 1.0 | 0.5 | 2.4 | 1.4 | 1.7 | 0.4 | 3.0 | 0.04 | 0.3 |
| Juniper | 5.8 | 0.0 | 1.0 | 4.0 | 0.8 | 0.2 | 10.2 | 0.0 | 0.0 |
| Kudzu | 6.3 | 0.0 | 0.0 | 15.8 | 10.5 | 5.6 | 17.0 | 5.3 | 5.4 |
| Manzanita | 3.0 | 0.1 | 1.1 | 2.7 | 3.1 | 0.5 | 5.5 | 0.8 | 1.5 |
| Montana Grass | 30.0 | 0.9 | 3.4 | 4.7 | 4.2 | 1.2 | 24.8 | 0.0 | 4.1 |
| Phragmites | 28.9 | 0.0 | 0.0 | 0.0 | 11.1 | 7.3 | 12.3 | 5.9 | 5.9 |
| Ponderosa Pine | 5.8 | 0.04 | 1.0 | 2.3 | 4.4 | 2.0 | 5.2 | 2.2 | 3.5 |
| Rabbitbrush/Sage | 17.0 | 0.4 | 1.3 | 10.6 | 1.9 | 0.5 | 40.0 | 0.0 | 0.0 |
| Sage | 23.1 | 0.7 | 0.8 | 10.4 | 1.8 | 1.5 | 39.7 | 0.09 | 0.3 |
| White Spruce | 4.9 | 0.7 | 0.0 | 0.0 | 1.2 | 1.3 | 2.5 | 0.1 | 0.3 |

**3.3 IMPROVE Site Data**

*3.3.1 Grand Canyon, AZ (HANC)*

At the Grand Canyon, Arizona (HANC) site, levoglucosan concentrations ranged from 0.007 to 0.034 $\mu gC/m^3$, with an average of 0.015 ± 0.009 $\mu gC/m^3$ (± one standard deviation), over the summer of 2005 (Figure 3.3). During the study period, concentrations of levoglucosan showed higher concentrations and greater variability in July than in August. Levoglucosan decreased at the beginning of July, increased for the sample beginning July 13th to the maximum value seen (0.034 $\mu gC/m^3$), decreasing afterwards and remaining fairly constant through the end of the summer. Concentrations of $K^+$, OC, and EC showed similar trends, though changes in $K^+$ and OC were much more drastic (note that OC and EC are on a separate axis than $K^+$ and levoglucosan). Concentrations of OC and EC shown in this section are from analyses using the NIOSH-TOT method at CSU. After the maximum on the July 13th sample, $K^+$ and OC decreased for three weeks and then increased slightly for the August 10th sample. Concentrations of $K^+$ ranged from 0.009 to 0.3 $\mu g/m^3$, with an average of 0.09 ± 0.1 $\mu g/m^3$ (± one standard deviation); OC ranged from 0.8 to 4.2 $\mu gC/m^3$, averaging 2.1 ± 1.2 $\mu gC/m^3$. EC showed similar trends as levoglucosan; concentrations ranged from below detection limits to 0.7 $\mu gC/m^3$, with an average of 0.1 ± 0.2 $\mu gC/m^3$ (± one standard deviation).

*3.3.2 Mount Rainier, WA (MORA)*

The data from the Mount Rainier, WA (MORA) site show marked differences between the summer (2004) and winter (2004-2005) seasons (Figure 3.4). Concentrations of $K^+$, and OC were higher and showed more variability in the summer

than in the winter (note that OC and EC are on a separate axis than $K^+$ and levoglucosan).

Concentrations of levoglucosan remained below 0.03 μgC/m$^3$ and were relatively

constant during the summer. However, concentrations of levoglucosan increased and

were much more variable during the winter, ranging from 0.010 μgC/m$^3$ on the January

12$^{th}$ sample to 0.13 μgC/m$^3$ on the February 16$^{th}$ sample. Also, concentrations of

levoglucosan, $K^+$, OC, and EC followed each other relatively well during the winter,

while there does not appear to be much correlation between them during the summer.

During the winter, concentrations of levoglucosan, $K^+$, and OC decreased at the

beginning of December, increasing again around the December 22$^{nd}$ sample, and

decreasing again through the January 12$^{th}$ sample. Concentrations increased again, with a

seasonal maximum in the February 16$^{th}$ sample. Concentrations of EC were low and

relatively constant during both seasons, with slightly more variability during the winter.

Average concentrations for the entire sampling period, ± one standard deviation, were

0.029 ± 0.027 μgC/m$^3$ for levoglucosan, 0.04 ± 0.05 μg/m$^3$ for $K^+$, 1.4 ± 0.7 μgC/m$^3$ for

OC, and 0.03 ± 0.06 μgC/m$^3$ EC.

### 3.3.3 Phoenix, AZ (PHOE)

During the summer of 2005, there appears to be good correlation between $K^+$ and

OC at the Phoenix, AZ (PHOE) site (Figure 3.5; note that OC and EC are on a separate

axis from $K^+$ and levoglucosan). Levoglucosan remained fairly constant during this

period, while EC was variable but does not show any apparent correlation with other

species. The concentrations of OC, $K^+$, and levoglucosan all increased from summer to

winter. Levoglucosan and $K^+$ show fairly good correlation during the winter, while

changes in OC were more pronounced. All four species reached maximum study values

during the winter; levoglucosan (0.20 $\mu$gC/m$^3$) and OC (12.3 $\mu$gC/m$^3$) reached maximum

values in December (during the December 7$^{th}$ and 21$^{st}$ samples, respectively).  The

maximum value of EC, 2.4 $\mu$gC/m$^3$, was reached during the November 30$^{th}$ sample, while

K$^+$, 0.413 $\mu$g/m$^3$, was reached during the February 1$^{st}$ sample.  Samples in late January

were interesting because they show a general decrease in OC, followed by the maximum

K$^+$ concentration.  While levoglucosan followed the trends of K$^+$ fairly well at the

beginning of the winter, its concentrations did not mirror the large increases seen during

this late winter period described above.  Looking at overall trends, OC decreased slightly

throughout the winter, K$^+$ increased, and levoglucosan decreased.  EC behaved in an

opposite manner, becoming more constant and close to zero concentration during the

winter season.  Study averages for these species were 0.051 ± 0.055 $\mu$gC/m$^3$ for

levoglucosan, 0.2 ± 0.1 $\mu$g/m$^3$ for K$^+$,  5.2 ± 2.8 $\mu$gC/m$^3$ for OC, and 0.3 ± 0.6 $\mu$gC/m$^3$ for

EC (mean ± one standard deviation).

### 3.3.4 Puget Sound, WA (PUSO)

Trends in concentrations of levoglucosan, K$^+$, OC, and EC during the summer of

2004 and winter of 2004-2005 at the Puget Sound, WA (PUSO) site are shown in Figure

3.6.  Note that OC and EC are on a separate axis than K$^+$ and levoglucosan.  OC, EC, and

K$^+$ appear to track each other to some extent, except for the June 30$^{th}$ sample, which

shows a large increase in K$^+$ while OC and EC concentrations remained relatively

constant.  Another exception to this trend is seen in August when OC and EC appear to

be anti-correlated.  The site maximum of 0.98 $\mu$gC/m$^3$ for EC was seen in the July 28$^{th}$

sample.  Levoglucosan concentrations remained below 0.015 $\mu$gC/m$^3$ and were fairly

constant throughout the summer.  However, levoglucosan concentrations increased and

became much more variable during the winter, reaching a maximum concentration of 0.16 µgC/m³ in the February 16th sample.  The February 16th sample also had the maximum OC concentration of 5.2 µgC/m³; though the K⁺ concentration was also high in this sample, the maximum concentration of 0.5 µg/m³ was seen during the summer, in the June 30th sample.  OC, levoglucosan, and K⁺ appear to have correlated well during the winter, with the exception of the sample from January 5th, where K⁺ again showed a much more drastic increase than the other two species.  EC remained relatively constant at concentrations below the LOD for most samples during the winter.  Overall, each of the species showed high variability, resulting in high standard deviations with respect to study averages.  Levoglucosan averaged $0.033 \pm 0.037$ µgC/m³, K⁺ was $0.1 \pm 0.1$ µg/m³ on average, and OC and EC were $2.1 \pm 1.1$ µgC/m³ and $0.3 \pm 0.4$ µgC/m³ on average, respectively (listed as mean ± one standard deviation).
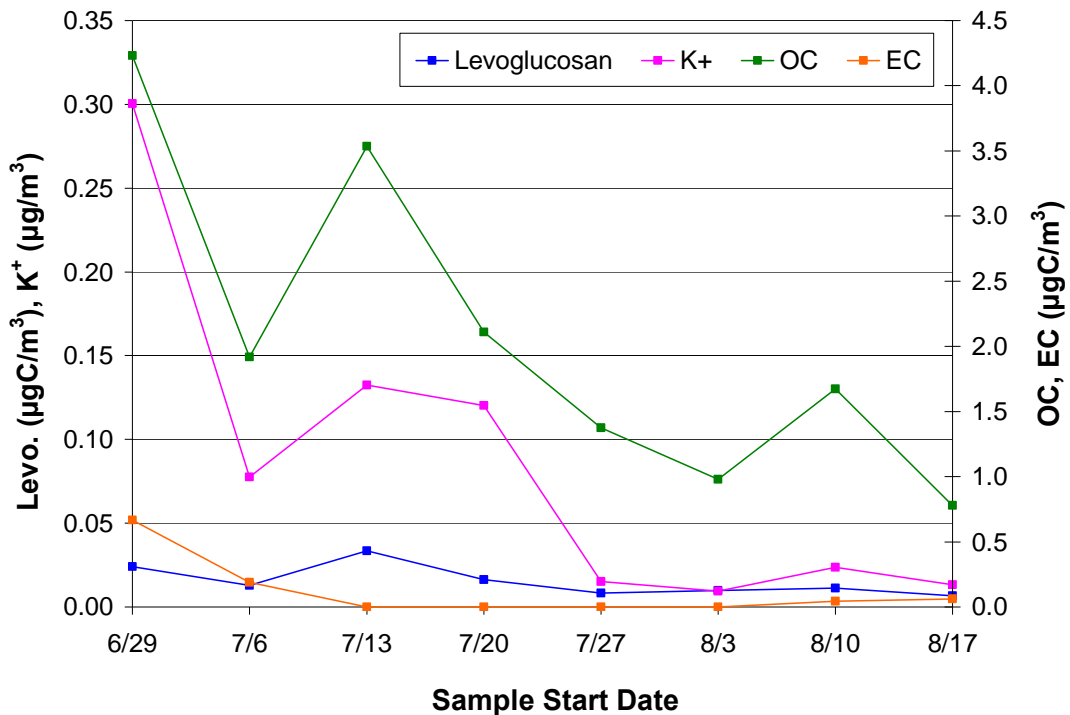


**Figure 3.3** *Timelines of levoglucosan, K⁺, OC, and EC concentrations during sampling at the Grand Canyon (HANC) site in the summer of 2005.  Levoglucosan and K⁺ are on the left y-axis, and OC and EC are on the right y-axis.*
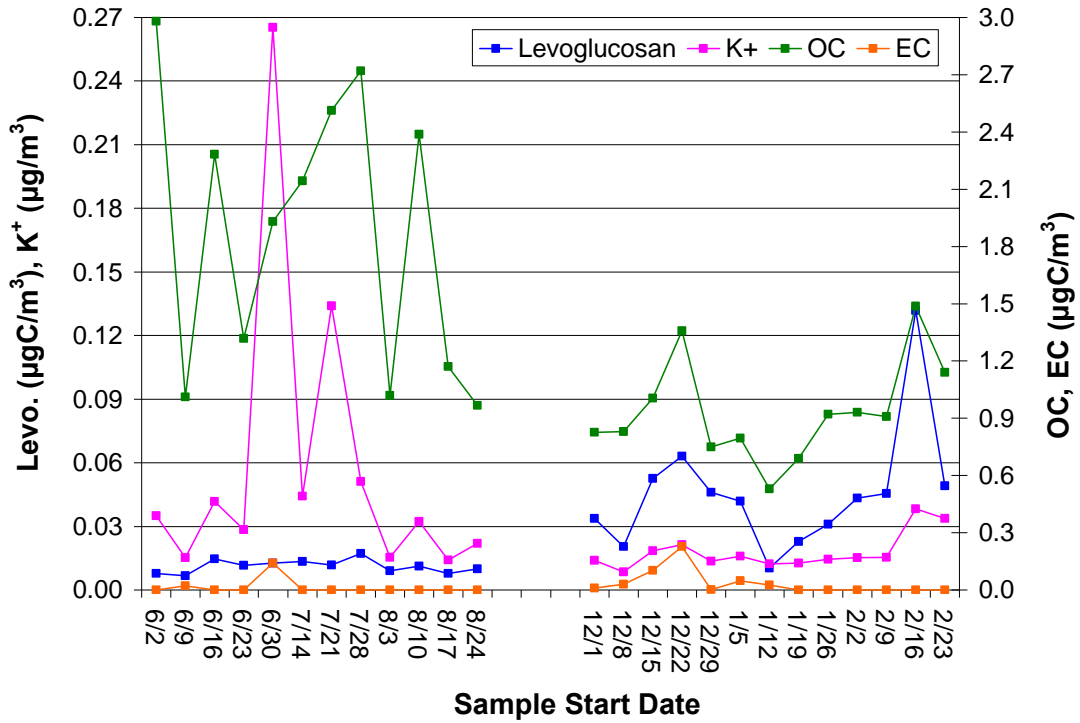
**Figure 3.4** *Timelines of levoglucosan, $K^+$, OC, and EC concentrations during sampling at the Mount Rainier (MORA) site in the summer of 2004 and winter of 2004-2005. Levoglucosan and $K^+$ are on the left y-axis, and OC and EC are on the right y-axis.*
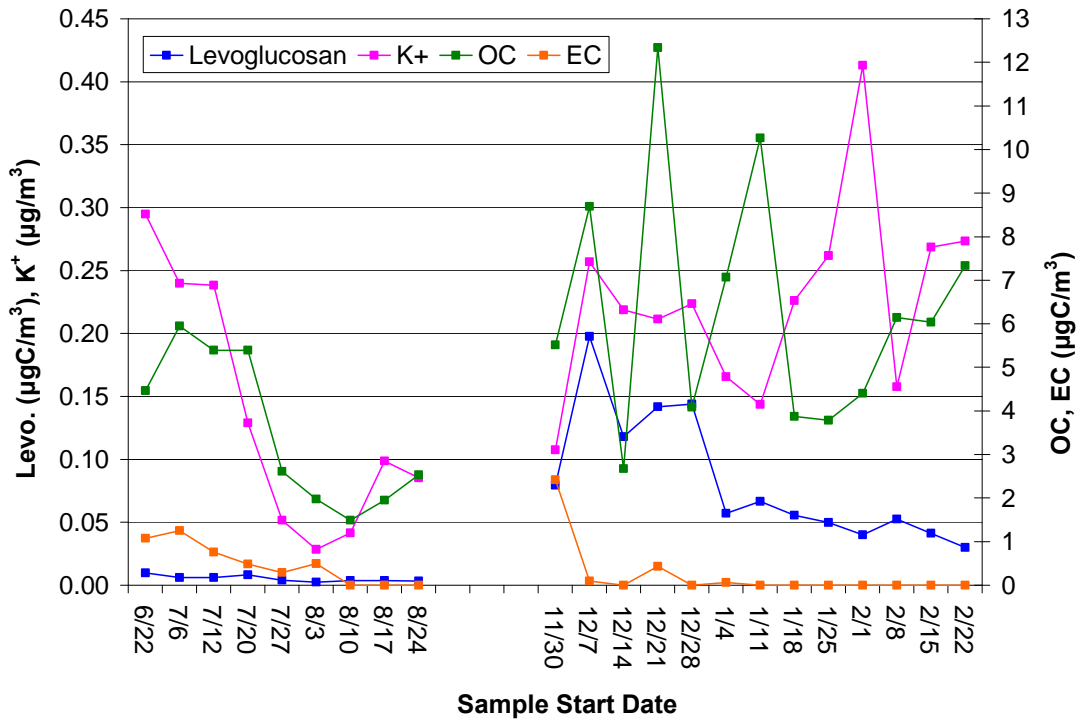


**Figure 3.5** *Timelines of levoglucosan, $K^+$, OC, and EC concentrations during sampling at the Phoenix (PHOE) site in the summer of 2005 and winter of 2005-2006. Levoglucosan and $K^+$ are on the left y-axis, and OC and EC are on the right y-axis.*

60
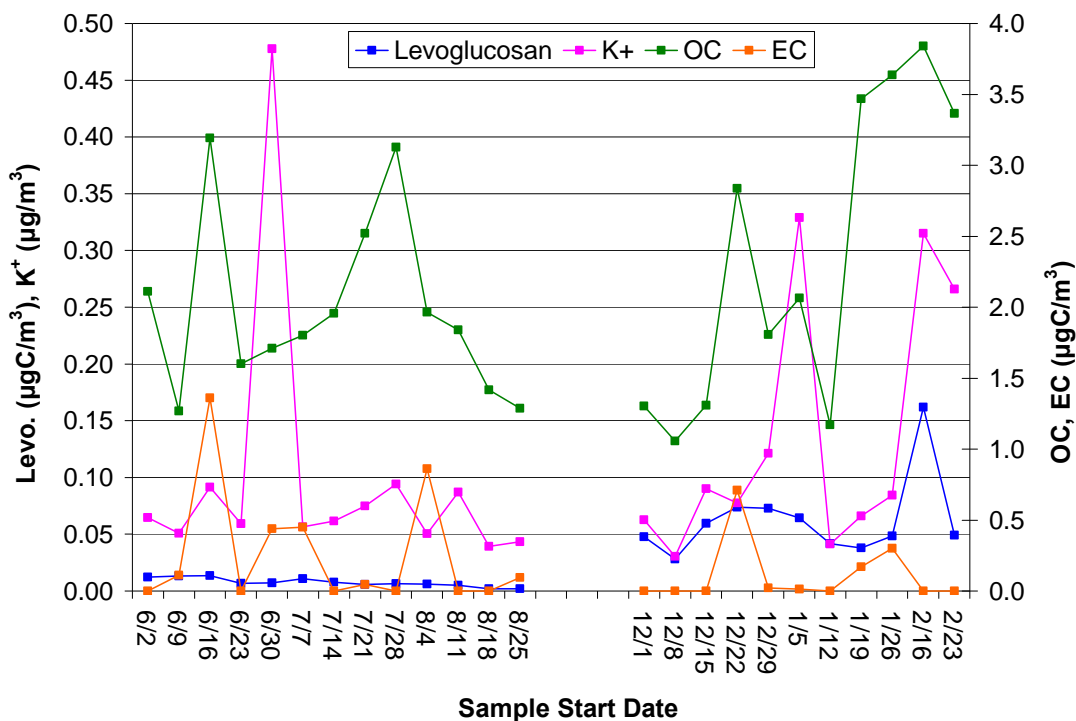
**Figure 3.6** *Timelines of levoglucosan, K⁺, OC, and EC concentrations during sampling at the Puget Sound (PUSO) site in the summer of 2004 and winter of 2004-2005. Levoglucosan and K⁺ are on the left y-axis, and OC and EC are on the right y-axis.*

### 3.3.5 Rocky Mountain National Park, CO (ROMO)

Levoglucosan, $K^+$, OC, and EC data for the summer of 2005 at the Rocky Mountain National Park, CO (ROMO) site are shown in Figure 3.7. Note that OC and EC are on a separate axis from the other two variables. At the beginning of the sampling period, in late June and early July, there appears to be a correlation between levoglucosan and $K^+$, with both showing an increase. OC also increased during this time, but unlike $K^+$ and levoglucosan, it continued to increase, reaching a maximum value of 4.6 $\mu gC/m^3$ during the July 19th sample. Following this peak, OC decreased throughout the rest of the study. $K^+$ also had a maximum of 0.2 $\mu g/m^3$ during the July 19th sample, then decreased into August, with one more increase during the week of August 9th. Levoglucosan, however, did not follow the same trends as $K^+$ during the latter part of the summer.

Levoglucosan began to increase as $K^+$ decreases in late July, reaching a maximum

concentration of 0.076 µgC/m$^3$ in the August 3$^{rd}$ sample, and decreasing for the rest of the

study. Levoglucosan and OC also appear to be anti-correlated throughout the sampling

period. EC did not show correlation between the other species examined here, increasing

slightly during the first week of August, but remaining relatively constant overall (0.02

µgC/m$^3$ on average, ranging from below detection limits to 0.1 µgC/m$^3$). Overall

averages, ± one standard deviation, were 0.036 ± 0.020 µgC/m$^3$, 0.08 ± 0.06 µg/m$^3$, and

3.5 ± 0.8 µgC/m$^3$ for levoglucosan, $K^+$, and OC, respectively.
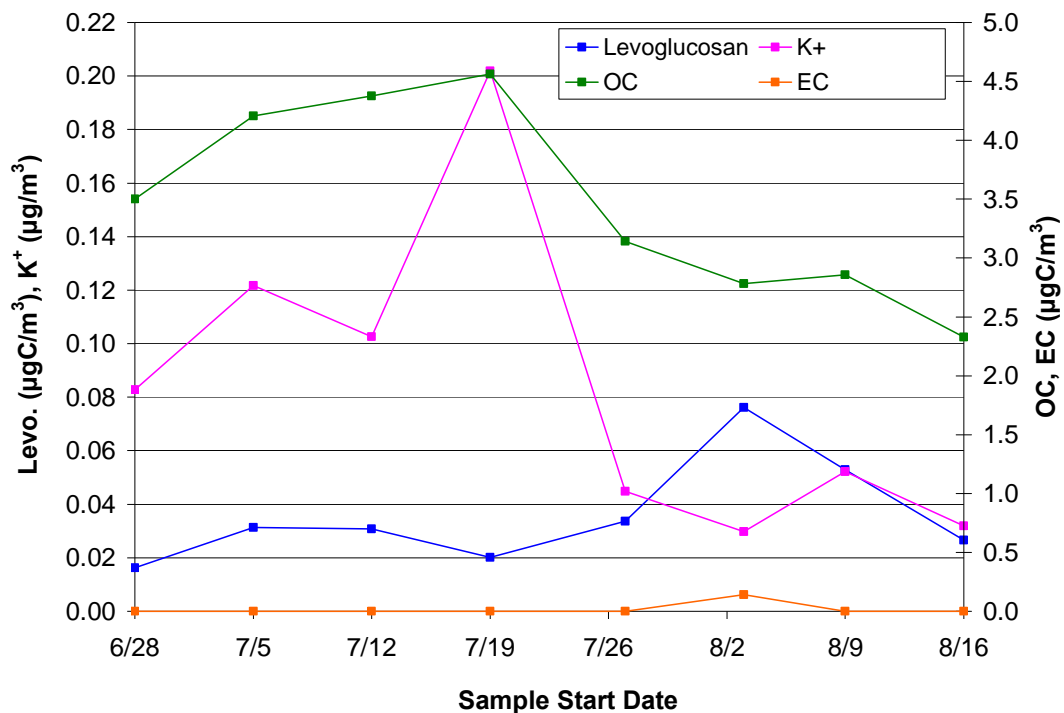


**Figure 3.7** *Timelines of levoglucosan, $K^+$, OC, and EC concentrations during sampling at the Rocky Mountain National Park (ROMO) site in the summer of 2005. Levoglucosan and $K^+$ are on the left y-axis, and OC and EC are on the right y-axis.*

*3.3.6 San Gorgonio Wilderness, CA (SAGO)*

Data from the San Gorgonio Wilderness, CA (SAGO) site, taken during the

summer of 2005, are shown below in Figure 3.8. Note that OC and EC are displayed on

a separate axis from $K^+$ and levoglucosan. As at the ROMO site, levoglucosan, $K^+$, and OC show similar trends throughout the study period. Levoglucosan and $K^+$ reached maximum concentrations (0.015 µgC/m$^3$ and 0.059 µg/m$^3$, respectively) during the July 5$^{th}$ sample and reached smaller peaks approximately every two weeks through the end of the summer. The study average concentrations of levoglucosan and $K^+$ were 0.005 ± 0.005 µgC/m$^3$ and 0.04 ± 0.02 µg/m$^3$, respectively (± one standard deviation). Concentrations of OC reached a maximum of 4.9 µgC/m$^3$ during the June 28$^{th}$ sample. Following this, concentrations decreased and then increased for the July 19$^{th}$ sample; concentrations decreased following this sample. Overall, OC averaged 2.0 ± 0.4 µgC/m$^3$ (± one standard deviation) during the study. Similar to the ROMO site, EC did not show much variation throughout the sample period, averaging 0.03 ± 0.05 µgC/m$^3$ (± one standard deviation).
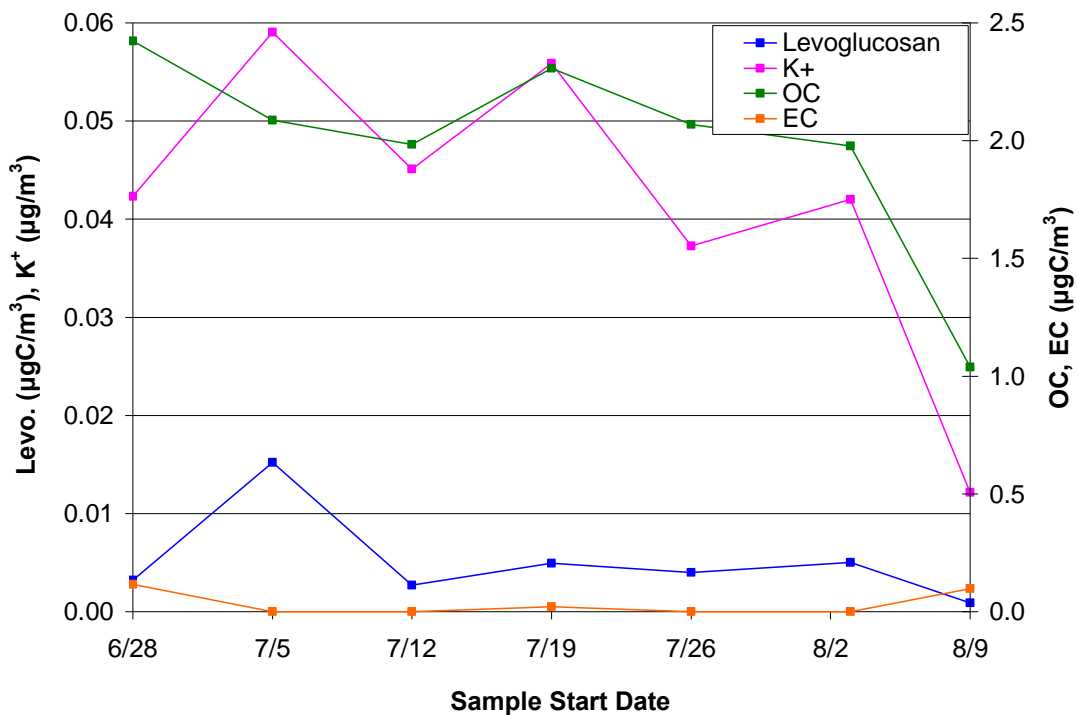


**Figure 3.8** *Timelines of levoglucosan, $K^+$, OC, and EC concentrations during sampling at the San Gorgonio Wilderness (SAGO) site in the summer of 2005. Levoglucosan and $K^+$ are on the left y-axis, and OC and EC are on the right y-axis.*

*3.3.7 Tonto National Monument, AZ (TONT)*

Like other sites, the data from the Tonto National Monument, AZ (TONT) site shows significant differences between the summer (2005) and winter (2005-2006) seasons, as seen in Figure 3.9 (note that OC and EC are displayed on a separate axis than $K^+$ and levoglucosan). Levoglucosan, $K^+$, OC, and EC followed the same trends during the summer season, with one exception. From week 1 to week 2, OC increases while the other species decrease in concentration. Levoglucosan (0.026 $\mu$gC/m$^3$), OC (4.9 $\mu$gC/m$^3$), and EC (0.8 $\mu$gC/m$^3$) reached maximum values for the study during the July 20$^{th}$ sample. The maximum concentration of $K^+$ (0.2 $\mu$g/m$^3$) was seen in the first sample of the summer, which began June 29$^{th}$. During the winter, the concentrations of $K^+$, OC, and EC were all lower than they were during the summer. The range of levoglucosan concentrations was similar between the two seasons. While $K^+$ and OC remained fairly well correlated during winter, EC and levoglucosan often did not show as much variability as the other two species. The overall averages for these four species were $0.007 \pm 0.006$ $\mu$gC/m$^3$ (levoglucosan), $0.06 \pm 0.06$ $\mu$g/m$^3$ ($K^+$), $1.7 \pm 1.0$ $\mu$gC/m$^3$ (OC), and $0.09 \pm 0.2$ $\mu$gC/m$^3$ (EC), listed as the mean $\pm$ one standard deviation.

*3.3.8 Comparison of TC from DRI and CSU Methods*

Total carbon, or TC, was measured for hi-vol filter samples from each IMPROVE site using TOT (thermal optical transmittance) and TOR (thermal optical reflectance). Samples were analyzed using TOT at CSU (CSU-TC) and TOR at DRI (DRI-TC). Though different methods were used, the concentrations of TC should be the same from each set of analyses. A comparison of the TC from these two methods is shown in Figure 3.10. As the figure shows, many points fall on the 1:1 line (the thick black line).

64

However, there are also many samples that are closer to one of the 1:2 lines (the gray lines), suggesting that for these samples the DRI measurements were twice as high as those using the CSU measurement technique, or vice versa. Underestimation of TC using the CSU method could be due to the method of storing the hi-vol filters. Particles were visibly coming off the filter samples onto the inside of the "Ziploc" plastic bags in which the filters were stored. It is also possible that uneven deposition of aerosols onto the filters led to differences in TC measured using the two methods.
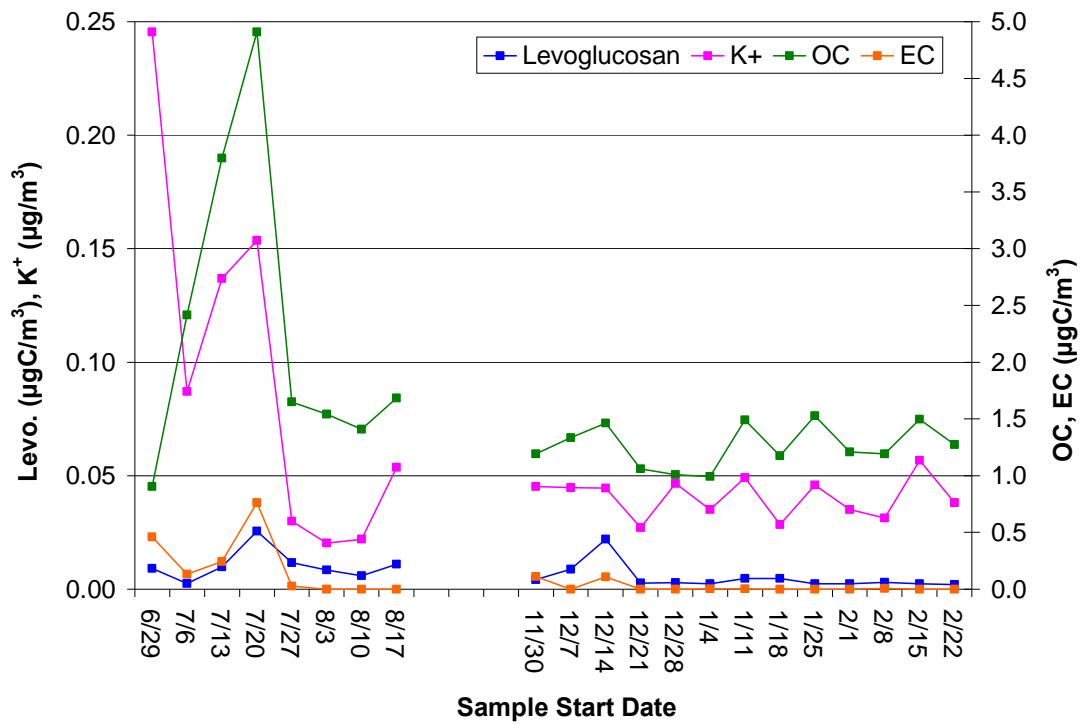


**Figure 3.9** *Timelines of levoglucosan, $K^+$, OC, and EC concentrations during sampling at the Tonto National Monument (TONT) site in the summer of 2005 and winter of 2005-2006. Levoglucosan and $K^+$ are on the left y-axis, and OC and EC are on the right y-axis.*

## 3.4 Application of Source Profiles to IMPROVE Samples

Source profiles, given as ratios of levoglucosan to total carbon, were applied to IMPROVE filter samples to estimate primary biomass combustion carbon concentrations. Residential wood combustion source profiles taken from the literature were applied to

65

winter samples, while wild/prescribed fire source profiles were calculated from FLAME experiment data and applied to the summer samples. Concentrations of fossil and contemporary carbon were estimated from carbon isotope data using accelerated mass spectrometry (AMS) at the Lawrence Livermore National Laboratory.
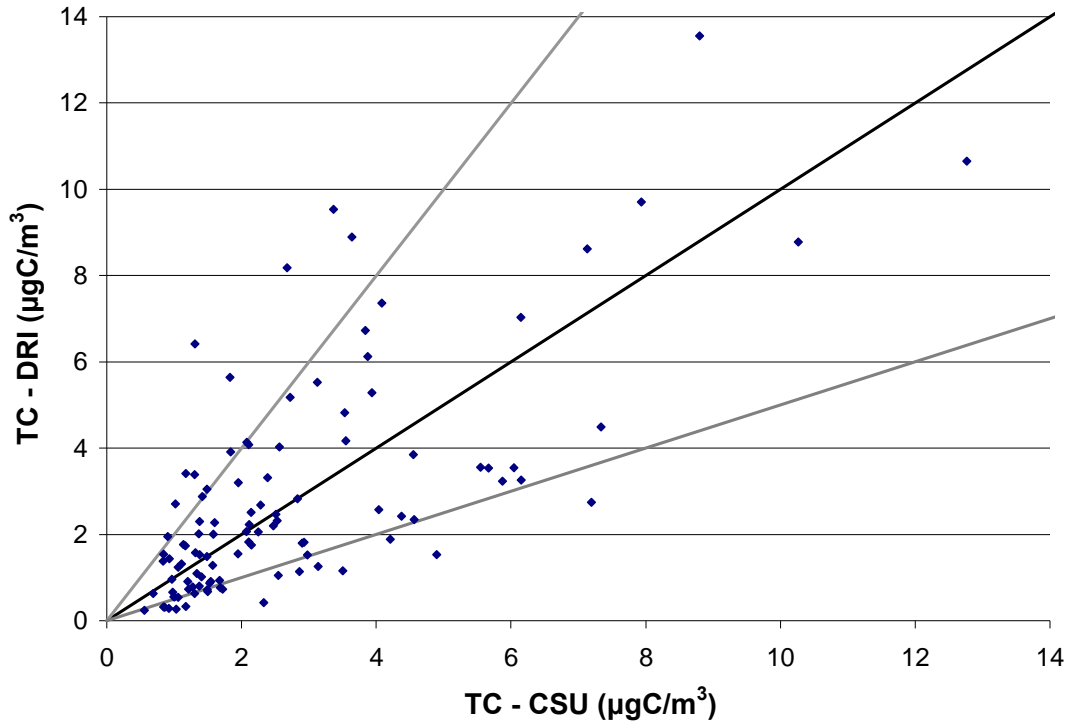


**Figure 3.10** *Total carbon measurements for IMPROVE filters measured by the CSU Method (TOT) compared to total carbon concentrations from measured at DRI (TOR). The thick black line represents a 1:1 relationship; the gray lines represent relationships of 1:2 (CSU:DRI on the top line, DRI:CSU on the bottom line).*

*3.4.1 Grand Canyon, AZ (HANC)*

Concentrations of fossil, contemporary, and primary biomass carbon measured in samples from the Grand Canyon, AZ (HANC) site are shown in Figure 3.11. These carbon types each showed much variability throughout the summer of 2005. During all of the samples, total carbon was dominated by contemporary carbon, as expected in a remote location like the Grand Canyon. Primary biomass burning carbon was estimated

66

to contribute 31-60% of contemporary carbon. Fossil carbon concentrations in the June 29th, July 20th, and August 10th samples were low enough to where they cannot be distinguished in the figure. Fossil carbon was seen at higher concentrations in the other samples, reaching a maximum of 0.24 $\mu gC/m^3$ during the July 13th sample. Concentrations of both contemporary and primary biomass combustion carbon were higher during the first half of the summer, decreasing in late July and into August.

The higher concentrations during the first four weeks correspond with periods of expected smoke influence, based on computed back trajectories and satellite smoke image data. These data predicted smoke plume presence at the site during the first half of the study (denoted by hatching), and no smoke influence in the latter half of the study. Interestingly, however, due to the lower concentrations of total carbon in August, fossil and primary biomass combustion carbon each appear to contribute larger percentages of measured TC during these last samples. It is possible that there were fires impacting the site which were too small to be seen by satellite. There is also a potential interference in the carbohydrate analysis with the sugar alcohol arabitol, which co-elutes with levoglucosan and could be causing over-estimations of levoglucosan concentrations. This could explain the higher estimates of primary biomass combustion when smoke plume presence was not expected. This possibility will be examined in more detail later in the chapter.

The lower contribution of primary biomass combustion to contemporary carbon in the first samples is most likely due to a missing source of contemporary carbon. As stated before, the estimates of biomass combustion in this study only include emissions from primary sources and do not include any secondary organic aerosols that could have

formed in the smoke plume as it aged. The combustion of biomass could therefore be contributing a larger amount of carbon than is estimated by the calculations in this study. In addition to SOA formed in smoke plumes, primary and secondary biogenic organic aerosols from non-combustion sources could make up a portion of the unidentified contemporary carbon.
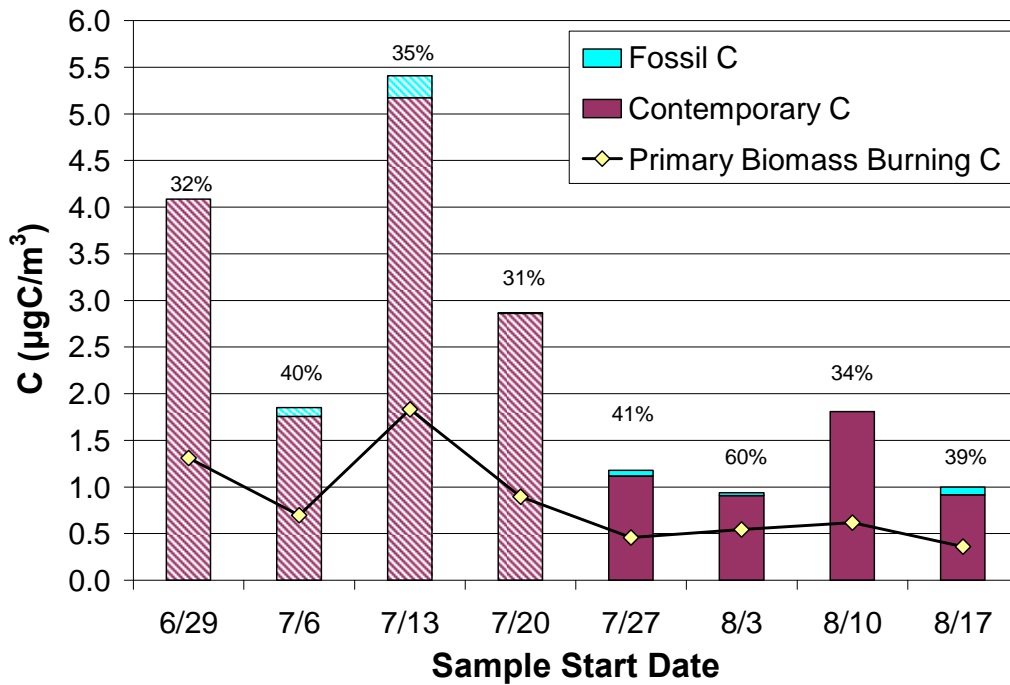


**Figure 3.11** *Fossil, contemporary, and primary biomass carbon concentrations during the summer of 2005 at the HANC (Grand Canyon, AZ) site. Fossil and contemporary carbon concentrations are bars stacked on top of one another, while biomass carbon concentrations are shown as points. The primary biomass burning carbon to contemporary carbon ratio is given as a percentage. Hatched bars represent samples expected to be influenced by smoke plumes from open/wildland fires.*

*3.4.2 Mount Rainier, WA (MORA)*

Fossil, contemporary, and primary biomass carbon data are shown in Figure 3.12 for the summer of 2004 and winter 2004-2005 at the Mount Rainier, WA (MORA) site. Note that each season is displayed on a separate graph. Considerable concentrations of fossil carbon are seen in the summer samples, more than often seen for other rural sites. For many of these samples, back trajectory data show transport from the Seattle/Tacoma,

WA and Portland, OR metropolitan areas. These urban areas would be large sources of fossil carbon, from the combustion of fossil fuels in automobiles and industrial facilities. During the winter, fossil carbon concentrations were much lower, probably due in part to the smaller number of visitors to the area. Similarly, total carbon concentrations were lower on average during the winter. Contemporary carbon dominated total carbon during each of the weeks during the two seasons sampled.

Primary biomass combustion carbon concentrations were relatively constant throughout the summer, ranging from approximately 0.26-0.67 $\mu gC/m^3$. However, because contemporary carbon concentrations varied much more during the season, the primary biomass combustion carbon/contemporary carbon ratios also varied. Primary biomass combustion carbon was estimated to contribute 14-54% of summer contemporary carbon. The percent contemporary carbon originating from primary biomass combustion does not clearly correlate with whether or not smoke was expected to influence the site during a sampling period. Some smaller fires might not be visible from the satellites that collect the data used in this study, leading to an underestimate in the weeks when smoke was present in the area. Similar to the HANC site, it is possible that some of the unexplained contemporary carbon was from SOA formation in aging smoke plumes and primary and secondary biogenic (non-combustion) organic aerosols. Arabitol influence could have also caused errors in the estimates of primary biomass combustion carbon.

During the winter, primary biomass combustion carbon was estimated to contribute 17-41% of the contemporary carbon, similar to the summer. It is assumed that all biomass combustion consists of residential wood burning during the winter. The high

contribution of primary biomass combustion during a cold winter, like the ones experienced in the Cascades of Washington, would make sense. This hypothesis will be explored in more detail later in this chapter.

### 3.4.3 Phoenix, AZ (PHOE)

At the Phoenix, AZ (PHOE) site there were high concentrations of fossil carbon during both the summer (2005) and winter (2005-2006) seasons (Figure 3.13). As this site was in a major urban area, this was expected. However, contemporary carbon still made up close to 50% of the total carbon. Primary biomass combustion was more influential during the warmer months, contributing 7-23% of the contemporary carbon in the summer and 4-16% of contemporary carbon in the winter. Low contributions of primary biomass combustion to contemporary carbon suggest that while residential wood combustion does occur here, it is not widespread. The low amounts of primary biomass combustion carbon, relative to contemporary carbon concentrations, also suggest an important unidentified source of contemporary carbon. Other non-combustion biogenic sources of primary and secondary organic aerosol, as well as SOA formed in smoke plumes, are likely important. Similar to other sites, the back trajectory and smoke plume image data did not predict every occurrence of biomass smoke at this site.

### 3.4.4 Puget Sound, WA (PUSO)

Like Phoenix, Puget Sound, WA (PUSO) also had high concentrations of fossil carbon in both the summer (2004) and winter (2004-2005) seasons (Figure 3.14), consistent with its urban location. However, contemporary carbon still made up more than half of the total carbon for each sample. Concentrations of primary biomass

combustion carbon were relatively constant in the beginning of the summer and decreased towards the end of the summer. Overall, primary biomass combustion carbon made up 7-38% of the contemporary carbon at the Puget Sound site. Many samples had similar contributions of primary biomass combustion carbon though not all of these samples were expected to be influenced by biomass smoke, according to back trajectory and satellite smoke data. For example, in the sample beginning August 11th, back trajectory data showed transport of particles from a smoke plume, and primary biomass combustion was estimated to contribute to approximately 7% of the contemporary carbon. In the sample beginning August 25th, however, back trajectory data did not suggest any smoke plume transport into the region, but biomass combustion was estimated to contribute approximately 8% of contemporary carbon. This could be a result of the satellite data not showing smaller fires, or from the presence of non-fire sources of contemporary carbon, as suggested previously. Similar to other sites, the interference of arabitol is a potential source of error in calculating concentrations of primary biomass combustion carbon.

During the winter, we see higher concentrations of primary biomass combustion carbon, resulting in greater contributions to contemporary carbon (10-34%). This is consistent with knowledge that residential wood combustion is frequently used in the winter months to heat homes in this region. It is also interesting to note that in both the summer and winter seasons at the PUSO site, we see the same trend that has been seen at the other IMPROVE sites so far, the suggestion of a missing source of contemporary carbon. This extra contemporary carbon contribution is relatively lower during the winter months at PUSO, as contributions from primary biomass combustion are greater.
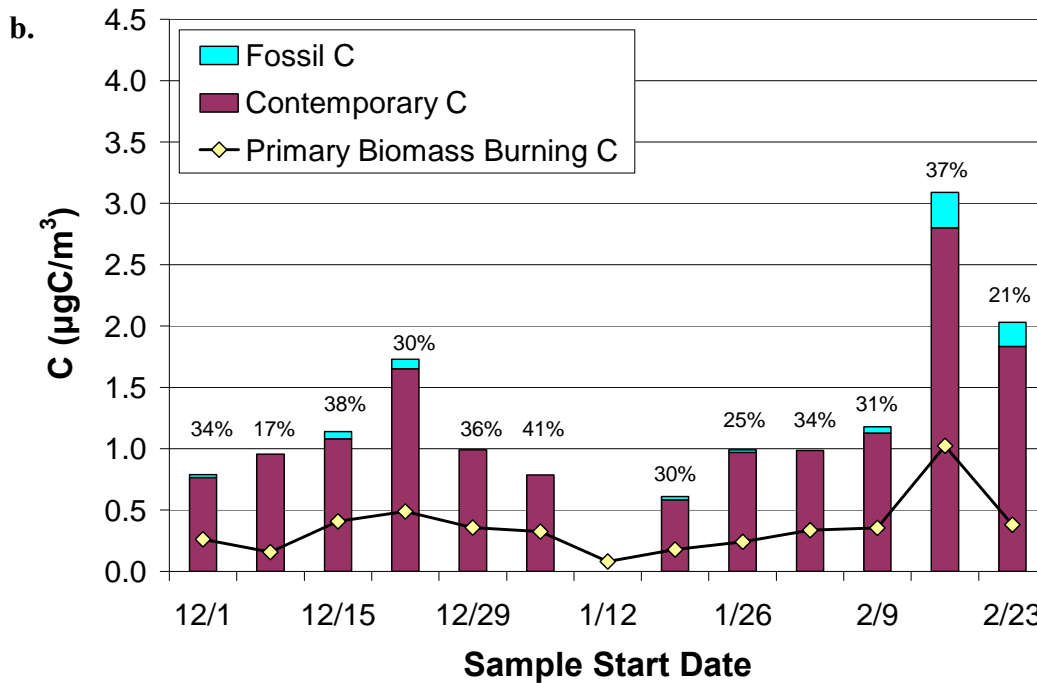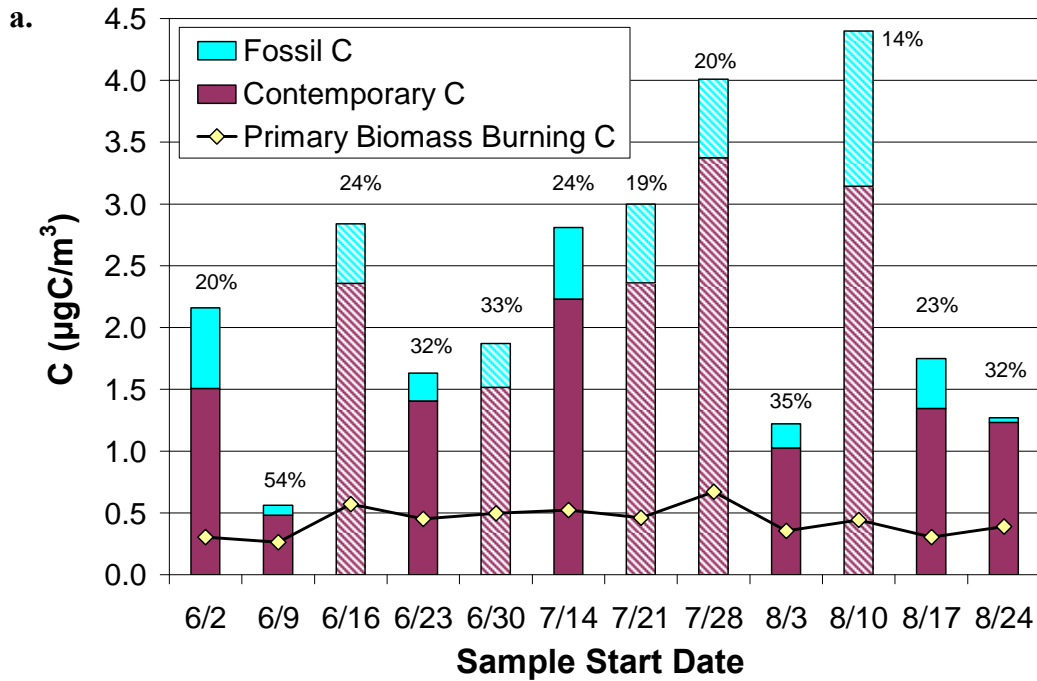
**Figure 3.12** *Fossil, contemporary, and primary biomass carbon concentrations during (a) Summer 2004 and (b) Winter 2004-2005 at the MORA (Mount Rainier National Park, WA) site. Fossil and contemporary carbon concentrations are bars stacked on top of one another, while biomass carbon concentrations are shown as points. The primary biomass burning carbon to contemporary carbon ratio is given as a percentage. Hatched bars represent samples expected to be influenced by smoke plumes from open/wildland fires. No filter sample was available for July 7 and no $^{14}C$ data was available for January 12.*
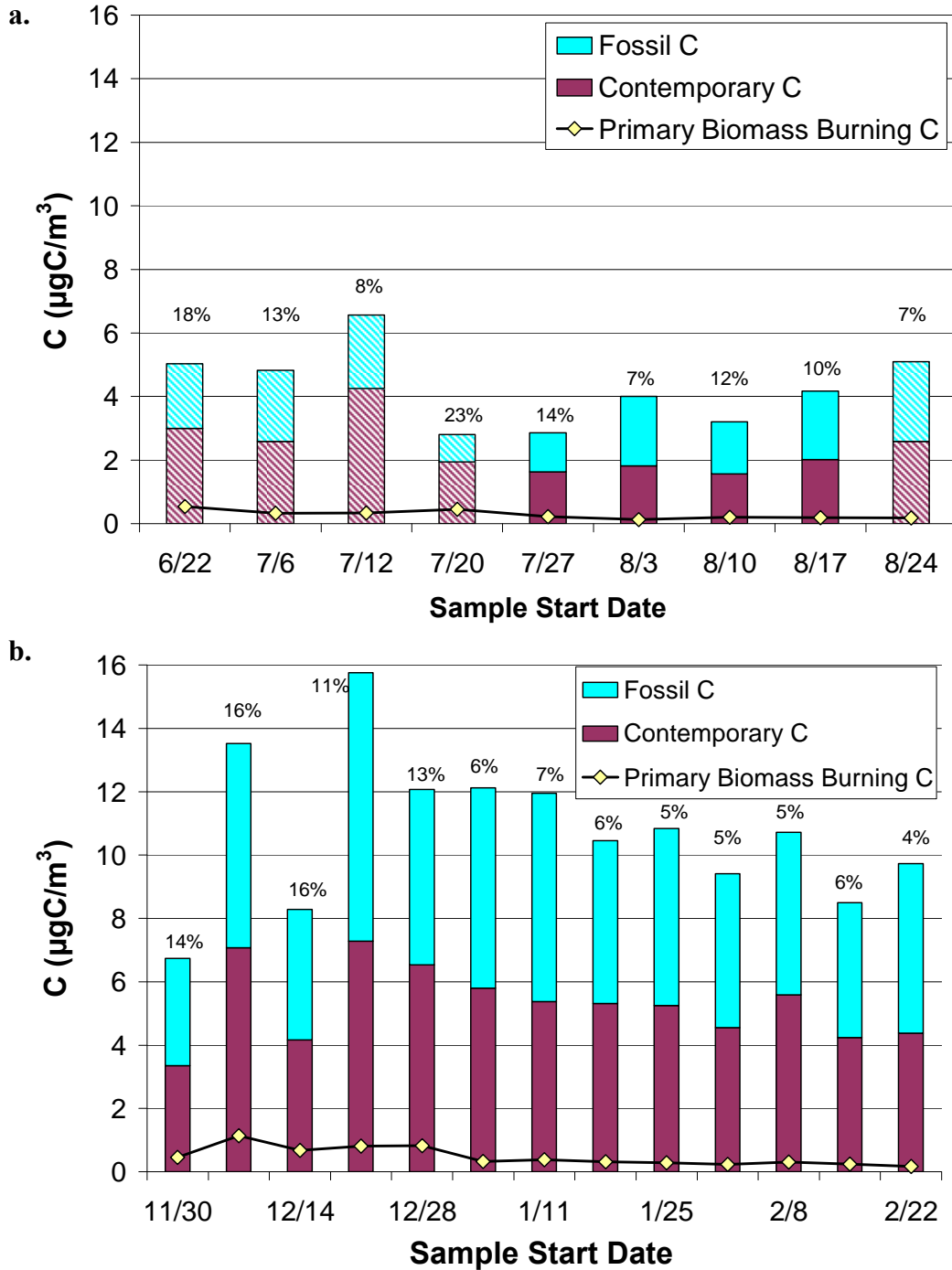
**Figure 3.13** *Fossil, contemporary, and primary biomass carbon concentrations during (a) Summer 2005 and (b) Winter 2005-2006 at the PHOE (Phoenix, AZ) site. Fossil and contemporary carbon concentrations are bars stacked on top of one another, while biomass carbon concentrations are shown as points. The primary biomass burning carbon to contemporary carbon ratio is given as a percentage. Hatched bars represent samples expected to be influenced by smoke plumes from open/wildland fires. No sample was available for June 29.*
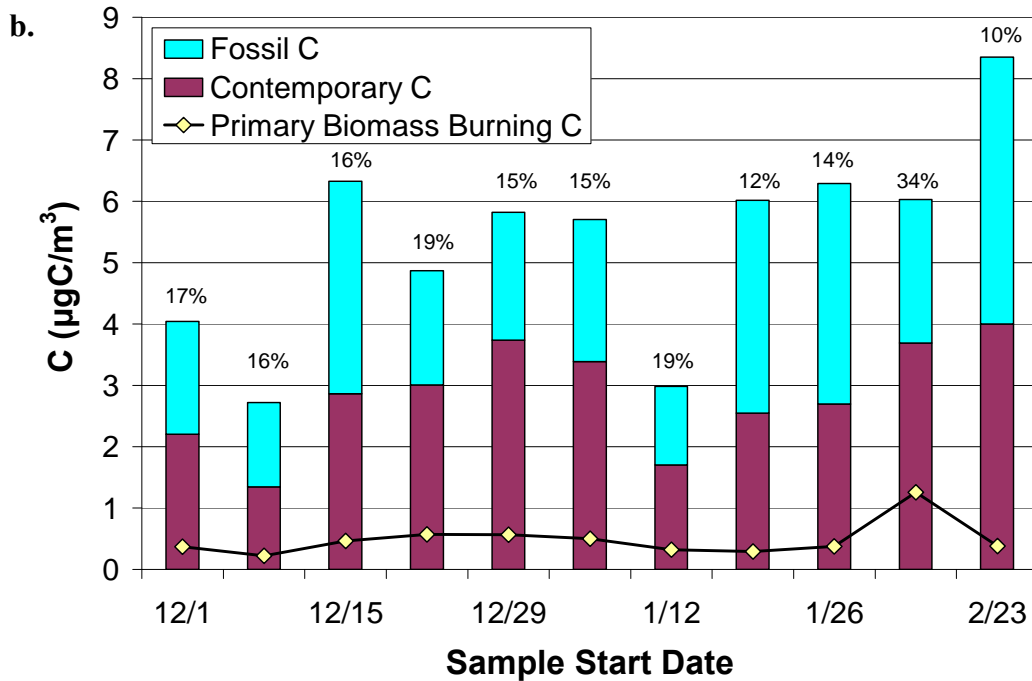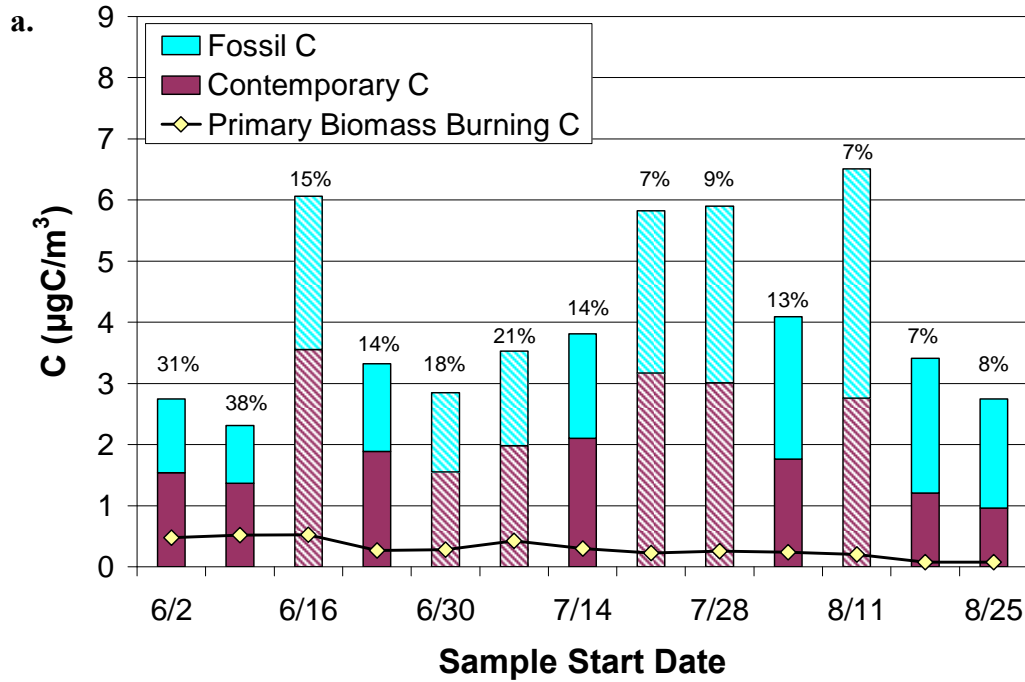
**Figure 3.14** *Fossil, contemporary, and primary biomass carbon concentrations during (a) Summer 2004 and (b) Winter 2004-2005 at the PUSO (Puget Sound, WA) site. Fossil and contemporary carbon concentrations are bars stacked on top of one another, while biomass carbon concentrations are shown as points. The primary biomass burning carbon to contemporary carbon ratio is given as a percentage. Hatched bars represent samples expected to be influenced by smoke plumes from open/wildland fires.*

*3.4.5 Rocky Mountain National Park, CO (ROMO)*

At the Rocky Mountain National Park site (ROMO) during the summer of 2005, total carbon was dominated by contemporary carbon, similar to other rural sites (Figure 3.15). However, fossil carbon concentrations were relatively high for a rural site. This could be due to automobile emissions from the many visitors that drive through the large park winter and summer or the influence of large population centers along the Colorado Front Range east of the park. This site also had high concentrations of primary biomass carbon, which led to the highest primary biomass combustion influence of all the sites examined in this study. During the first four weeks of the summer, primary biomass combustion was estimated to contribute approximately 50-81% of the contemporary carbon. The last four weeks of the summer showed estimated concentrations of primary biomass combustion carbon greater than those of contemporary and total carbon concentrations. It is interesting that all of the samples were expected to be influenced by biomass smoke (shown as hatched bars in Figure 3.15), based on computed back trajectories and satellite smoke images, except the samples beginning August 3$^{rd}$ and August 16$^{th}$. Again, we see that even in some samples where biomass smoke influence was expected, there is still a large unknown source of contemporary carbon. Similar to other sites, this excess contemporary carbon is most likely due to a combination of sources, including SOA in the biomass smoke that has not been accounted for in our calculations, along with other non-combustion biogenic contributions.

Obviously, concentrations of primary biomass combustion carbon greater than total carbon measured are not possible and there must be an error somewhere in the analysis and/or calculations. It is likely that the simple regional source profile applied

was not appropriate for all of the samples at this site.  This possibility will be examined

further when we look at possible relationships between emissions and type of fuel

component burned.
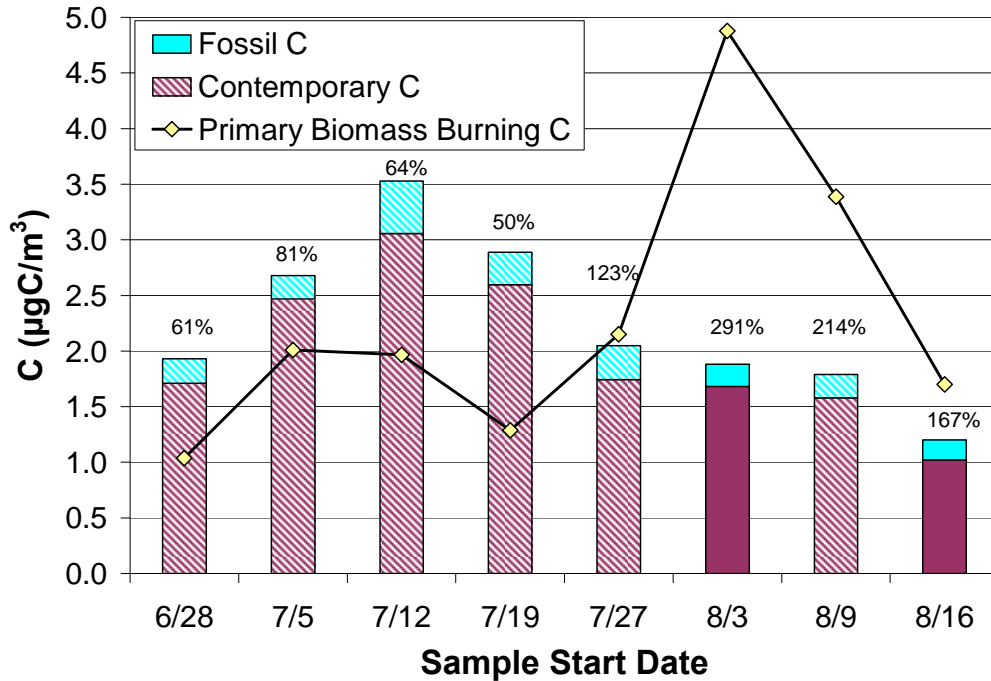


**Figure 3.15** *Fossil, contemporary, and primary biomass carbon concentrations during Summer 2005 at the ROMO (Rocky Mountain National Park, CO) site.  Fossil and contemporary carbon concentrations are bars stacked on top of one another, while biomass carbon concentrations are shown as points.  The primary biomass burning carbon to contemporary carbon ratio is given as a percentage. Hatched bars represent samples expected to be influenced by smoke plumes from open/wildland fires.*

*3.4.6 San Gorgonio Wilderness, CA (SAGO)*

At the San Gorgonio Wilderness, CA (SAGO) site in the summer of 2005, fossil

carbon was very low and even negative during some weeks.  This was possibly due to the

method of calculating the concentrations of contemporary and fossil carbon.  As stated in

Chapter 1, contemporary carbon concentrations are calculated based on the $^{14}C/C$ ratio.

Total carbon was measured separately, and then fossil carbon was defined as the

difference between contemporary carbon and total carbon.  However, in some cases the

concentration of contemporary carbon was calculated to be higher than the total carbon

measured, resulting in negative concentrations of fossil carbon. The data from this site was excluded from a study on the ^{14}C data shown in Schichtel et al. (2008) because it was suspected that a large ^{14}C source, such as a hospital incinerator, had influenced filter samples. Because of this uncertainty in the split between fossil and contemporary carbon, concentrations of primary biomass combustion carbon are compared to total carbon measured during ^{14}C analyses (Figure 3.16).
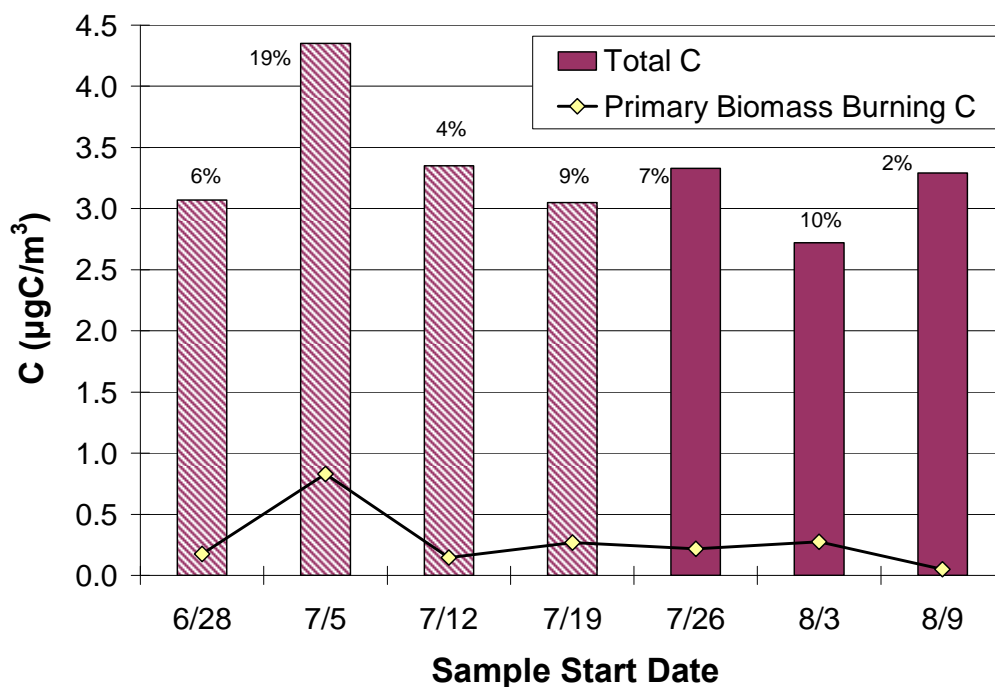


**Figure 3.16** *Fossil, contemporary, and primary biomass carbon concentrations during Summer 2005 at the SAGO (San Gorgonio Wilderness, CA) site. Fossil and contemporary carbon concentrations are bars stacked on top of one another, while biomass carbon concentrations are shown as points. The primary biomass burning carbon to total carbon ratio is given as a percentage. Hatched bars represent samples expected to be influenced by smoke plumes from open/wildland fires.*

Primary biomass combustion carbon did not largely contribute to total carbon at the SAGO site. Approximately 2-19% of total carbon was made up by primary biomass carbon during the summer. Despite these low apparent contributions, biomass smoke was expected to influence the site during four of the seven weeks sampling took place (weeks highlighted in Figure 3.16). This is another example of the possibility of SOA

formation in a biomass smoke plume, as well as primary and secondary biogenic organic aerosols, contributing to contemporary carbon.

### 3.4.7 Tonto National Monument, AZ (TONT)

The final site analyzed was the Tonto National Monument, AZ (TONT) site, which was sampled during the summer of 2005 and winter of 2005-2006. During the summer at this site, there were relatively low concentrations of fossil carbon, with the majority of total carbon coming from contemporary carbon sources (Figure 3.17). The fossil carbon seen here could be due to visitors driving to the national monument or transport from the nearby metropolitan area of Phoenix, as supported by back trajectory data. Contributions of primary biomass combustion to contemporary carbon ranged from 8-48%. Back trajectory data, along with smoke plume images, suggested biomass smoke influence during the first four weeks of the summer sampling. It is interesting that, similar to previous sites, the relative contribution of primary biomass combustion to contemporary carbon was actually higher during the last four weeks of the summer, when little or no influence from biomass smoke was expected at the site. However, as Figure 3.9 showed previously, concentrations of organic carbon were higher during the weeks where smoke influence was expected.

During the winter, concentrations of contemporary carbon were much lower than during the summer. Primary biomass combustion carbon also decreased, making up only 1-11% of contemporary carbon. Conversely, fossil carbon appears to have contributed more to total carbon than during the summer. Again, this could be due to transport from Phoenix, where high levels of fossil carbon were seen during the winter (see above).

Finally, as seen in the previous sites, the majority of contemporary carbon was found to consist of carbon from some other source besides primary biomass combustion.
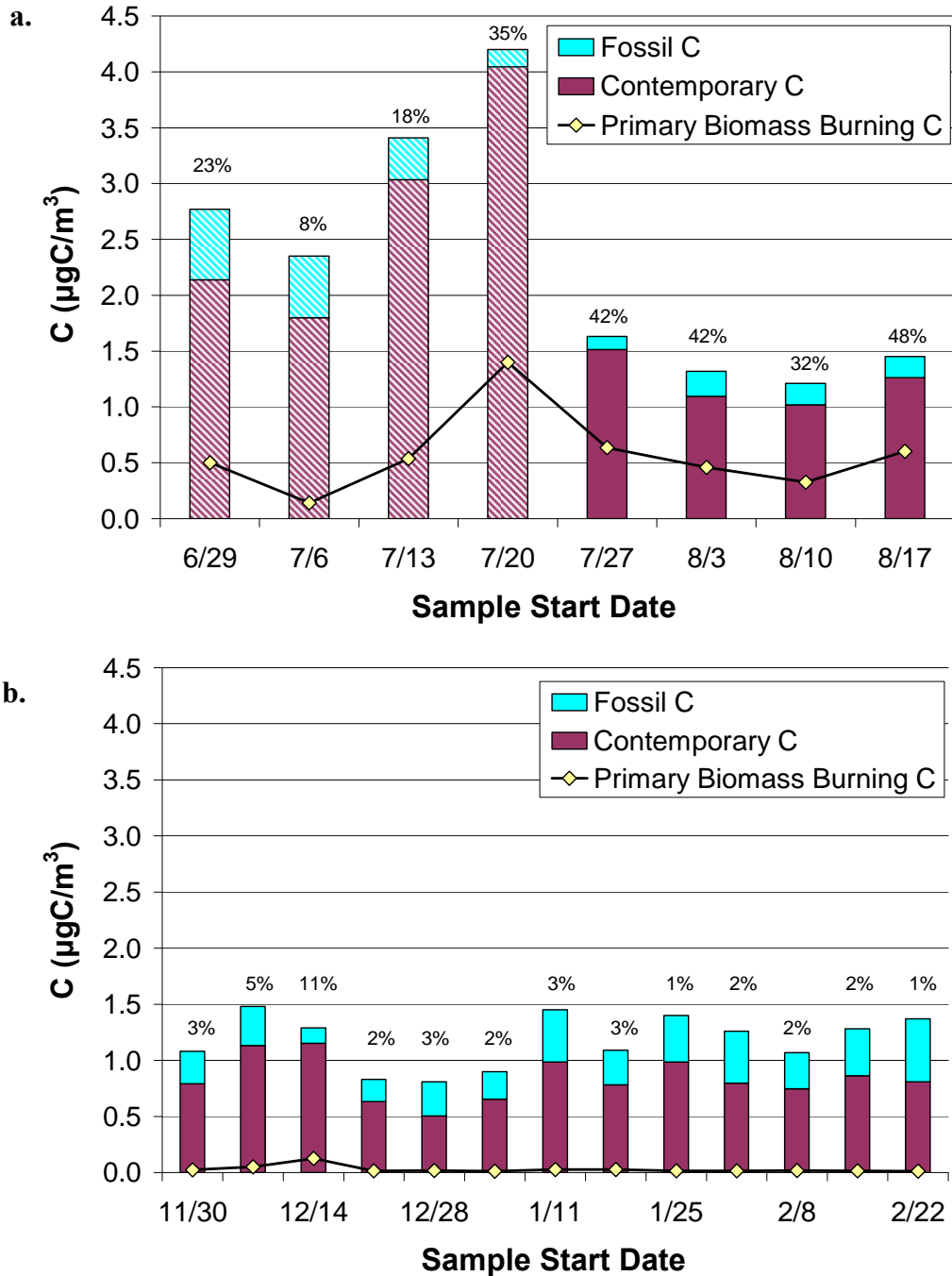


**Figure 3.17** *Fossil, contemporary, and primary biomass carbon concentrations during (a) Summer 2005 and (b) Winter 2005-2006 at the TONT (Tonto National Monument, AZ) site. Fossil and contemporary carbon concentrations are bars stacked on top of one another, while biomass carbon concentrations are shown as points. The primary biomass burning carbon to contemporary carbon ratio is given as a percentage. Hatched bars represent samples expected to be influenced by smoke plumes from open/wildland fires.*

*3.4.8 Comparisons Between IMPROVE Sites*

After looking at data from each of the IMPROVE sites individually, we can look for patterns in the data between sites of different climates, regions, and population densities, as shown in the following sections. The seven sites share two main similarities in the data. The first is that there is a missing source of contemporary carbon, as shown in low percent contributions of primary biomass combustion. It is likely that this discrepancy between biomass carbon and contemporary carbon is partly due to secondary organic aerosols that form in the smoke plumes as they age. Previous studies have suggested the need to understand SOA formation in biomass smoke plumes. Liousse et al. (1995) found in their study of savanna fires that biomass smoke can age quickly, possibly within the first 100 meters of the fire source. As Engling et al. (2006b) suggest, the farther these plumes are transported from the fire, the more aged the smoke plume and the longer time there is for SOA to be produced, resulting in higher concentrations of SOA. The back trajectory data, along with images of smoke plumes from satellite data, show that transported smoke plumes are likely a major source of biomass carbon at each of the sites. In fact, for most of the samples, the influence of biomass combustion was expected to be from particles transported many kilometers from the site, allowing much time for plume aging and SOA production. It is therefore likely that SOA exist in large quantities in the smoke plumes that impacted the sites discussed here. As mentioned previously, since the calculations for the estimation of concentrations of biomass carbon use a primary chemical tracer, levoglucosan, the data here act as more of a lower limit to the potential influence biomass combustion has on ambient particulate matter.

A second possibility could be the presence of non-combustion sources of organic aerosols contributing to contemporary carbon concentrations. Primary biogenic organic gases, such as isoprene and monoterpenes, are naturally emitted by vegetation. These gas-phase compounds can be oxidized by species such as OH radicals to produce secondary organic compounds (Shallcross and Monks, 2000), which can condense into the particle phase and be collected on $PM_{2.5}$ filters. Estimates of global emissions have shown that isoprene is a considerable contributor of contemporary carbon in the atmosphere, with studies suggesting 175-503 TgC emitted per year (Dignon and Logan, 1990; Guenther et al., 1995; Muller, 1992; Rasmussen and Khalil, 1988; Taylor et al., 1990; Turner et al., 1991; Zimmerman, 1979). It is also interesting to note that emissions of isoprene are known to increase with higher temperatures, such as those seen near wild and prescribed fires (Shallcross and Monks, 2000). Fires would not only add to contemporary carbon concentrations by producing levoglucosan and smoke plume SOA, but also by contributing to the amount of isoprene in the atmosphere, which could lead to an increase in secondary biogenic organic aerosol formation.

It is also possible that some levoglucosan is lost during transport of the smoke plume. Research discussed in Chapter 2 suggested that levoglucosan is relatively stable in acidic clouds and in a laboratory environment (Fraser and Lakshmanan, 2000; Sullivan, 2008). However, recent studies by colleagues at the Institute for Tropospheric Research in Leipzig, Germany suggest that hydroxyl radical attack on levoglucosan in the aqueous phase can be rapid, suggesting potential degradation during cloud processing. It is also possible that levoglucosan can partition to the gas phase, which is not measured using the current methods. This process is not well understood, but could have

significant impacts on the amount of total levoglucosan measured. Degradation of levoglucosan by microbes is also possible. Consumption of levoglucosan would lead to an underestimation of primary biomass combustion concentrations. Finally, errors in creating source profiles could account for some of the unidentified contemporary carbon. If the profiles overestimated the levoglucosan/TC emitted in a typical fire, concentrations of primary biomass combustion carbon would appear to be less than their true values.

The other similar aspect of each of the IMPROVE sites analyzed here was the lack of correlation between biomass contributions to contemporary carbon and estimates of biomass smoke influence from satellite data. It is important to remember that the process of estimating fire influence is not quantitative. That is, the satellite and back trajectory data are used to determine the presence of smoke plumes and estimate whether they will impact a site during a given time period. The data do not, however, give any information of the degree to which a fire is influencing a sample. There were many samples which showed similar contributions of primary biomass combustion to TC, though not all of these were expected to show any biomass combustion influence. It is possible that there were more fires present than seen in the satellite data. Smaller smoke plumes might not be as visible from satellites. Yokelson et al. (2007) suggest that cloud cover also interferes with the satellite's view of smoke plumes and fires. Another possibility would be that we are somehow overestimating the influence of biomass combustion on ambient particulate matter, perhaps by not including additional sources that could be emitting levoglucosan in addition to biomass combustion. Burning of paper products, such as cardboard, are an example of a potential source of levoglucosan not included in our estimates.

*3.4.8.1 Seasonal Differences*

When comparing data between the summer and winter, some obvious trends appear. Figure 3.18 displays the percent contribution of primary biomass combustion to total carbon for each of the samples discussed previously. Note that two points exceed 100% at the ROMO site. Also, all seven sites had summer data but winter data were only analyzed for four sites. In the summer, there were higher relative contributions of primary biomass carbon at the rural sites (HANC, MORA, ROMO, and TONT) than at the urban sites (PHOE, PUSO). This trend is consistent with the assumption that primary biomass combustion in the summer is due mostly to wild and prescribed fires. While wild fires do impact urban areas, they are more often found in rural areas such as forests and parks, where there is a large amount of vegetation to burn. Prescribed burns also follow this trend. The only exception to this trend was SAGO, a rural site that showed low contributions of primary biomass combustion. Conversely, urban areas show higher relative contributions of fossil carbon than rural areas. Similarly, rural sites showed higher contributions of primary biomass combustion to contemporary carbon (Figure 3.19). Table 3.8 gives the average and range of relative contributions of primary biomass combustion.

Contributions of primary biomass combustion to TC decreased from summer to winter at the Arizona sites. However, at the northern sites, the fraction of TC made up by primary biomass combustion carbon increased from summer to winter. This increase led to consistently higher primary biomass carbon contributions to TC during the winter at the northern sites; the only exception was one TONT sample with high contributions of primary biomass carbon to TC. Again, this agrees with previous assumptions that

primary biomass combustion is from mostly residential wood burning during the winter.

Nizich et al. (2000) found that residential wood combustion contributes approximately 8-14% of the $PM_{2.5}$ mass in WA, OR, and CA, supporting the idea that it is an important emission source in the Pacific Northwest.  These sites in the north experience lower temperatures, leading to increased numbers of fires in fire places and wood stoves to warm houses.  Figure 3.20 shows that for most of the winter, the WA sites did experience lower minimum temperatures than the southern sites in AZ.
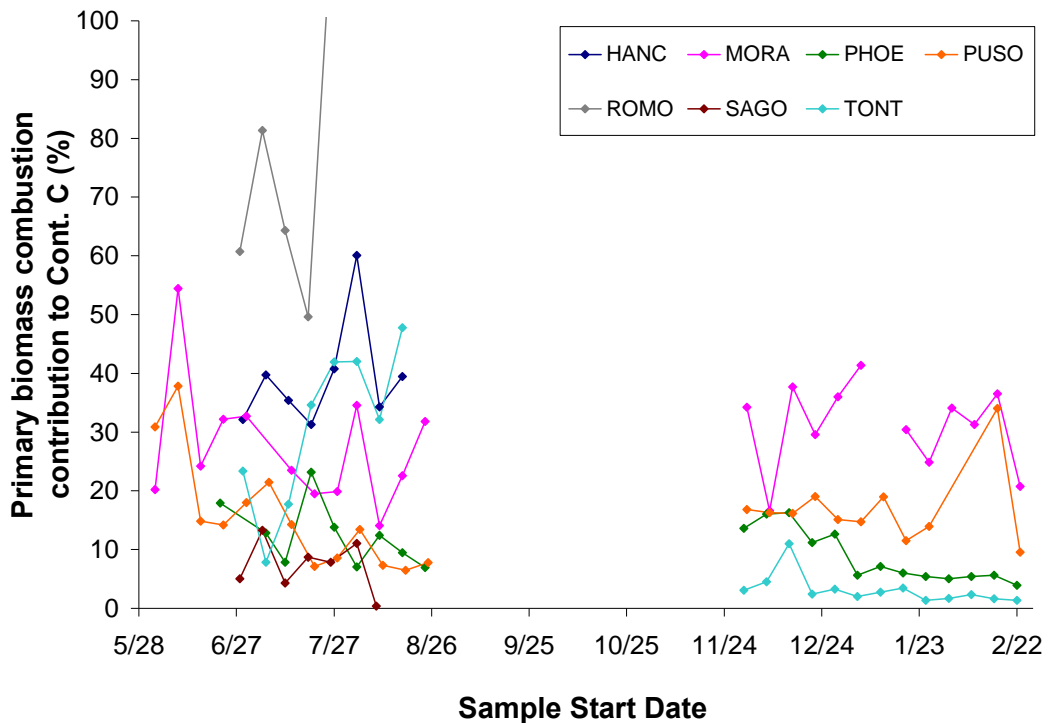


**Figure 3.18** *Percent primary biomass combustion contributions to TC (fossil + contemporary carbon) at each of the IMPROVE sites analyzed in this study.  Note that the vertical scale only goes to 100%, though there are two samples at the ROMO site which have contributions higher than this (8/3-160.5%, 8/9-117.0%).*

The temperature data, taken from the NOAA NCDC (National Oceanic and Atmospheric Administration National Climatic Data Center, http://www.ncdc.noaa.gov/oa/ncdc.html), can provide other useful information about

some of the assumptions made here. Though meteorological data were not available at the exact sites where PM$_{2.5}$ filter samples were taken, data were available from nearby stations and are assumed to be generally representative of the IMPROVE sites. As stated previously, colder weather at the WA sites should correlate with higher estimates of primary biomass burning carbon relative to TC. This statement can be verified on a sample-by-sample basis, looking at whether samples during colder periods showed higher amounts of primary biomass carbon.
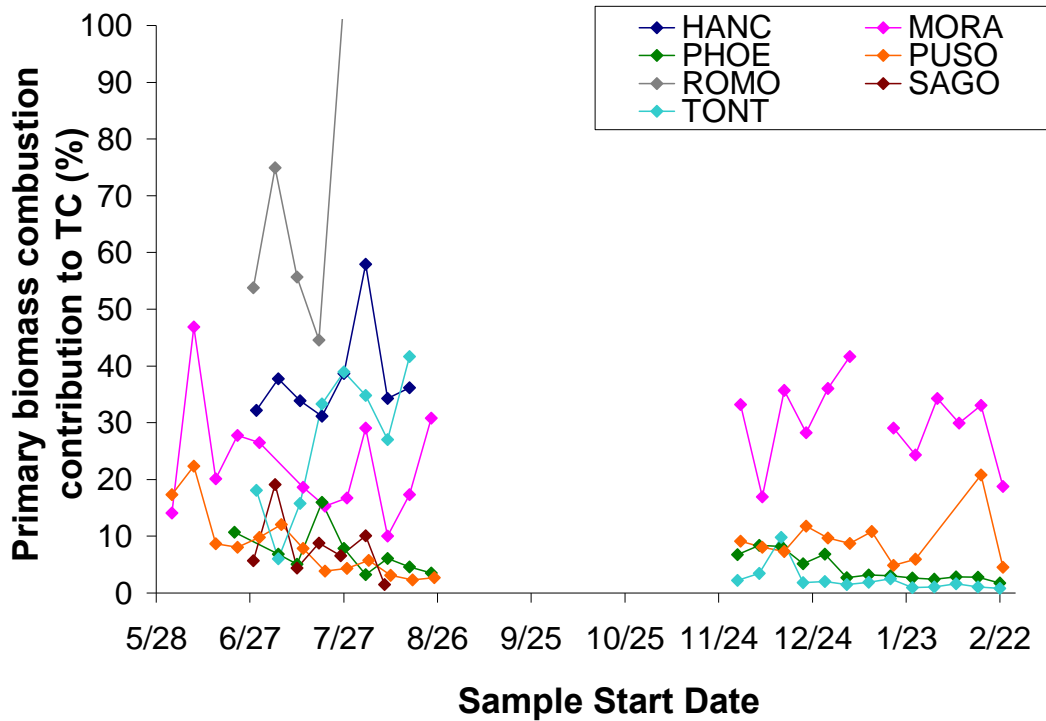


**Figure 3.19** *Percent primary biomass combustion contributions to contemporary carbon at each of the IMPROVE sites analyzed in this study. Note that the vertical scale only goes to 100%, though there are four samples at the ROMO site which have contributions higher than this; (7/27- 123.4%, 8/3- 290.5%, 8/9- 214.4%, 8/16- 166.9%).*

There are a few periods of interest at the four sites during the winter. At the MORA and PUSO sites, there was a decrease in temperature in about mid-December, lasting until temperatures rose again in about mid-January. The contribution of primary biomass combustion carbon to TC seems to mirror this trend well. Temperatures

85

decreased again in mid-February, reaching the lowest values of the season. The estimates of primary biomass combustion carbon also increased dramatically at PUSO and remained high at MORA during this time. There were two major "dips" in temperature at the PHOE and TONT sites in Arizona, one in mid-December and the other in mid-January. The primary biomass combustion estimates show a sharp increase during mid-December and a less drastic increase in mid-January at the TONT site. Data at the PHOE site also show increases in primary biomass combustion influence during these periods, though not as drastic as those seen at TONT. Overall, it appears that there is weak relationship between lower temperatures and higher contributions of primary biomass combustion to contemporary carbon (Figure 3.21). Though this relationship is not strong at any of the sites, it seems to describe the data more accurately at the PUSO site. This observation makes sense, as this site is in the north and in a more densely populated area (as opposed to MORA). Partitioning of levoglucosan to the gas phase, mentioned previously, could also affect the relationship seen between temperature and contributions of primary biomass combustion to contemporary carbon. Changes in temperature affect the vapor pressure, which in turn determines whether levoglucosan would be in the gas or particle phase. This partitioning could result in underestimates of primary biomass combustion carbon depending on the ambient temperature. Although levoglucosan is traditionally thought to be non-volatile, this is an area where further investigation is needed.

Another assumption that was made that can be examined more closely is that in the summer biomass combustion is from wild and prescribed burns, while residential wood combustion contributes most of the primary biomass carbon during the winter.
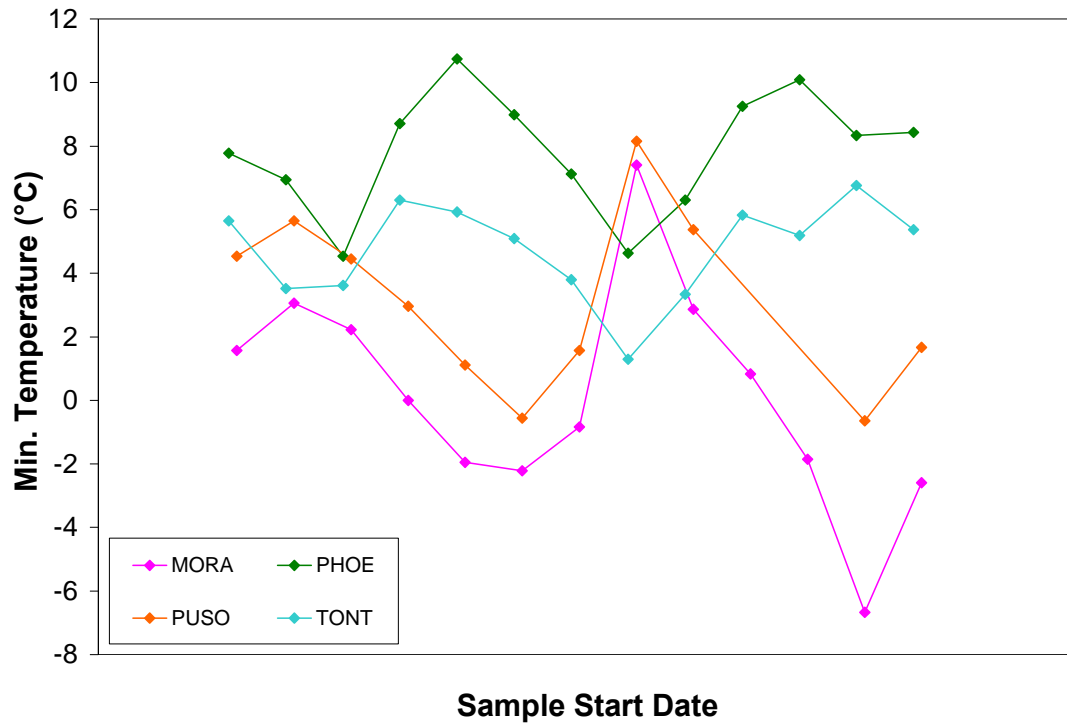
**Figure 3.20** *Daily minimum temperatures averaged over each sample period during the winter at the MORA, PHOE, PUSO, and TONT sites. Temperature data from the NOAA NCDC.*
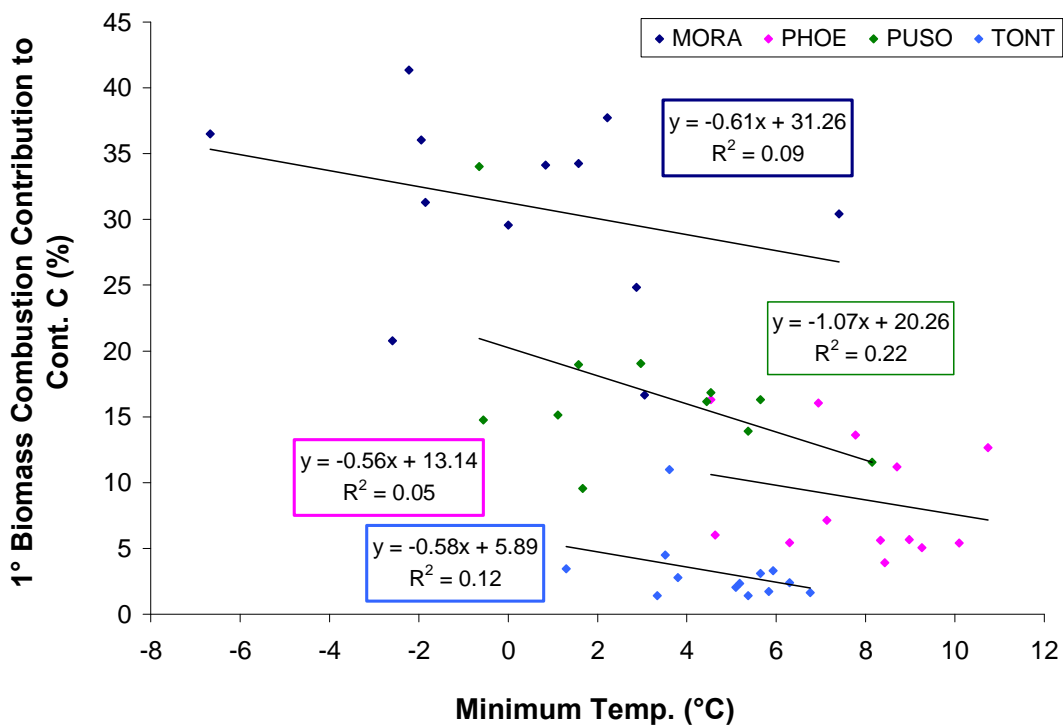


**Figure 3.21** *Daily minimum temperatures averaged over each sampling period compared to primary biomass combustion contributions to contemporary carbon.*
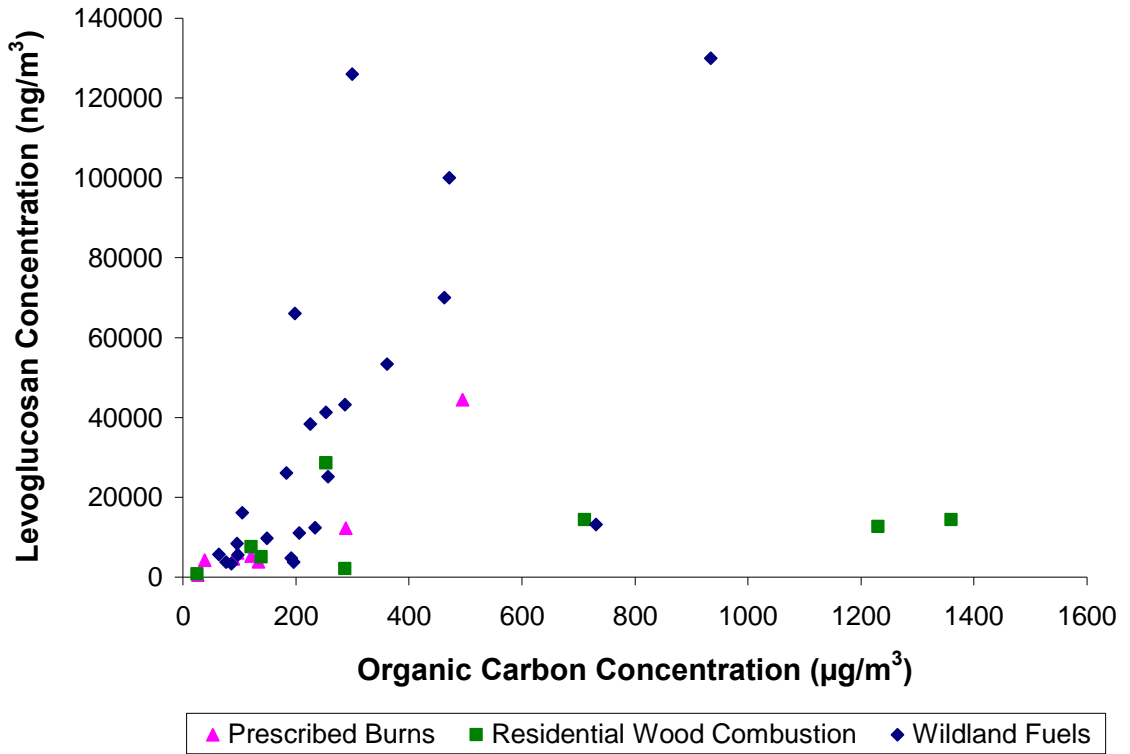
**Figure 3.22** *Organic carbon and levoglucosan concentrations for various types of biomass combustion. From Mazzoleni et al., 2007.*
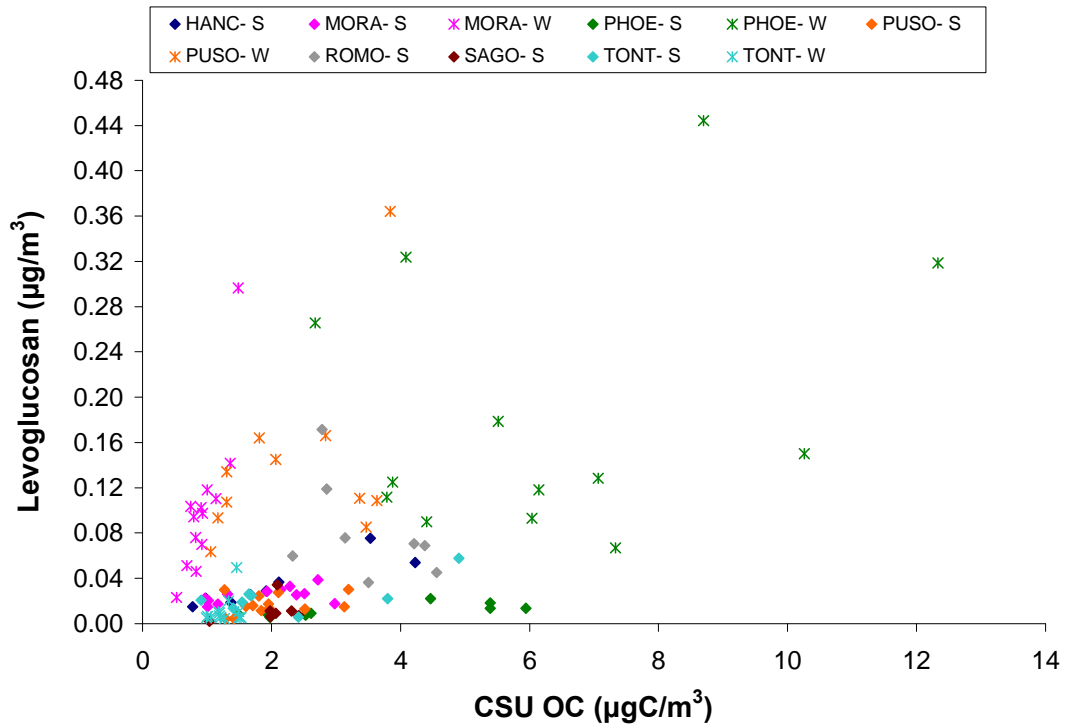


**Figure 3.23** *Comparison of OC and levoglucosan measured in the IMPROVE PM$_{2.5}$ samples split by site and season.*

Mazzoleni et al. (2007) found differences in levoglucosan/OC ratios when looking at various combustion types. Their results showed higher ratios of levoglucosan/OC during wild and prescribed burns than during residential wood combustion (Figure 3.22). It is interesting that we see the opposite trends in this study. Figure 3.23 shows levoglucosan versus OC for each of the samples from the IMPROVE sites; average and $R^2$ values for each of these relationships are listed in Table 3.9. Ratios of levoglucosan/OC are higher for the winter samples, when residential wood combustion was expected to occur. However, these higher levoglucosan/OC ratios are more likely due to changes in OC sources during the winter. The source profiles used in this study also disagree with values shown in Mazzoleni et al. Average levoglucosan/OC ratios (μg/μg) from Mazzoleni et al. were 0.126 for wild and prescribed fires and 0.031 for residential wood combustion. The opposite relationship was seen with the source profiles used in this study, where FLAME levoglucosan/OC ratios averaged 0.052 μg/μg and residential source profiles from the literature averaged 0.14 μg/μg (Figure 3.24).

**Table 3.8** *Primary biomass combustion contributions (%) to contemporary carbon for the IMPROVE sites analyzed in this study.*

| Site | Season | 1° Biomass Combustion C/Contemporary C (%) | |
|---|---|---|---|
| | | Average | Range |
| HANC | Summer | 39 | 31-60 |
| MORA | Summer | 28 | 14-54 |
| | Winter | 31 | 17-41 |
| PHOE | Summer | 12 | 7-23 |
| | Winter | 9 | 4-16 |
| PUSO | Summer | 16 | 7-38 |
| | Winter | 17 | 10-34 |
| ROMO | Summer | 131 | 50-291 |
| SAGO | Summer | 7 | 0-13 |
| TONT | Summer | 31 | 8-48 |
| | Winter | 3 | 1-11 |

Puxbaum et al. (2007) found that wild/prescribed fires and residential wood combustion also differ in their K/levoglucosan ratios (ng/ng). Comparing different published studies, they found that ratios <0.2 were measured in emissions from fire places and wood ovens, while "open fires" gave ratios of approximately 0.5. The levoglucosan and $K^+$ data for the IMPROVE sites also differ between the summer, when primarily "open fires" were expected to occur, and the winter, when biomass combustion was expected to be mostly from residential wood combustion (Figure 3.25). Similar to the results from Puxbaum et al., higher ratios of $K^+$/levoglucosan were seen in the summer ("open fires"). However, the ratios of $K^+$/levoglucosan were higher on average in the IMPROVE site data than those found by Puxbaum et al. Puxbaum et al. suggest that $K^+$/levoglucosan ratios higher than 0.5 are due to an additional source of potassium, such as coal combustion or biogenic sources (*e.g.*, vegetative emissions). These data support the suggestion that $K^+$/levoglucosan ratios can be one tool to help differentiate contributions from wild/prescribed fires and residential wood combustion.

**Table 3.9** *Slope and $R^2$ values for linear trendlines comparing OC (independent variable) and levoglucosan (dependent variable) in IMPROVE and FLAME data.*

| Site | Season | Average | $R^2$ |
|---|---|---|---|
| HANC | Summer | 0.017 | 0.80 |
| MORA | Summer | 0.015 | 0.26 |
| | Winter | 0.10 | 0.74 |
| PHOE | Summer | 0.0035 | 0.59 |
| | Winter | 0.034 | 0.077 |
| PUSO | Summer | 0.0090 | 0.096 |
| | Winter | 0.066 | 0.20 |
| ROMO | Summer | 0.026 | 0.21 |
| SAGO | Summer | 0.0056 | 0.10 |
| TONT | Summer | 0.012 | 0.46 |
| | Winter | 0.0086 | 0.13 |
| All Sites | - | 0.030 | 0.23 |
| FLAME | - | 0.052 | 0.82 |
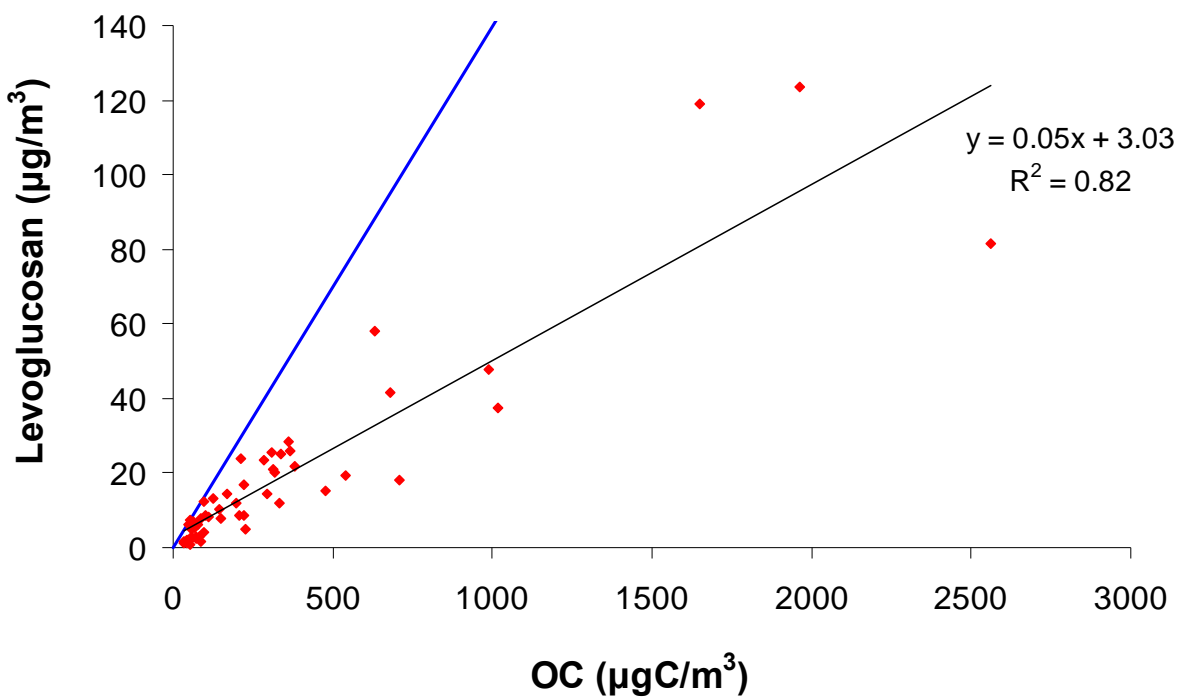
**Figure 3.24** *Comparison of OC and levoglucosan measured in the FLAME PM$_{2.5}$ samples and the residential source profiles. The average ratio for the residential source profiles is represented by the blue line; the red points represent the FLAME samples.*
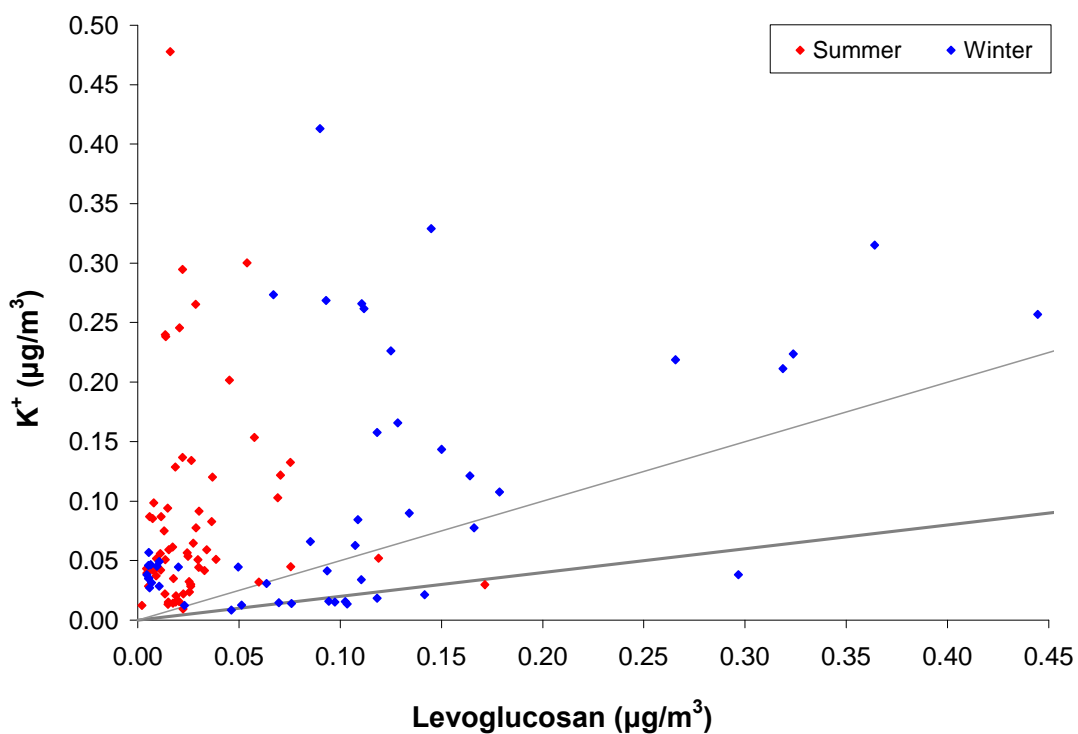


**Figure 3.25** *Levoglucosan and K$^+$ concentrations for PM$_{2.5}$ samples from IMPROVE sites. The thick gray line represents a K$^+$/levoglucosan ratio of 0.2; the thin line represents a ratio of 0.5.*

*3.4.8.2 Differences in Population Density*

There were also differences in carbon concentrations between rural and urban sites. Some of these differences were seen when comparing seasonal trends at the various sites. For example, during the summer, primary biomass combustion contributed a larger percent of TC (contemporary + fossil carbon) at rural sites (46.3% versus 14.3% at urban sites). In the summer, contemporary carbon at rural sites also made up more of the TC than at urban sites (97.4% at the rural sites, 52.5% at the urban sites). Conversely, fossil carbon made up more of the TC at the urban sites. Total carbon concentrations were also higher year-round at the urban sites. On average, TC at urban sites was 6.3 μgC/m$^3$, while TC at rural sites was 2.0 μgC/m$^3$.

**3.5 Further Analysis**

*3.5.1 Fuel Type Source Profiles*

Closer inspection of the data from the FLAME campaigns suggests fingerprint information about various types of fuels may be contained in sample chromatograms. Two peaks elute before levoglucosan in the analysis of each fuel sample (Figure 3.26). Work by A. Sullivan (CSU Department of Atmospheric Science) has found that the first compound, labeled "a" in Figure 3.26, is probably glycerol, a sugar alcohol. The second peak ("b") could either be inositol or a combination of the stereoisomers threitol and erythritol, all sugar alcohols. These three compounds all elute at approximately the same time, which causes some uncertainty in determining which is in a sample. Molecular structures of these four sugar alcohols are shown below in Figure 3.27.
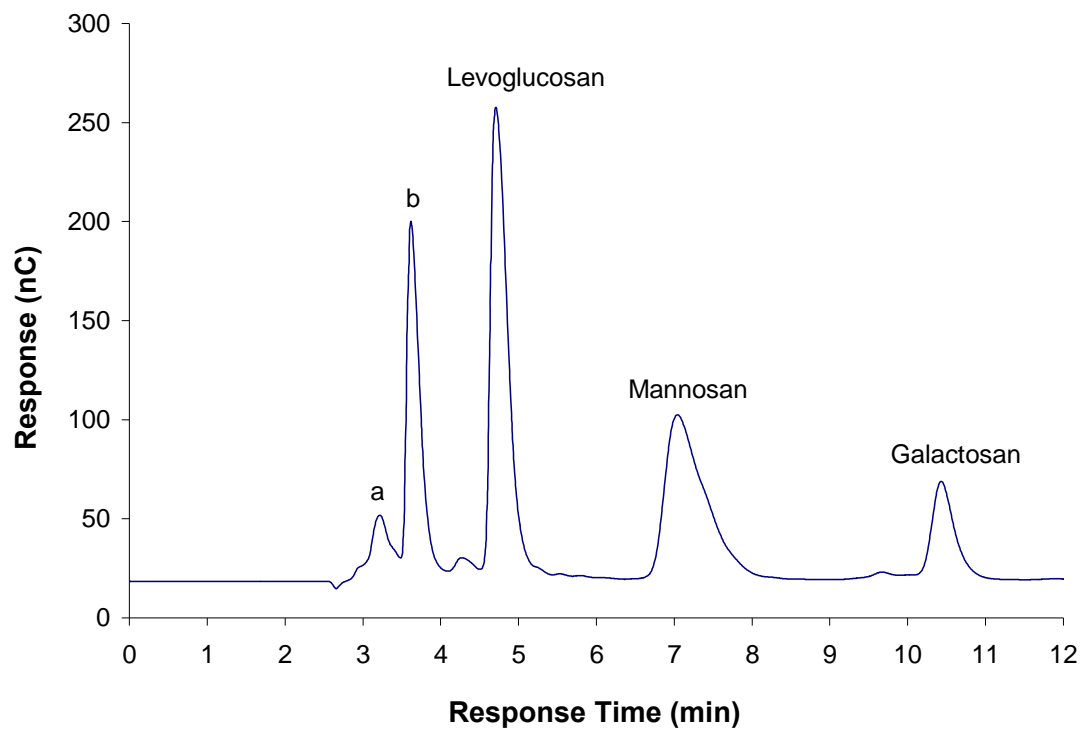
**Figure 3.26** *Chromatogram showing first 12 minutes of sugar separation with the HPAEC-PAD method.*
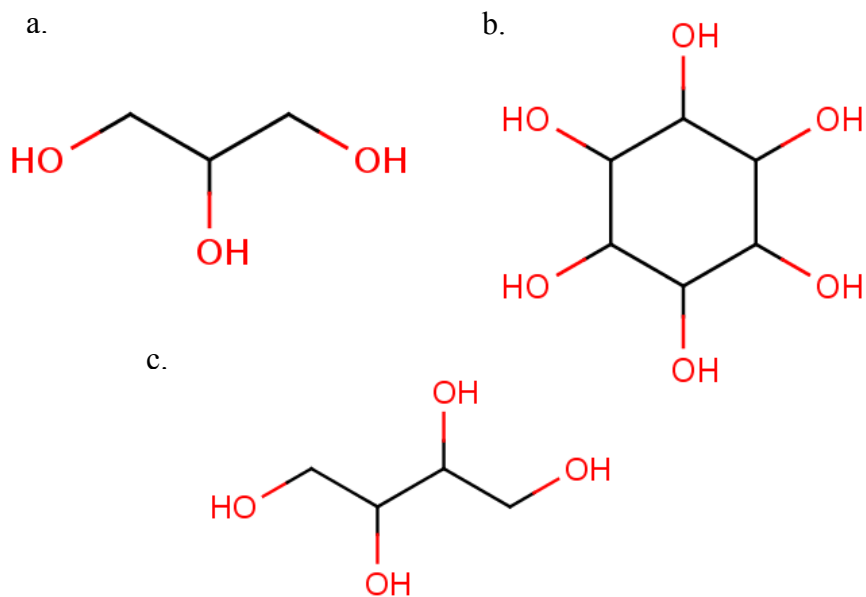


**Figure 3.27** *Molecular structures of (a) glycerol, (b) inositol, and (c) threitol/erythritol. Images from http://www.bmrb.wisc.edu/metabolomics/metabolomics_standards.html.*

These compounds show unique relationships based on the type of fuels burned, as shown in Figure 3.28 (Sullivan et al., 2008). Fuel components, such as grasses and branches, provide a unique ratio of the responses of glycerol to inositol or threitol/erythritol when burned. This provides a useful tool in determining what source profiles are appropriate for a specific sample. The IMPROVE site samples from this study can be examined in conjunction with these fuel data to estimate what types of fuels were included in any biomass combustion impacting that site during that specific time period (Figure 3.29). The fuel types that best match each sample composition can be compared with back trajectory data to determine if combustion of that fuel type is likely in that area. New source profiles can then be created based on the selected fuel types to update estimates of primary biomass combustion contributions to total carbon.
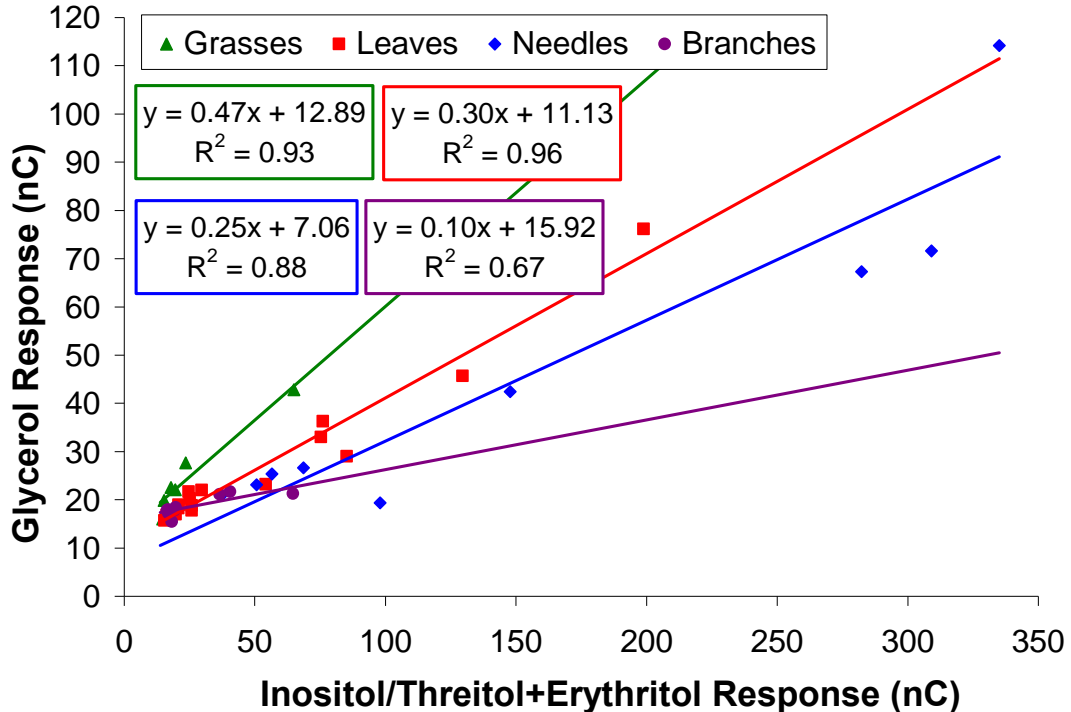


**Figure 3.28** *FLAME fuels plotted by their response for the "mystery" peaks, estimated to be glycerol and either inositol or a combination of the stereoisomers threitol and erythritol . The colored lines and points split the data into different fuel types. The gray line shows a 1:1 relationship.*
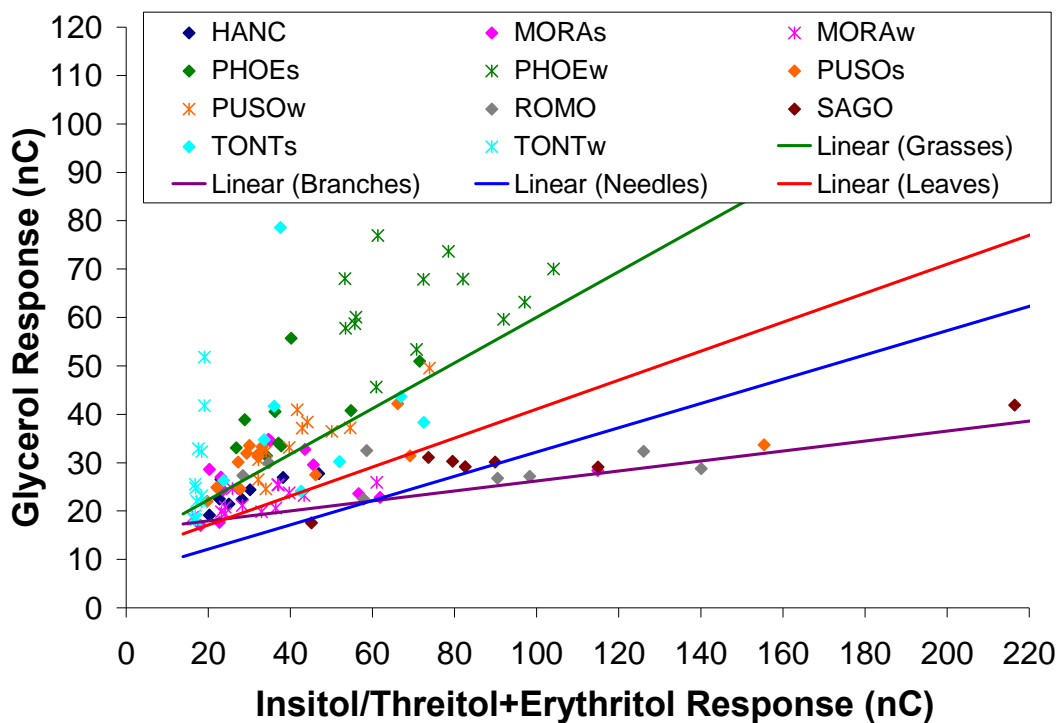
**Figure 3.29** *Instrument response for glycerol and either inositol or threitol and erythritol for fuel types and samples from the IMPROVE sites. Colored lines represent the linear trendlines for the different fuel types as determined in the previous figure.*

Figure 3.29 gives us much information about the possible fuel types combusted for each IMPROVE site sample, though only a few selected samples will be discussed in this section. For each of the following cases, estimates of primary biomass combustion contributions to contemporary carbon will be presented, calculated from revised source profiles based on fuel type (using the ratios of sugar alcohols, described previously). These estimates will be compared to the original estimates of primary biomass combustion contributions, based on our original regional source profiles. Only summer samples were considered in this reanalysis since the FLAME data are only relevant during this season.

As shown in Figure 3.29, ratios of the sugar alcohols for the PHOE site samples fall on and above the line for grasses. When compared to the back trajectory data, we see

that points on or near the line for grasses were for samples that had mostly southerly

winds.  The points that were above the line for grasses, however, correlated with samples

that had mostly northerly winds.  Southerly winds would be coming from places like

southern Arizona, California, and northwest Mexico with desert and scrub ecosystems.  It

would make sense for fires in these areas to include different grasses.  However, the

samples with northerly winds make less sense.  With winds coming from the north, we

would expect to see a better correlation with plant components, such as grasses.  It is

possible that there is another fuel component that is missing from this analysis, or that an

additional source of glycerol is causing the ratios to be higher.  Since the data for grasses

fit the IMPROVE site data best, grasses-based source profiles were used for this site.

Plants included in each type of fuel-based source profile are listed in Table 3.10.  After

applying these fuel-based source profiles, we can compare them to results using region-

based source profiles (Figure 3.30).  In every sample in this re-analysis, using the fuel-

based source profiles lead to slightly lower primary biomass carbon contributions to

contemporary carbon (11.4% on average) than using region-based source profiles (12.4%

on average).

**Table 3.10** *Composition and average value of fuel-based source profiles. The average value for the source profile was taken as the average of each plant species average.*

| Source Profile | Plant Species | Avg. Value (g levo/g TC) |
|---|---|---|
| Grasses | Montana grass (dry and fresh), Phragmites | 0.020 |
| Branches | Manzanita branches, Chamise branches (dry and fresh), Ponderosa pine branches (dry and fresh) | 0.041 |
| Needles | Black Spruce needles (dry and fresh), Ponderosa Pine needles, White Spruce needles | 0.036 |
| Grasses + Leaves | Ceanothus leaves, Chamise leaves (dry and fresh), Juniper foliage, Kudzu leaves, Manzanita leaves, Rabbitbrush & Sage leaves, Sage leaves, Montana grass (dry and fresh), Phragmites | 0.015 |
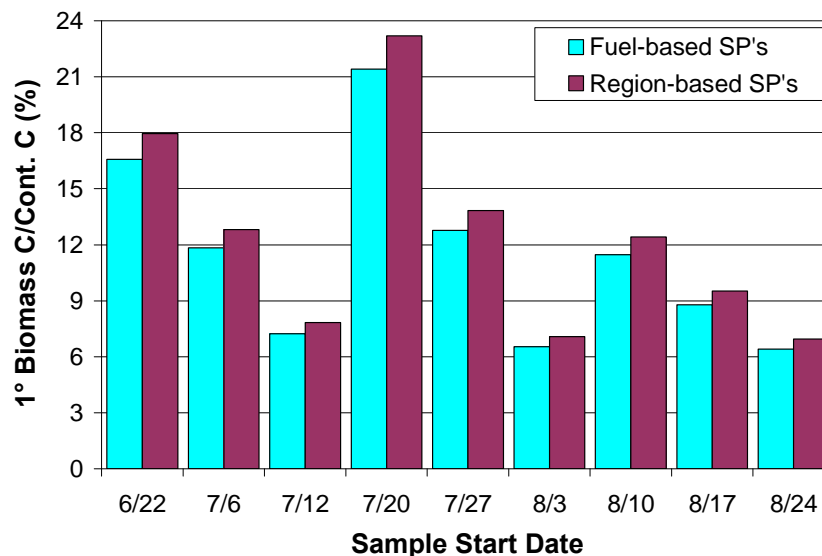
**Figure 3.30** *Contributions of primary biomass C as a percent of contemporary C during the summer of 2005 at the PHOE site based on regional- and fuel-based source profiles. No sample was taken on 6/29.*

Data at the SAGO site also show interesting trends with the sugar alcohol ratios in Figure 3.29. During the July 12 and August 3 samples, the ratios fall on the line for branches, while all other data points are more consistent with burning of needles. Unlike the PHOE samples, there are no changes in the back trajectories to suggest why this change in fuel components would be occurring. Differences in fire intensity throughout sampling at the site could lead to changes in chemical composition. A source profile representative of needles was applied to all of the samples except those beginning July 12 and August 3, to which a branches source profile was applied (see Table 3.10 for source profile compositions). Because of potential contemporary carbon contamination at this site, discussed previously, the concentrations of primary biomass combustion carbon are again compared to total carbon concentrations (Figure 3.31). Using fuel-based source profiles leads to a smaller contribution of primary biomass combustion to total carbon (4.0% on average) than using the source profiles based on region (8.0% on average).
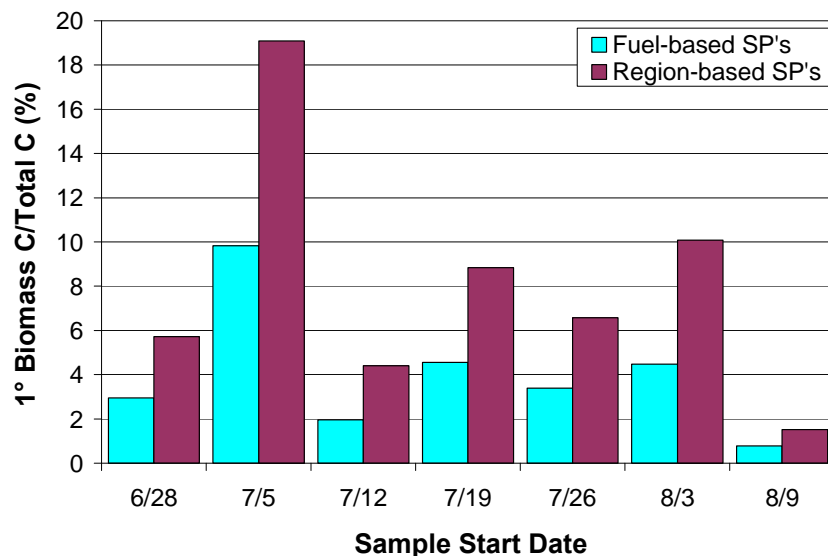
**Figure 3.31** *Contributions of primary biomass C as a percent of total C during the summer of 2005 at the SAGO site based on regional- and fuel-based source profiles.*

Data at the HANC (Grand Canyon) site were interesting because all points fell between the lines for grasses and leaves in Figure 3.29. Back trajectory data showed that winds were not constant in their direction during sampling. This suggests that fires impacting the site were similar in nature, despite differences in wind direction. The fuel-based source profiles for this site were created by averaging the source profiles for grasses and leaves. This site is also interesting because when comparing the two types of source profiles, we see that fuel-based source profiles lead to an increase in the estimated contribution of primary biomass combustion to contemporary carbon (Figure 3.32). Using fuel-based source profiles, primary biomass combustion was estimated to contribute approximately 47.3% of contemporary carbon, while region-based source profiles only estimated a contribution of about 39.1%. However, without having any data about the specific fires impacting the area, including their location and the amounts and types of fuels burned, it is difficult to determine which source profile produces the most accurate results.
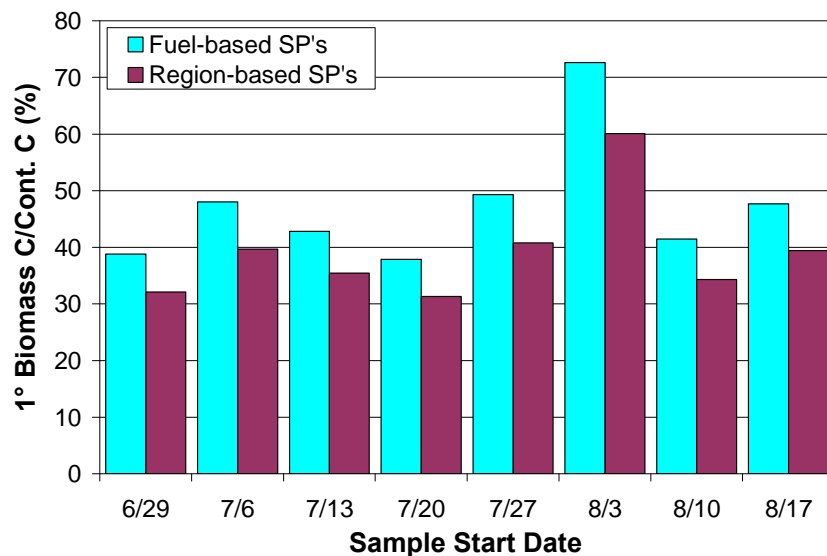
**Figure 3.32** *Contributions of primary biomass C as a percent of contemporary C during the summer of 2005 at the HANC site based on regional- and fuel-based source profiles.*

The final data examined in this re-analysis using sugar alcohol ratios were the samples collected at the ROMO site during the summer of 2005. Looking at Figure 3.29, we see that there is a split between points on the grasses and branches lines. The back trajectory data for these samples give some interesting information (Figure 3.33). The data show two samples with winds entirely from the west (samples beginning June 28 and July 27), while the other samples display a combination of winds from the west and the east. For the last three weeks of sampling, the presence of easterly winds correlate with burning of grasses (samples ending August 9, 15, and 23). The ROMO site is unique in its position relative to multiple ecosystems. To the west are the Rocky Mountains and many forested areas, while the land to the east comprises mostly plains and grassland areas. Therefore, an estimate of burning grasses with winds coming from the east is logical. Similarly, the samples with only westerly winds show sugar alcohol ratios suggesting burning of branches, which would make sense in a forest fire. Though the winds during the last three samples were primarily westerly, the data in Figure 3.29

99

suggest that the site was impacted by burning of grasses and leaves.  It is possible that during this sample there were no fires to the west and the transport of particles from the east, though not as large as that from the west, introduced the only smoke particles to the site.
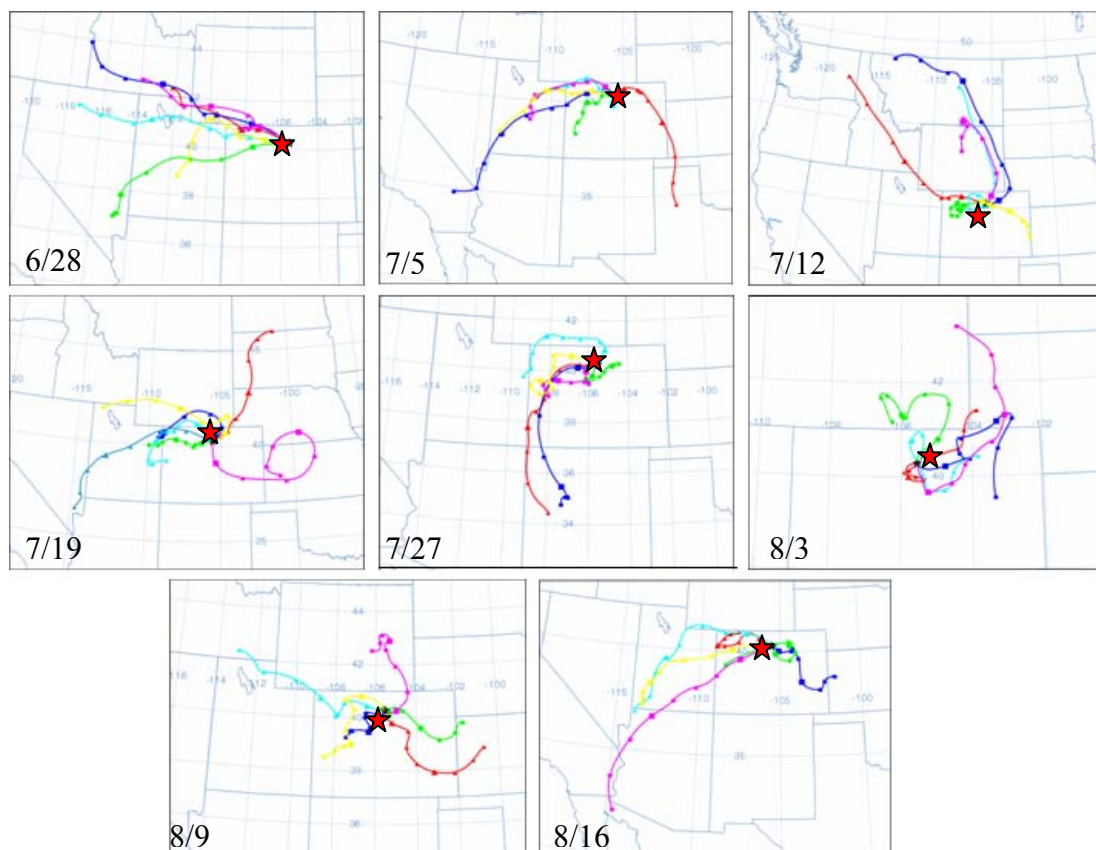


**Figure 3.33** *Back trajectories for the ROMO site (beginning the last day of sampling, each trajectory is 48-hours long and a new trajectory begins every 24 hours).  Dates listed are sample start dates. The site location is denoted by a star.*

Similar to the PHOE and SAGO data discussed above, applying the fuel-based source profiles (representative of burning of either grasses or branches, depending on the sample) to data from the ROMO site leads to a decrease in contributions of primary biomass combustion to contemporary carbon (Figure 3.34).  On average, using fuel-based source profiles estimated an 84.1% contribution of primary biomass combustion to

contemporary carbon, while with region-based source profiles this estimate was 131.4% on average. Using the fuel-based source profiles appears to have produced more reasonable data, since the average contributions are now below 100% of the contemporary carbon.
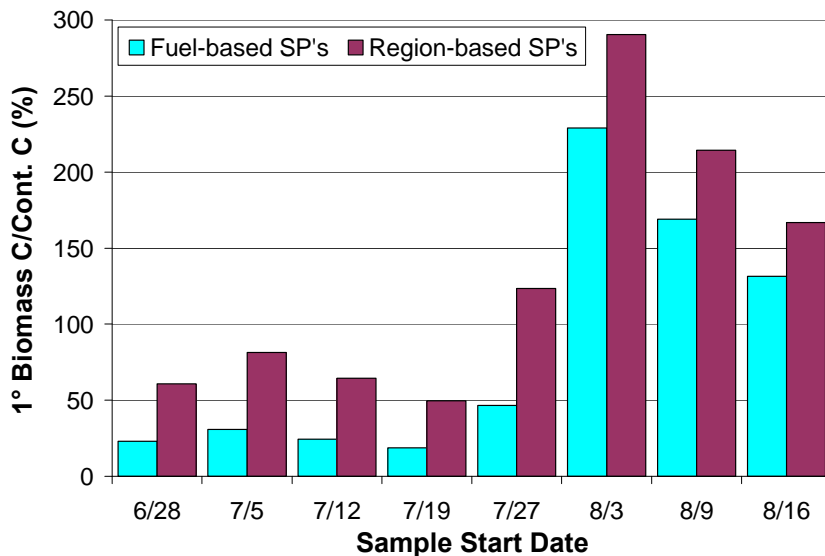


**Figure 3.34** *Contributions of primary biomass C as a percent of contemporary C during the summer of 2005 at the ROMO site based on regional- and fuel-based source profiles.*

*3.5.2 Ratios of Other Species*

Potassium ($K^+$) has often been used in the past as a marker of biomass combustion (*e.g.*, Park et al., 2007; Gao et al., 2003). As mentioned previously, some studies have used relationships between $K^+$ and levoglucosan to differentiate between biomass combustion types. Other researchers have used ratios of $K^+$/OC to apportion particulate matter from different sources, including biomass combustion. Duan et al. (2004) measured $K^+$/OC ratios ranging approximately 0.02-0.14 μg/μg in China to be representative of biomass burning. Similar ratios were measured for agricultural burning, approximately 0.04-0.13 μg/μg (Andreae and Merlet, 2001). Biomass burning in the

101

savanna ecosystem also produced similar ratios ranging from 0.08 to 0.10 μg/μg (Cachier et al., 1991; Cachier et al., 1995; Echalar et al., 1995; Maenhaut et al., 1996).

The $K^+$/OC ratios measured in the IMPROVE site samples appear to fall in the lower range of values seen in other studies, with an average value of 0.037 μg/μg. This is most likely due to the presence of other important sources of OC in addition to primary biomass burning. Some of the sites and seasons show a better relationship between these two variables than others, as seen in Figure 3.35 and in the $R^2$ values in Table 3.10. The data for the HANC, MORA (winter), PHOE (summer), ROMO, and SAGO sites showed strong relationships between $K^+$ and OC, with $R^2$ values ranging from 0.66-0.86. The $K^+$/OC ratios at these sites also agreed with data seen in other studies, averaging between 0.019-0.036 μg/μg. Ratios of $K^+$/OC were higher in the FLAME data (0.11 μg/μg), suggesting that wood smoke is the dominant source of $K^+$, though additional OC sources are present. This agreed well with results from previous studies with fairly good agreement (Figure 3.36).

However, there isn't a strong relationship between these two species when looking at all the IMPROVE data together, as is shown in Figure 3.35. A linear trendline applied to all of the IMPROVE site data has an $R^2$ value of only 0.32, meaning that it only represents about 32% of the variability in the data (Table 3.11). Lee et al. (2008) also found a non-linear relationship between OC and fine $K^+$. They suggested that this meant that OC did not depend entirely on primary emissions and that SOA played a significant part in biomass combustion. This agreed with their measurements of water soluble organic carbon (WSOC) and increases in biogenic SOA compounds such as isoprene and monoterpenes. The lack of a good linear relationship between $K^+$ and OC in

the IMPROVE data also supports the possibility of SOA production in the biomass smoke plumes, as well as additional sources of OC. This is likely to be a larger factor at the sites which did not show the strong $K^+$/OC relationship discussed above. Though a relationship between $K^+$/OC ratio and percent contributions of primary biomass combustion to TC might be expected, this is not seen in the data (Figure 3.37).
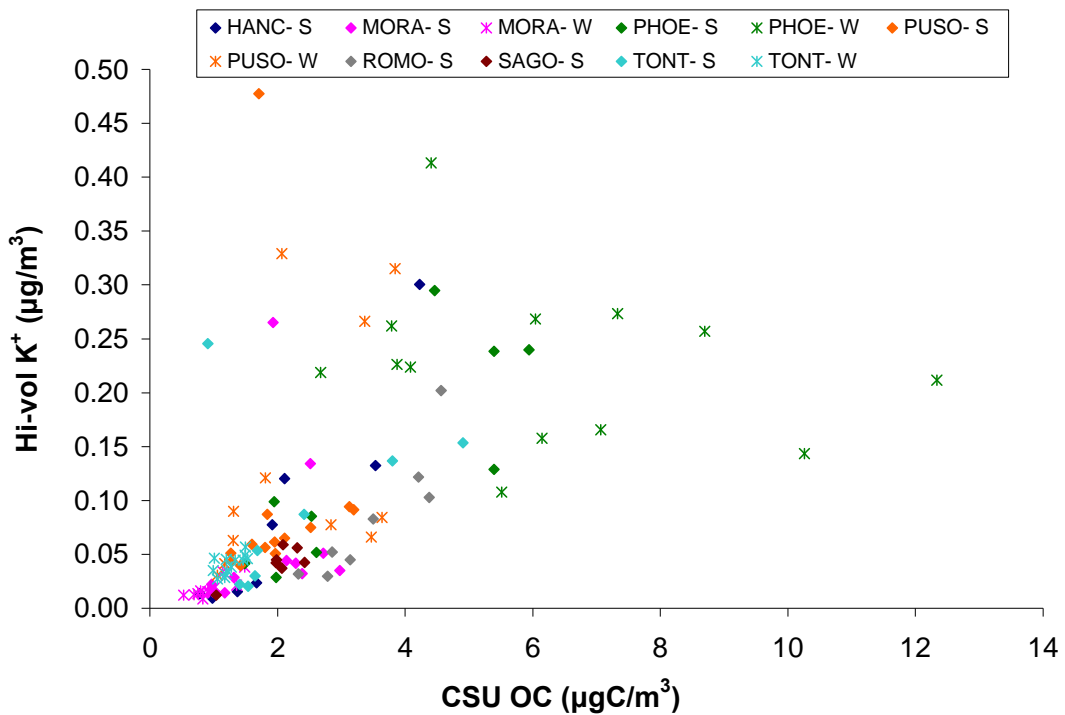


**Figure 3.35** *Comparison of OC and $K^+$ measured in the IMPROVE PM$_{2.5}$ samples.*

Ratios of EC/OC are also interesting because they tell us about the combustion efficiency of the fire. As discussed previously, increases in EC are due to more flaming combustion, while lower amounts of EC (and hence, higher OC) are due to more smoldering combustion. As seen with most of the FLAME burns, OC dominates TC in the majority of IMPROVE site samples (Figure 3.38). This suggests that any fires impacting the sites during the sampling periods were mostly smoldering. Higher OC

could also be due to other sources of OC, such as SOA formation.  However, there are

some sites which show higher EC/OC ratios (Table 3.12), suggesting the presence of

more flaming fires or other sources of high EC (*e.g.*, diesel truck emissions).  It is

interesting that three of the four sampling periods that have higher EC/OC ratios also

show a stronger relationship between OC and EC, based on the $R^2$ value.  The samples

for PHOE (summer), PUSO (summer), and TONT (summer and winter) all show EC/OC

ratios greater than 0.1.  HANC, PHOE (summer), and TONT (summer) also show the

highest $R^2$ values, meaning that the trendlines explain 42-65% of the variability in the

data.  These sites also show a stronger relationship between EC and OC than in the

FLAME samples, which had an $R^2$ value of only 0.11 (Figure 3.39).  The higher $R^2$

values at these sites might not necessarily be due to biomass burning contributions;

however, changes in OC and EC could be due to other sources, particularly urban

emissions.

**Table 3.11** *Average and $R^2$ values (for linear trendlines) comparing $K^+$ (dependent variable) and OC (independent variable) in IMPROVE and FLAME data.*

| Site | Season | Average | $R^2$ |
|---|---|---|---|
| HANC | Summer | 0.032 | 0.86 |
| MORA | Summer | 0.030 | 0.073 |
|  | Winter | 0.019 | 0.67 |
| PHOE | Summer | 0.036 | 0.66 |
|  | Winter | 0.044 | 0.065 |
| PUSO | Summer | 0.052 | 7E-6 |
|  | Winter | 0.058 | 0.20 |
| ROMO | Summer | 0.022 | 0.80 |
| SAGO | Summer | 0.021 | 0.69 |
| TONT | Summer | 0.057 | 0.064 |
|  | Winter | 0.032 | 0.40 |
| All Sites | - | 0.037 | 0.32 |
| FLAME | - | 0.11 | 0.55 |
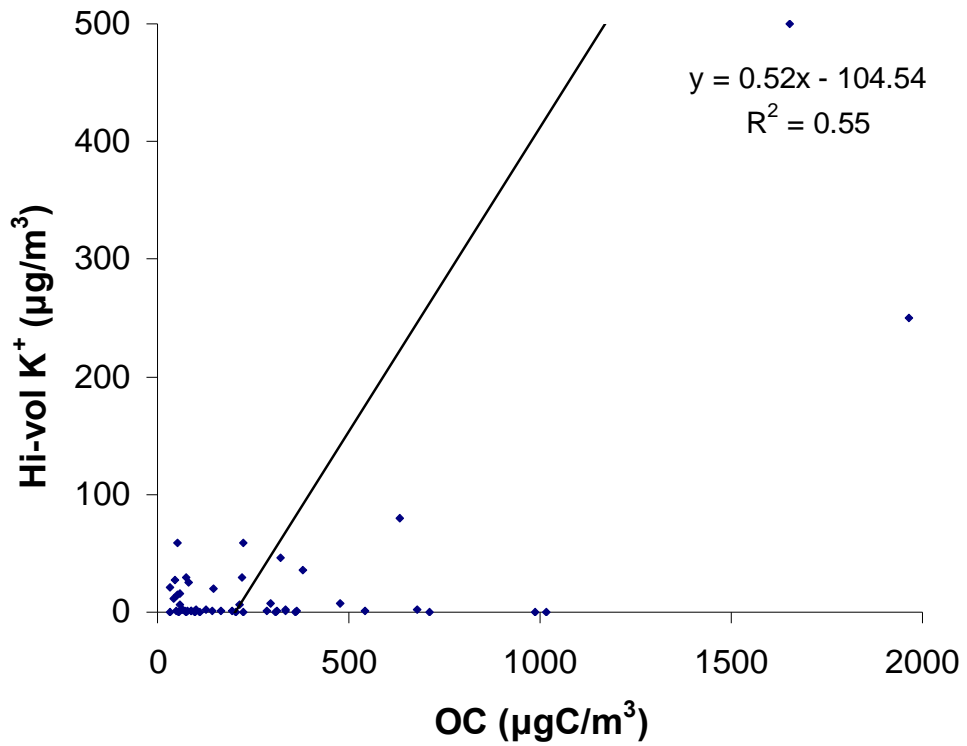
**Figure 3.36** *Comparison of OC and K$^+$ measured in the FLAME PM$_{2.5}$ samples.*
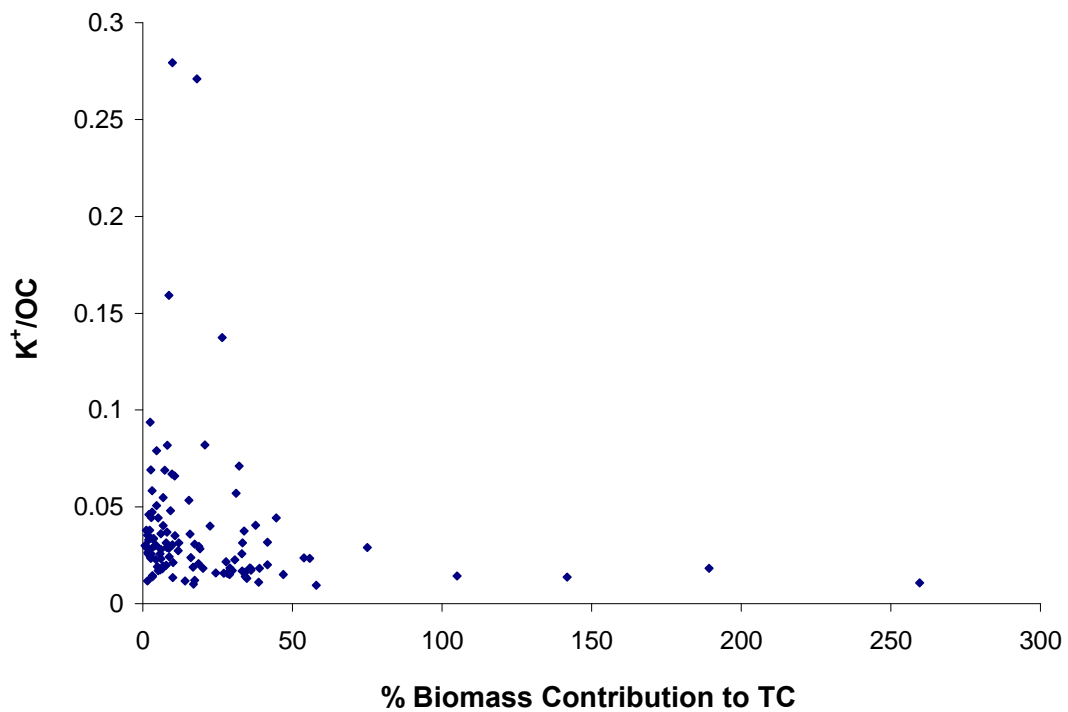


**Figure 3.37** *Percent Biomass contributions to TC, based on regional source profile groups, and K$^+$/OC ratios for PM$_{2.5}$ filter samples taken at seven IMPROVE sites in the western U.S.*
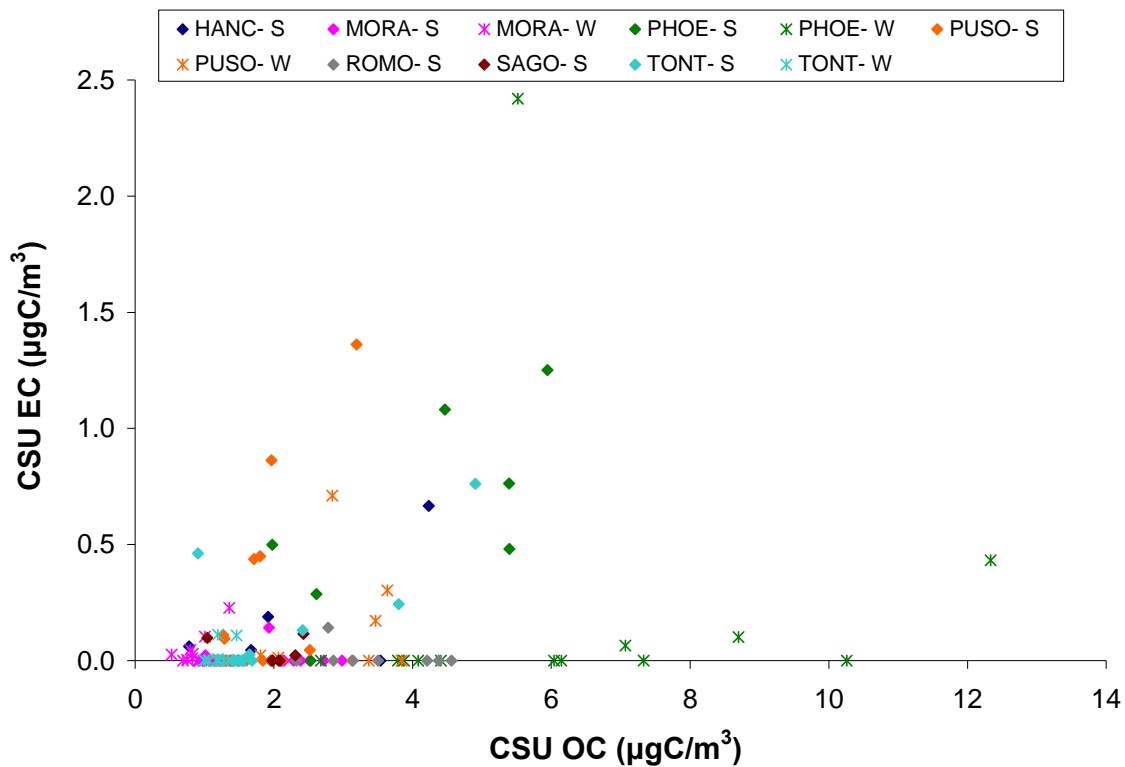
**Figure 3.38** *Comparison of OC and EC measured in the IMPROVE PM$_{2.5}$ samples.*

**Table 3.12** *Slope and $R^2$ values for linear trendlines comparing OC (independent variable) and EC (dependent variable) in IMPROVE and FLAME data.*

| Site | Season | Average | $R^2$ |
|---|---|---|---|
| HANC | Summer | 0.045 | 0.45 |
| MORA | Summer | 0.0079 | 0.001 |
| | Winter | 0.033 | 0.15 |
| PHOE | Summer | 0.12 | 0.65 |
| | Winter | 0.038 | 0.0017 |
| PUSO | Summer | 0.12 | 0.17 |
| | Winter | 0.037 | 0.14 |
| ROMO | Summer | 0.0063 | 0.11 |
| SAGO | Summer | 0.022 | 0.064 |
| TONT | Summer | 0.10 | 0.42 |
| | Winter | 0.14 | 0.022 |
| All Sites | - | 0.048 | 0.092 |
| FLAME | - | 0.15 | 0.11 |
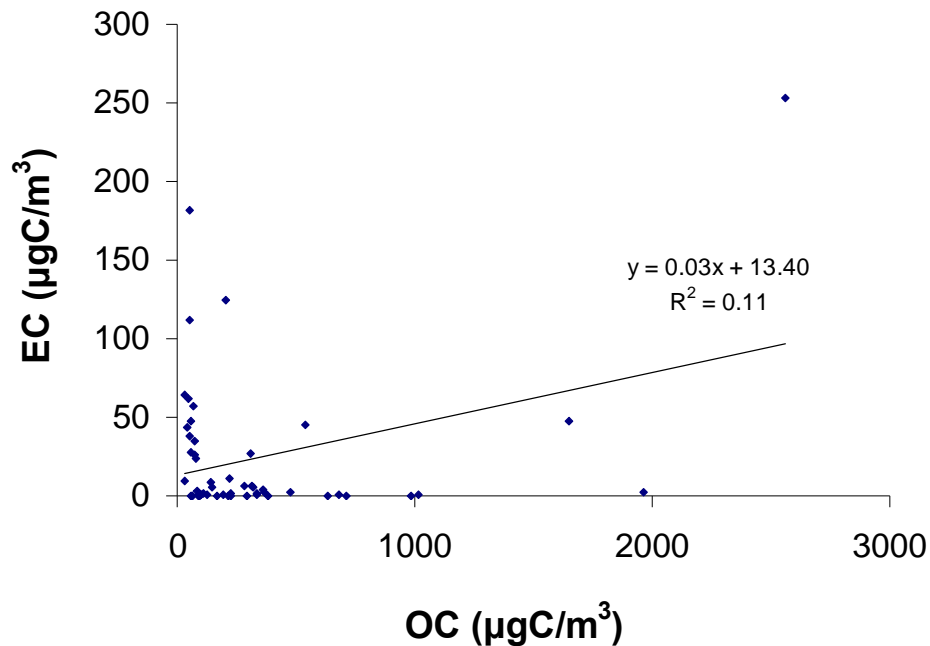
**Figure 3.39** *Comparison of OC and EC measured in the FLAME PM$_{2.5}$ samples.*

*3.5.3* Arabitol Interferences

Recent work with levoglucosan quantification by HPAEC-PAD in ambient samples in other laboratories has found instrumental signal interference by the sugar alcohol arabitol (Puxbaum et al., 2007), which originates from fungal spores (Lewis and Smith, 1967). Work by A. Sullivan at CSU has found that arabitol accounts for anywhere from 17-84% of levoglucosan measured using the HPAEC-PAD method in ambient filter samples from the Midwest U.S. The interference was most important during a summer measurement period, due to greater fungal activity in warmer seasons. This interference, if neglected, can lead to a large overestimation of primary biomass combustion contributions to TC. These results suggest that arabitol may significantly impact ambient samples and its concentration should be identified to avoid overestimation of primary biomass combustion estimates. The similar retention times of arabitol and levoglucosan

cause difficulty in separating their concentrations. The method used by A. Sullivan involves using a standard solution containing mannitol, a sugar alcohol variant of the anhydrous sugar mannosan. A modified instrumental method (different column and elution protocol) allows for the separation of these two compounds using HPAEC-PAD. The concentration of mannitol (in $\mu g/m^3$) is consistently found to be 1.5 times greater than the concentration of arabitol (Bauer et al., 2008). Therefore, concentrations of arabitol can be calculated using the mannitol data and, based on an independent arabitol calibration, the co-eluting levoglucosan/arabitol peak can be corrected to remove the arabitol contribution to determine the true levoglucosan concentration.

Though time did not allow the calculation of arabitol concentrations in all of the IMPROVE site samples, a preliminary analysis was completed of the Phoenix summer samples. Arabitol was found in each of these samples; however, at the time of analysis, the instrument was experiencing lower sensitivity when measuring levoglucosan than is normally seen. The interference of arabitol, though present, cannot be currently quantified. Future analyses will determine the amount of interference by this compound in each of the IMPROVE site samples discussed in this study. Based on results from the Midwestern U.S. and from Europe, we expect the necessary correction to be largest in summer when fungal emissions are more important. We also expect the correction to be largest during periods when the influence of fires is small, since levoglucosan concentrations will be lower at these times.

Chapter 4 Summary and Conclusions

This study estimated the influence of primary biomass combustion on total fine

particle carbon concentrations at various sites in the western United States by using

source profiles representing both residential and wild/prescribed biomass burning.

Wild/prescribed burning source profiles were created using data from the FLAME

campaigns, conducted at the USDA/USFS Fire Science Lab in Missoula, Montana during

the summers of 2006 and 2007. Residential wood burning source profiles were collected

from multiple studies in the literature. Both types of source profiles were defined as the

ratio of levoglucosan (gC) to total carbon (gC) emitted during the burn. The source

profiles were applied to Hi-vol filter sample data from seven sites operated by the

IMPROVE network during Summer and Winter 2004-2006: two urban (Puget Sound,

WA and Phoenix, AZ) and five rural/remote (Grand Canyon, AZ; Mount Rainier, WA;

Rocky Mountain National Park, CO; San Gorgonio Wilderness, CA; and Tonto National

Monument, AZ). The concentrations of primary biomass combustion carbon were

compared to values of fossil and contemporary carbon determined at Lawrence

Livermore National Laboratory using carbon isotope analysis.

The rural sites had higher relative contributions of primary biomass combustion to

contemporary carbon than the urban sites, which showed greater relative contributions of

fossil carbon. Primary biomass combustion also contributed more to total carbon

concentrations at rural sites.  Increased vegetation and open land for burning most likely allowed for more fires in these rural areas.  Conversely, more industrial plants and mobile sources (*e.g.,* automobiles) led to greater amounts of fossil carbon at the urban sites.  The urban sites also had higher concentrations of total fine particle carbon, more than tripling TC from rural sites.

Contributions of primary biomass combustion to TC also differed between seasons and regions.  At the Arizona sites, the fraction of TC made up by primary biomass combustion was highest during the summer, while it was higher in the winter at the sites in Washington.  The increases in relative primary biomass combustion contributions at the more northern sites showed a weak correlation with decreases in temperature, suggesting that residential wood combustion was an important source at these sites.

A common finding for each of the sites examined was an unidentified source (or sources) of contemporary carbon.  Secondary organic aerosol formation associated with fire emissions likely contributes to a portion of this "extra" contemporary carbon.  Calculations of biomass carbon used in this study only used a primary chemical tracer, levoglucosan, and therefore did not include any carbon in the form of secondary organics produced during reactions in aging smoke plumes.  Additional likely sources of contemporary carbon include primary aerosol emissions from vegetation, secondary organic aerosol produced from atmospheric reaction of vegetative volatile organic compound emissions, and primary biological aerosol particles (including fungal spores and bacteria).  Finally, it is possible that a fraction of the levoglucosan emitted at a fire is

lost during transport of the smoke plume to the sampling site, causing the applied source profiles to underestimate primary smoke amounts at the monitoring locations.

An additional similarity of the IMPROVE site samples was the lack of strong correlation between biomass contributions to contemporary carbon and estimates of biomass smoke influence from satellite data. It is important to remember that the process of estimating fire influence is not quantitative and that satellite data only suggest the presence of a fire, not its size. Smoke plumes could be overlooked due to their small size or the presence of cloud cover. The local combustion of paper products, such as cardboard, could also be contributing to levoglucosan emissions but not be recognized as traditional smoke plumes in satellite data. These problems suggest the use of satellite smoke data as only a tool to help estimate fire presence, in addition to chemical analysis of samples.

HPAEC-PAD is a relatively simple, cost-effective analytical method for looking at smoke markers, such as levoglucosan, in ambient aerosol samples. However, there are many potential sources of error which need to be avoided during analysis. It is important to choose the right type of source profiles (*i.e.,* residential or wild fire) because of the significant differences between them. Choosing an inappropriate source profile can lead to large errors in estimating contributions of primary biomass combustion to ambient particulate matter. The results of this study have also shown that arabitol, a product of fungal spores, is present in the IMPROVE site samples and is causing an overestimation in concentrations of levoglucosan. This has led to currently unquantified errors in the estimates of primary biomass combustion carbon. This study has, however, brought to

light many of these sources of error, as well as suggested future work that can help

continue to advance the study of biomass burning emissions and behavior.

Chapter 5 Future Work

As this study has shown, there are still many unanswered questions about the contributions of biomass combustion to total carbon in the western United States.  Future studies should address these questions to gain a better understanding of how biomass burning affects the global environment.  This will help improve the accuracy of global climate models and be necessary in any mitigation attempts.

This study focused on chemical emissions from combustion of vegetation, including plants burned in forest fires and tree logs used in residential wood combustion.  However, burning of other objects occurring worldwide may also emit similar compounds.  In many less-industrialized countries, trash is burned to prevent the spread of diseases and save space.  Even in the U.S., incinerators are sometimes used to burn waste.  It is possible that when burning products that have a biomass background, such as paper which originally came from trees, we would see similar chemical species emitted as during the combustion of more "traditional" biomass fuels.  It would be interesting to determine source profiles for the burning of these products and estimate the contributions they make towards ambient particulate matter.

As suggested in Puxbaum et al. (2007) and confirmed with a set of the IMPROVE site samples, arabitol interferes with the signal for levoglucosan during analysis, causing an over-estimation of primary biomass combustion contributions.  Each of the IMPROVE site samples should be re-analyzed to determine the actual amount of levoglucosan present, and therefore, the true contribution of primary biomass combustion to total

113

carbon.  Development of a method which successfully separates these two compounds would lead to fewer problems with over-estimation in the future.

Sampling directly from a fire would also answer many questions brought up during this study.  By being able to know what types of fuels were burning and the intensity and extent of the fire, we would have a better understanding of what source profiles to use.  This type of experiment would also allow for higher time resolution of samples and the ability to sample at various points downwind of the fire source.  This would increase understanding of the transport and aging of a smoke plume.  Knowing this would improve estimates of smoke plume influence of ambient particulate matter many kilometers from a prescribed or wild fire.  These data could also be used to identify secondary biomass combustion markers.  Secondary markers could be used to determine the amount of contemporary carbon emitted by biomass combustion that could not be explained using levoglucosan.  This would also provide greater understanding of a potentially major source of organic aerosols to the environment, which could have large implications on global climate change.

## References

Andreae, M. O. and Merlet, P. (2001). Emission of trace gases and aerosols from biomass burning. *Global Biogeochemical Cycles* 15:955-966.

Bauer, H., Claeys, M., Vermeylen, R., Schueller, E., Weinke, G., Berger, A. and Puxbaum, H. (2008). Arabitol and mannitol as tracers for the quantification of airborne fungal spores. *Atmospheric Environment* 42:588-593.

Bench, G. and Herckes, P. (2004). Measurement of contemporary and fossil carbon contents of PM2.5 aerosols: Results from Turtleback Dome, Yosemite National Park. *Environmental Science & Technology* 38:2424-2427.

Bench, G., Fallon, S., Schichtel, B., Malm, W. and McDade, C. (2007). Relative contributions of fossil and contemporary carbon sources to PM 2.5 aerosols at nine Interagency Monitoring for Protection of Visual Environments (IMPROVE) network sites. *Journal of Geophysical Research-Atmospheres* 112:doi: 10.1029/2006JD007708.

Birch, M. E. and Cary, R. A. (1996). Elemental carbon-based method for monitoring occupational exposures to particulate diesel exhaust. *Aerosol Science and Technology* 25:221-241.

Cachier, H., Ducret, J., Brémond, M. P., Gaudichet, A., Lacaux, J. P., Yoboué, V. and Baudet, J. (1991). Characterization of biomass burning aerosols in a savannah region of the Ivory Coast, in *Global Biomass Burning*, J. Levine, ed., MIT Press, Cambridge, MA, 174-180.

Cachier, H., Liousse, C., Buat-Menard, P. and Gaudichet, A. (1995). Particulate content of savanna fire emissions. *Journal of Atmospheric Chemistry* 22:123-148.

Chow, J. C., Watson, J. G., Kuhns, H., Etyemezian, V., Lowenthal, D. H., Crow, D., Kohl, S. D., Engelbrecht, J. P. and Green, M. C. (2004). Source profiles for industrial, mobile, and area sources in the Big Bend Regional Aerosol Visibility and Observational study. *Chemosphere* 54:185-208.

Christian, T. J., Kleiss, B., Yokelson, R. J., Holzinger, R., Crutzen, P. J., Hao, W. M., Shirai, T. and Blake, D. R. (2004). Comprehensive laboratory measurements of biomass-burning emissions: 2. First intercomparison of open-path FTIR, PTR-MS, and GC-MS/FID/ECD. *Journal of Geophysical Research-Atmospheres* 109.

Crutzen, P. J. and Andreae, M. O. (1990). BIOMASS BURNING IN THE TROPICS - IMPACT ON ATMOSPHERIC CHEMISTRY AND BIOGEOCHEMICAL CYCLES. *Science* 250:1669-1678.

Dignon, J. and Logan, J. (1990). Biogenic emissions of isoprene: A global inventory. *EOS, Trans. AGU* 71.

Duan, F. K., Liu, X. D., Yu, T. and Cachier, H. (2004). Identification and estimate of biomass burning contribution to the urban aerosol organic carbon concentrations in Beijing. *Atmospheric Environment* 38:1275-1282.

Echalar, F., Gaudichet, A., Cachier, H. and Artaxo, P. (1995). Aerosol emissions by tropical forest and savanna biomass burning: characteristic trace elements and fluxes. *Geophysical Research Letters* 22:3034-3042.

Eller, P. M. and Cassinelli, M. E., eds. (1996). *NIOSH Manual of Analytical Methods, 4th Edition (1st Supplement)*. National Institute for Occupational Safety and Health, Cincinnati, OH.

Engling, G. (2006). Characterizing Biomass Combustion Emission Contributions to Ambient Aerosol Concentrations (Ph.D. Thesis), Department of Atmospheric Science, Colorado State University: Fort Collins, CO.

Engling, G., Carrico, C. M., Kreidenweis, S. M., Collett, J. L., Day, D. E., Malm, W. C., Lincoln, E., Hao, W. M., Iinuma, Y. and Herrmann, H. (2006a). Determination of levoglucosan in biomass combustion aerosol by high-performance anion-exchange chromatography with pulsed amperometric detection. *Atmospheric Environment* 40:S299-S311.

Engling, G., Herckes, P., Kreidenweis, S. M., Malm, W. C. and Collett, J. L. (2006b). Composition of the fine organic aerosol in Yosemite National Park during the 2002 Yosemite Aerosol Characterization Study. *Atmospheric Environment* 40:2959-2972.

Fine, P. M., Cass, G. R. and Simoneit, B. R. T. (2001). Chemical characterization of fine particle emissions from fireplace combustion of woods grown in the northeastern United States. *Environmental Science & Technology* 35:2665-2675.

Fine, P. M., Cass, G. R. and Simoneit, B. R. T. (2002). Chemical characterization of fine particle emissions from the fireplace combustion of woods grown in the southern United States. *Environmental Science & Technology* 36:1442-1451.

Fine, P. M., Cass, G. R. and Simoneit, B. R. T. (2004a). Chemical Characterization of Fine Particle Emissions from the Wood Stove Combustion of Prevalent United States Tree Species. *Environmental Engineering Science* 21:705-721.

Fine, P. M., Cass, G. R. and Simoneit, B. R. T. (2004b). Chemical characterization of fine particle emissions from the fireplace combustion of wood types grown in the Midwestern and Western United States. *Environmental Engineering Science* 21:387-409.

Finlayson-Pitts, B. J. and J.N. Pitts, J. (2000). *Chemistry of the Upper and Lower Atmosphere: Theory, Experiments, and Applications*. Academic Press, San Diego, CA.

Fraser, M. P. and Lakshmanan, K. (2000). Using levoglucosan as a molecular marker for the long-range transport of biomass combustion aerosols. *Environmental Science & Technology* 34:4560-4564.

Gao, S., Hegg, D. A., Hobbs, P. V., Kirchstetter, T. W., Magi, B. I. and Sadilek, M. (2003). Water-soluble organic components in aerosols associated with savanna fires in southern Africa: Identification, evolution, and distribution. *Journal of Geophysical Research-Atmospheres* 108:doi: 10.1029/2002JD002324.

Gelencsér, A. (2004). *Carbonaceous Aerosol*. Springer, Dordrecht, The Netherlands.

Gorin, C. A., Collett, J. L. and Herckes, P. (2006). Wood smoke contribution to winter aerosol in Fresno, CA. *Journal of the Air & Waste Management Association* 56:1584-1590.

Guenther, A., Hewitt, C. N., Erickson, D., Fall, R., Geron, C. D., Graedel, T., Harley, P. C., Klinger, L., Lerdau, M., McKay, W. A., Pierce, T., Scholes, B., Steinbrecher, R., Tallamraju, R., Taylor, J. and Zimmerman, P. (1995). A global model of natural volatile organic compound emissions. *Journal of Geophysical Research* 100:8873-8892.

Hays, M. D., Geron, C. D., Linna, K. J., Smith, N. D. and Schauer, J. J. (2002). Speciation of gas-phase and fine particle emissions from burning of foliar fuels. *Environmental Science & Technology* 36:2281-2295.

Hays, M. D., Fine, P. M., Geron, C. D., Kleeman, M. J. and Gullett, B. K. (2005). Open burning of agricultural biomass: Physical and chemical properties of particle-phase emissions. *Atmospheric Environment* 39:6747-6764.

Hedberg, E., Kristensson, A., Ohlsson, M., Johansson, C., Johansson, P. A., Swietlicki, E., Vesely, V., Wideqvist, U. and Westerholm, R. (2002). Chemical and physical characterization of emissions from birch wood combustion in a wood stove. *Atmospheric Environment* 36:4823-4837.

Herckes, P., Engling, G., Kreidenweis, S. M. and Collett, J. L. (2006). Particle size distributions of organic aerosol constituents during the 2002 Yosemite Aerosol Characterization Study. *Environmental Science & Technology* 40:4554-4562.

Hobbs, P. V., Reid, J. S., Herring, J. A., Nance, J. D., Weiss, R. E., Ross, J. L., Hegg, D. A., Ottmar, R. D. and Liousse, C. (1996). Particle and Trace-Gas Measurements in the Smoke from Prescribed Burns of Forest Products in the Pacific Northwest, in *Biomass Burning and Global Change, Vol. 2: Biomass Burning in South America, Southeast Asia, and Temperate and Boreal Ecosystems, and the Oil Fires of Kuwait*, J. S. Levine, ed., The MIT Press, Cambridge, MA, 697-715.

Iinuma, Y., Bruggemann, E., Gnauk, T., Muller, K., Andreae, M. O., Helas, G., Parmar, R. and Herrmann, H. (2007). Source characterization of biomass burning particles: The combustion of selected European conifers, African hardwood, savanna grass, and German and Indonesian peat. *Journal of Geophysical Research-Atmospheres* 112:doi: 10.1029/2006JD007120.

Interagency Monitoring of Protected Visual Environments (IMPROVE) (2004). Location Table, in IMPROVE Aerosol Data. <http://vista.cira.colostate.edu/DatawareHouse/IMPROVE/Data/AEROSOL/Help/IMPR OVELocTable.txt>.

Johansson, L. S., Tullin, C., Leckner, B. and Sjovall, P. (2003). Particle emissions from biomass combustion in small combustors. *Biomass & Bioenergy* 25:435-446.

Kaufman, Y. J. and Fraser, R. S. (1997). The effect of smoke particles on clouds and climate forcing. *Science* 277:1636-1639.

Kjallstrand, J. and Olsson, M. (2004). Chimney emissions from small-scale burning of pellets and fuelwood - examples referring to different combustion appliances. *Biomass & Bioenergy* 27:557-561.

Lacourse, W. R. and Johnson, D. C. (1993). OPTIMIZATION OF WAVE-FORMS FOR PULSED AMPEROMETRIC DETECTION OF CARBOHYDRATES BASED ON PULSED VOLTAMMETRY. *Analytical Chemistry* 65:50-55.

Lakshmanan, C. M., Gal-Or, B. and Hoelscher, H. E. (1969). PRODUCTION OF LEVOGLUCOSAN BY PYROLYSIS OF CARBOHYDRATES. *Industrial & Engineering Chemistry Product Research and Development* 8:261-&.

Lee, S., Baumann, K., Schauer, J. J., Sheesley, R. J., Naeher, L. P., Meinardi, S., Blake, D. R., Edgerton, E. S., Russell, A. G. and Clements, M. (2005). Gaseous and particulate emissions from prescribed burning in Georgia. *Environmental Science & Technology* 39:9049-9056.

Lee, S., Kim, H. K., Yan, B., Cobb, C. E., Hennigan, C., Nichols, S., Chamber, M., Edgerton, E. S., Jansen, J. J., Hu, Y. T., Zheng, M., Weber, R. J. and Russell, A. G. (2008). Diagnosis of aged prescribed burning plumes impacting an urban area. *Environmental Science & Technology* 42:1438-1444.

Lee, T. (2007). Characterizing Ionic Compounds of Aerosol in Rural Environments: Temporal Variability, Size Distributions, and the Form of Particle Nitrate, Ph.D. Thesis, Department of Atmospheric Science, Colorado State University: Fort Collins, CO.

Levin, I., Dromer, B., Schock-Fisher, H., Bruns, M., Munnich, M., Berdau, D., Vogel, J. C. and Munnich, K. O. (1985). 25 Years of Tropospheric C-14 Observations in Central-Europe. *Radiocarbon* 27:1-19.

Levin, I. and Kromer, B. (2004). The Tropospheric $^{14}CO_2$ level in mid latitudes of the northern hemisphere (1959-2003). *Radiocarbon* 14:1261-1272.

Lewis, D. H. and Smith, D. C. (1967). Sugar alcohols (polyols) in fungi and green plants. I. Distribution, physiology and metabolism. *New Phytology* 66:143-184.

Liousse, C., Devaux, C., Dulac, F. and Cachier, H. (1995). AGING OF SAVANNA BIOMASS BURNING AEROSOLS - CONSEQUENCES ON THEIR OPTICAL-PROPERTIES. *Journal of Atmospheric Chemistry* 22:1-17.

Liu, W., Wang, Y. H., Russell, A. and Edgerton, E. S. (2005). Atmospheric aerosol over two urban-rural pairs in the southeastern United States: Chemical composition and possible sources. *Atmospheric Environment* 39:4453-4470.

Locker, H. B. (1988). The Use of Levoglucosan to Assess the Environmental Impact of Residential Wood-Burning on Air Quality, Dartmouth College: Hanover, New Hampshire. 137 pp.

Maenhaut, W., Salma, I., Cafmeyer, J., Annegarn, H. J. and Andreae, M. O. (1996). Regional atmospheric aerosol composition and sources in the eastern Transvaal, South Africa and impact of biomass burning. *Journal of Geophysical Research* D19:23631-23650.

Malm, W. C., Schichtel, B. A., Pitchford, M. L., Ashbaugh, L. L. and Eldred, R. A. (2004). Spatial and monthly trends in speciated fine particle concentration in the United States. *Journal of Geophysical Research-Atmospheres* 109:doi: 10.1029/2003JD003739.

Mazzoleni, L. R., Zielinska, B. and Moosmuller, H. (2007). Emissions of levoglucosan, methoxy phenols, and organic acids from prescribed burns, laboratory combustion of wildland fuels, and residential wood combustion. *Environmental Science & Technology* 41:2115-2122.

McDonald, J. D., Zielinska, B., Fujita, E. M., Sagebiel, J. C., Chow, J. C. and Watson, J. G. (2000). Fine particle and gaseous emission rates from residential wood combustion. *Environmental Science & Technology* 34:2080-2091.

McMeeking, G. R., Sullivan, A., Holden, A., Carrico, C. M., Kreidenweis, S. M., J.L. Collett, J., Chow, J., Moosmüller, H., Baker, S., Wold, C. E., Hao, W. M., Malm, W. C. and Ashbaugh, L. (2008, submitted). Aerosol emissions from the laboratory combustion of several North American wildland plant species during the Fire Laboratory at Missoula Experiment (FLAME).

Muller, J. F. (1992). GEOGRAPHICAL-DISTRIBUTION AND SEASONAL-VARIATION OF SURFACE EMISSIONS AND DEPOSITION VELOCITIES OF ATMOSPHERIC TRACE GASES. *Journal of Geophysical Research-Atmospheres* 97:3787-3804.

Nizich, S. V., Pope, A. A. and Driver, L. M. (2000). National Air Pollutant Emission Trends, 1900-1998 (EPA Report 454/R-00-002), Office of Air Quality Planning and Standards, U.S. Environmental Protection Agency, Research Triangle Park, NC.

Oros, D. R. and Simoneit, B. R. T. (2001a). Identification and emission factors of molecular tracers in organic aerosols from biomass burning Part 2. Deciduous trees. *Applied Geochemistry* 16:1545-1565.

Oros, D. R. and Simoneit, B. R. T. (2001b). Identification and emission factors of molecular tracers in organic aerosols from biomass burning Part 1. Temperate climate conifers. *Applied Geochemistry* 16:1513-1544.

Park, R. J., Jacob, D. J. and Logan, J. A. (2007). Fire and biofuel contributions to annual mean aerosol mass concentrations in the United States. *Atmospheric Environment* 41:7389-7400.

Puxbaum, H., Caseiro, A., Sanchez-Ochoa, A., Kasper-Giebl, A., Claeys, M., Gelencser, A., Legrand, M., Preunkert, S. and Pio, C. (2007). Levoglucosan levels at background sites in Europe for assessing the impact of biomass combustion on the European aerosol background. *Journal of Geophysical Research-Atmospheres* 112:doi: 10.1029/2006JD008114.

Rasmussen, R. A. and Khalil, M. A. K. (1988). ISOPRENE OVER THE AMAZON BASIN. *Journal of Geophysical Research-Atmospheres* 93:1417-1421.

Rogge, W. F., Hildemann, L. M., Mazurek, M. A., Cass, G. R. and Simoneit, B. R. T. (1998). Sources of fine organic aerosol. 9. Pine, oak and synthetic log combustion in residential fireplaces. *Environmental Science & Technology* 32:13-22.

Ruellan, S., Cachier, H., Gaudichet, A., Masclet, P. and Lacaux, J. P. (1999). Airborne aerosols over central Africa during the experiment for regional sources and sinks of oxidants (EXPRESSO). *Journal of Geophysical Research-Atmospheres* 104:30673-30690.

Schauer, J. J., Kleeman, M. J., Cass, G. R. and Simoneit, B. R. T. (2001). Measurement of emissions from air pollution sources. 3. C-1-C-29 organic compounds from fireplace combustion of wood. *Environmental Science & Technology* 35:1716-1728.

Schichtel, B. A., Malm, W., Kreidenweis, S., J.L. Collett, J., Sullivan, A. and Holden, A. (2007). Contribution of Smoke to PM2.5 and Haze: Development of Smoke Source Profiles and Routine Source Apportionment Tools, in *Presentation to USFS Fire Science Lab*, Missoula, MT.

Schichtel, B. A., Malm, W. C., Bench, G., Fallon, S., McDade, C. E., Chow, J. C. and Watson, J. G. (2008). Fossil and contemporary fine particulate carbon fractions at 12 rural and urban sites in the United States. *Journal of Geophysical Research-Atmospheres* 113:doi: 10.1029/2006JD008114.

Seinfeld, J. H. and Pandis, S. N. (2006). *Atmospheric Chemistry and Physics: From Air Pollution to Climate Change*. John Wiley & Sons, Inc., Hoboken, NJ.

Shafizadeh, F. (1982). INTRODUCTION TO PYROLYSIS OF BIOMASS. *Journal of Analytical and Applied Pyrolysis* 3:283-305.

Shallcross, D. E. and Monks, P. S. (2000). New Directions: A role for isoprene in biosphere-climate-chemistry feedbacks. *Atmospheric Environment* 34:1659-1660.

Simoneit, B. R. T., Rogge, W. F., Mazurek, M. A., Standley, L. J., Hildemann, L. M. and Cass, G. R. (1993). LIGNIN PYROLYSIS PRODUCTS, LIGNANS, AND RESIN ACIDS AS SPECIFIC TRACERS OF PLANT CLASSES IN EMISSIONS FROM BIOMASS COMBUSTION. *Environmental Science & Technology* 27:2533-2541.

Simoneit, B. R. T., Schauer, J. J., Nolte, C. G., Oros, D. R., Elias, V. O., Fraser, M. P., Rogge, W. F. and Cass, G. R. (1999). Levoglucosan, a tracer for cellulose in biomass burning and atmospheric particles. *Atmospheric Environment* 33:173-182.

Stuiver, M. and Polach, H. A. (1977). Reporting of C-14 Data - Discussion. *Radiocarbon* 19:355-363.

Sullivan, A. P. (2008). Carbohydrate stability, Personal communication to A. S. Holden.

Sullivan, A. P., Holden, A. S., Patterson, L. A., Kreidenweis, S. M., Malm, W. C., Hao, W. M., Wold, C. E. and J.L. Collett, J. (2008). A Method for Smoke Marker Measurements and its Potential Application for Determining the Contribution of Biomass Burning from Wildfires and Prescribed Fires to Ambient PM$_{2.5}$ Organic Carbon. *Journal of Geophysical Research,* In press:doi: 10.1029/2008JD010216.

Taylor, J., Zimmerman, P. and Erickson, D. (1990). *A 3-D modelling study of the sources and sinks of atmospheric carbon monoxide, CRES Work. Pap. 1990/3*. Australian National University, Canberra.

Turner, D. P., Baglio, J. V., Wones, A. G., Pross, D., Vong, R., McVeety, B. D. and Phillips, D. L. (1991). CLIMATE CHANGE AND ISOPRENE EMISSIONS FROM VEGETATION. *Chemosphere* 23:37-56.

USDA Natural Resources Conservation Service (2008). PLANTS Database, in <http://plants.usda.gov/index.html>.

USGS Earth Surface Processes (2006). Tree Species Distribution Maps for North America, in <http://esp.cr.usgs.gov/data/atlas/little/>.

Wang, Q. Q., Shao, M., Liu, Y., William, K., Paul, G., Li, X. H., Liu, Y. A. and Lu, S. H. (2007). Impact of biomass burning on urban air quality estimated by organic tracers: Guangzhou and Beijing as cases. *Atmospheric Environment* 41:8380-8390.

Ward, T. J. and Smith, G. C. (2005). The 2000/2001 Missoula Valley PM2.5 chemical mass balance study, including the 2000 wildfire season - seasonal source apportionment. *Atmospheric Environment* 39:709-717.

Ward, T. J. (2007). The Missoula, Montana PM2.5 Source Apportionment Research Study, The University of Montana-Missoula Center for Environmental Health Services, Missoula, MT.

Whitby, K. T. and Cantrell, B. (1976). Fine Particles, in *International Conference on Environmental Sensing and Assessment*, Institute of Electrical and Electronic Engineers, Las Vegas, NV.

Yokelson, R. J., Karl, T., Artaxo, P., Blake, D. R., Christian, T. J., Griffith, D. W. T., Guenther, A. and Hao, W. M. (2007). The Tropical Forest and Fire Emissions Experiment: overview and airborne fire emission factor measurements. *Atmospheric Chemistry and Physics* 7:5175-5196.

Zheng, M., Cass, G. R., Schauer, J. J. and Edgerton, E. S. (2002). Source apportionment of PM2.5 in the southeastern United States using solvent-extractable organic compounds as tracers. *Environmental Science & Technology* 36:2361-2371.

Zimmerman, P. (1979). Testing of hydrocarbon emissions from vegetation, leaf litter and aquatic surfaces, and development of a method for compiling biogenic emission inventories. Rep. EPA-450-4-70-004, U.S. Environmental Protection Agency, Research Triangle Park, N.C.

## Appendix A. Sample Calculations and Formulae

**Hi-vol Filters**

*Carbohydrates*

$$\left(\frac{\mu g}{m^3}\right) = \frac{\mu g \times 5mL \times 1000\frac{\mu L}{mL} \times 400.5cm^2}{\left(\frac{L_{air}}{\min}\right) \times \min \times 1000\frac{cm^3}{L_{air}} \times \left(\frac{m}{100cm}\right)^3 \times 50\mu L \times 9.82cm^2}$$

The numerator contains the mass concentration given by chromatogram analysis, the extraction volume, a conversion factor, and the total area of the filter sampled, respectively. The denominator contains the flow rate, time sampled, two conversion factors, the injection volume, and the total area of the punches extracted, respectively.

*$K^+$*

$$\left(\frac{\mu g}{m^3}\right) = \frac{\frac{\mu eq}{L} \times 5mL \times \frac{L}{1000mL} \times 400.5cm^2 \times \frac{\mu mol}{1\mu eq} \times \frac{39.0983\mu g}{\mu mol}}{\frac{L_{air}}{\min} \times \min \times 1000\frac{cm^3}{L_{air}} \times \left(\frac{m}{100cm}\right)^3 \times 9.82cm^2}$$

The numerator contains the liquid extract concentration given by chromatogram analysis, the extract volume, a conversion factor, the total area of the filter sampled, the number of equivalents per mole of potassium, and the molecular weight of potassium, respectively. The denominator contains the flow rate, time sampled, two conversion factors, and the total area of the punches extracted, respectively.

**OC/EC Analysis**

$$\left(\frac{\mu g C}{m^3}\right) = \frac{\mu g C \times 400.5 cm^2}{2.27 cm^2 \, x \, \dfrac{L_{air}}{\min} \times \min \times 1000 \dfrac{cm^3}{L_{air}} \times \left(\dfrac{m}{100 cm}\right)^3}$$

The numerator of this equation contains the punch mass of OC or EC given by the Sunset Labs OC/EC analyzer, and the total area of the filter measured. The denominator contains the punch area, flow rate, time sampled, and two conversion factors, respectively.

**URG Cellulose and Nylon Filters**

$$\left(\frac{\mu g}{m^3}\right) = \frac{\dfrac{\mu eq}{L} \times 6 mL \times \dfrac{L}{1000 mL} \times \dfrac{\mu mol}{\mu eq} \times \dfrac{\mu g}{\mu mol}}{\dfrac{L_{air}}{\min} \times \min \times 1000 \dfrac{cm^3}{L_{air}} \times \left(\dfrac{m}{100 cm}\right)^3}$$

The numerator contains the liquid extract concentration given by chromatogram analysis, the extract volume, a conversion factor, the number of equivalents per mole, and the molecular weight of the species in question, respectively. The denominator contains the flow rate, time sampled, and two conversion factors, respectively.

**Limits of Detection**

The LOD were calculated using information from the blanks taken for that sampling method. LOD for URG filters (nylon and cellulose) extracts were calculated using field blanks from a previous study of ambient aerosol composition (Lee, 2007). The following equation was used to calculate the LOD for species on URG filters and for

OC/EC on hi-vol filters during the FLAME campaigns, as well as all species on hi-vol

filters from IMPROVE sampling.

$$LOD = x_b + \left( t \times s_b \times \sqrt{\frac{1 + N_b}{1 \times N_b}} \right)$$

The terms in the calculation are as follows (from left to right): average

concentration of the blanks, t-value (at 95% confidence level, two-tailed), standard

deviation of the blanks, and number of blanks.  Since the LOD calculation includes the

average blank concentration, samples were not blank corrected.  The calculation of LOD

for FLAME hi-vol filters (carbohydrates and $K^+$) uses the same equation except $x_b$ is not

added to the other terms because blank filters did not contain any $K^+$ or carbohydrates.

For these filters, LOD were calculated from the noise in the chromatogram for the DI

water blanks run with each set of samples.

## Appendix B.  Carbohydrate Stability Data

The legends for each figure are the same as in Figure B.1.
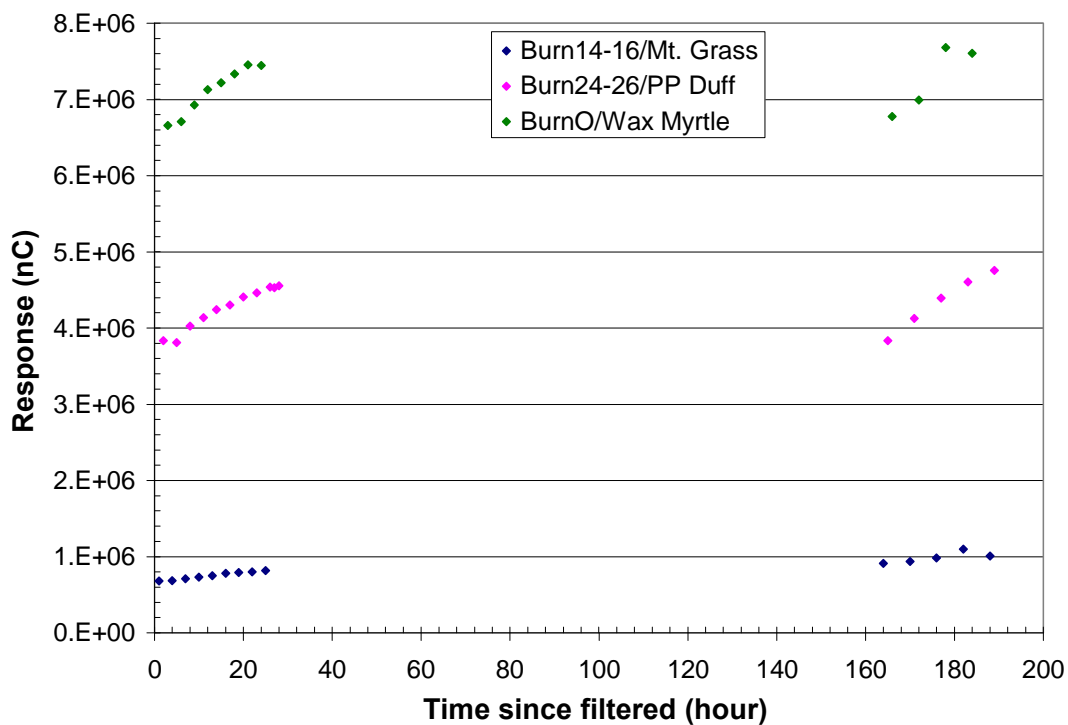


**Figure B.1** *Levoglucosan stability in selected FLAME PM$_{2.5}$ filter samples.  Time is since sample filtration. Data from A. Sullivan.*
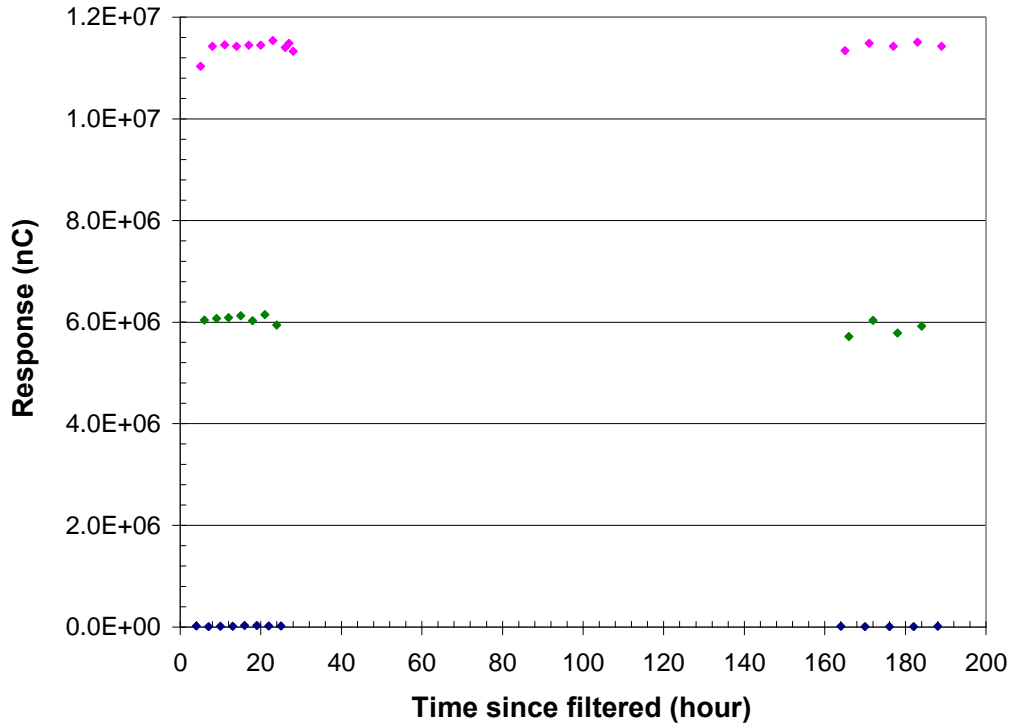
**Figure B.2** *Mannosan stability in selected FLAME PM$_{2.5}$ filter samples.  Time is since sample filtration. Data from A. Sullivan.*
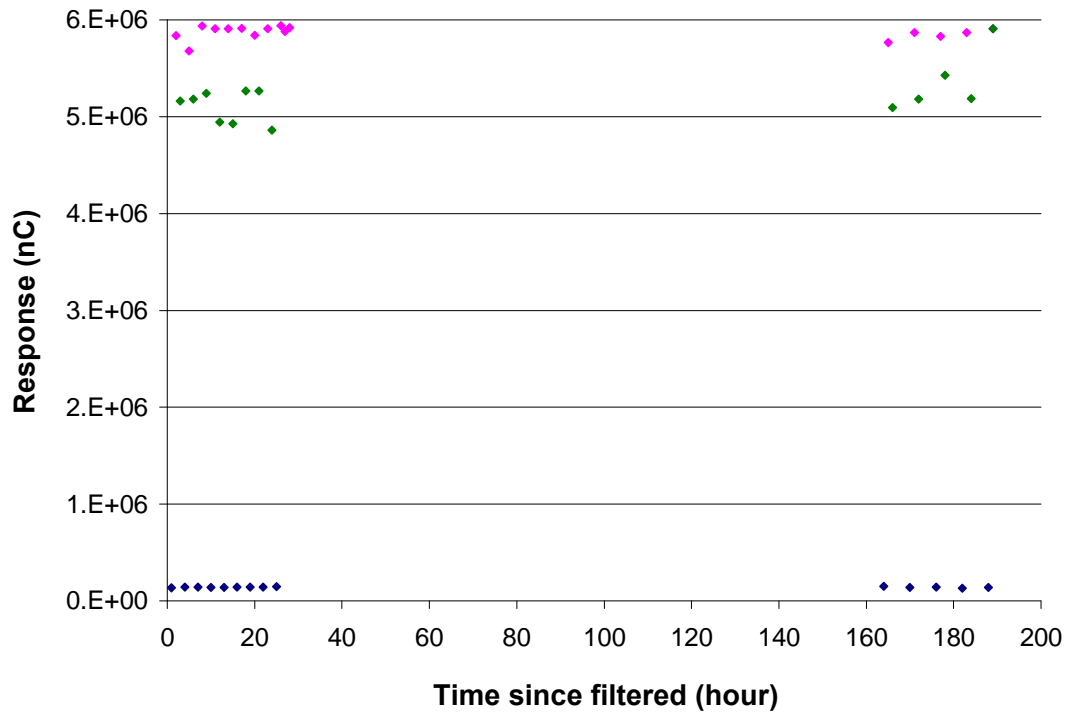


**Figure B.3** *Galactosan stability in selected FLAME PM$_{2.5}$ filter samples.  Time is since sample filtration. Data from A. Sullivan.*
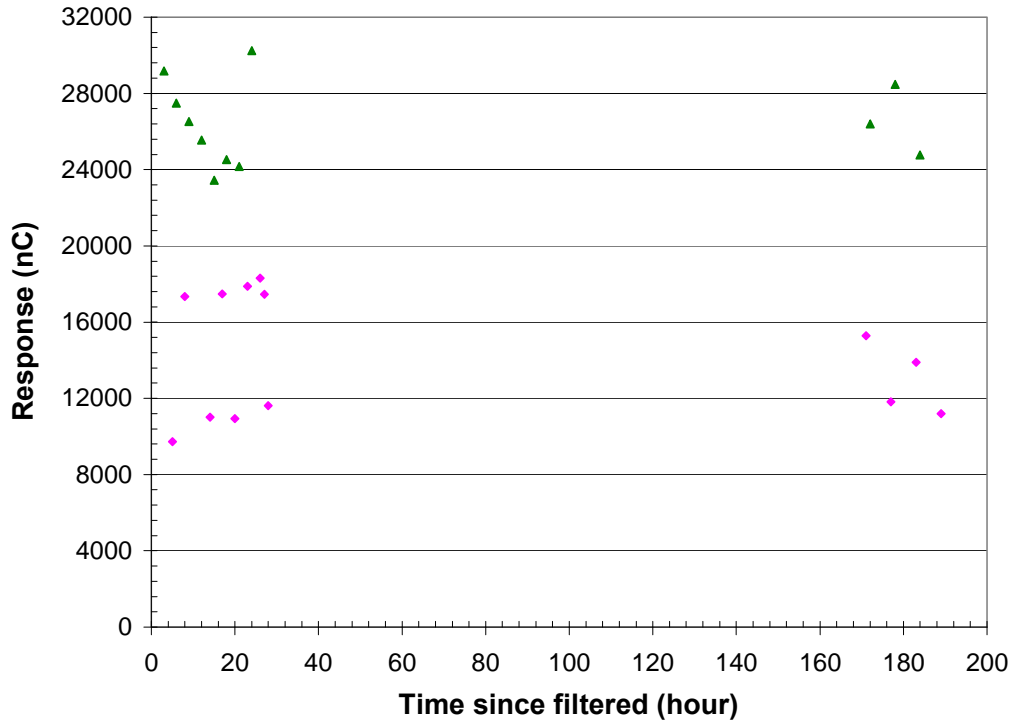
**Figure B.4** *Galactose stability in selected FLAME PM$_{2.5}$ filter samples. Time is since sample filtration. Data from A. Sullivan.*
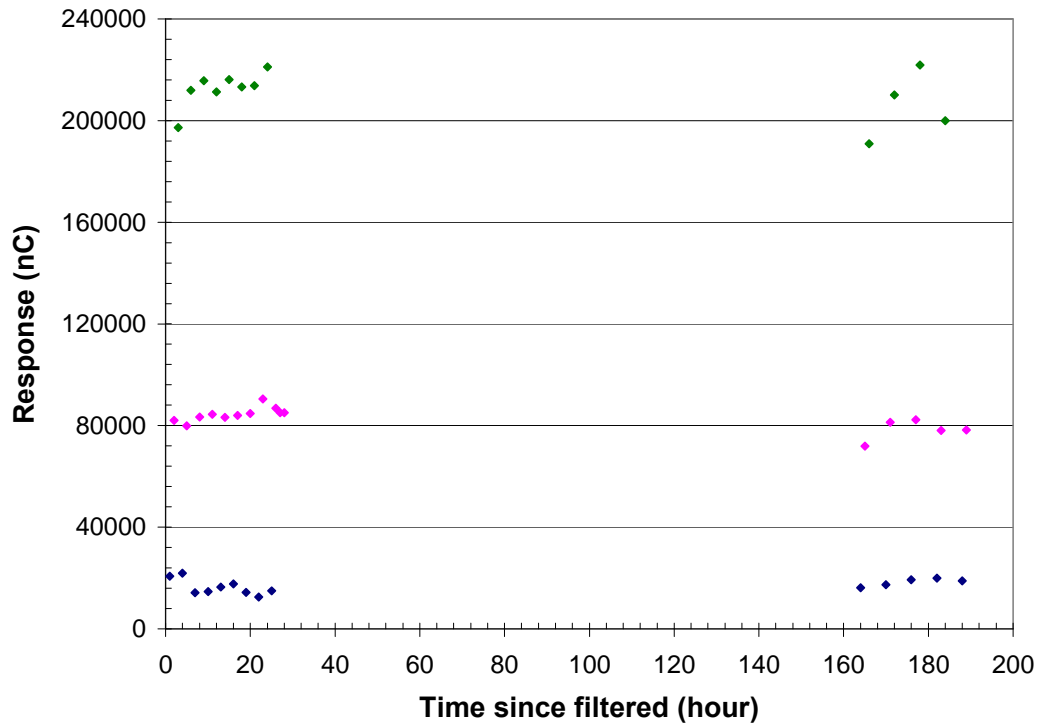


**Figure B.5** *Glucose stability in selected FLAME PM$_{2.5}$ filter samples. Time is since sample filtration. Data from A. Sullivan.*
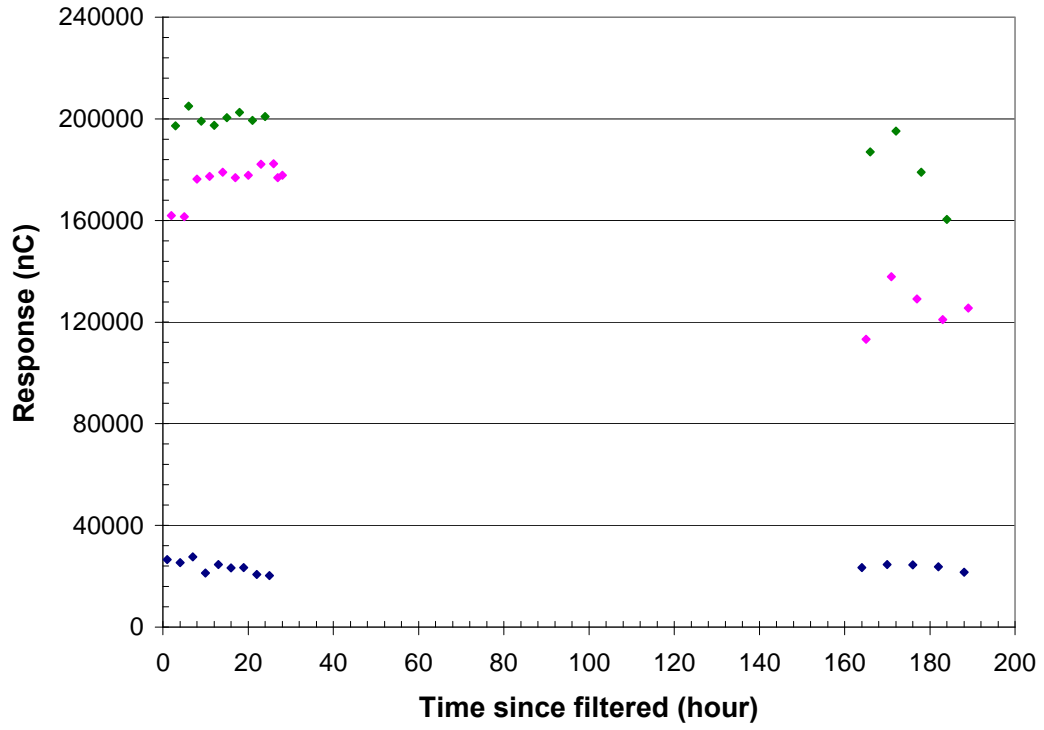
**Figure B.6** *Mannose stability in selected FLAME PM$_{2.5}$ filter samples. Time is since sample filtration. Data from A. Sullivan.*

# Appendix C.  Data from FLAME Campaigns

**Table C.1** *Species concentrations from hi-vol filters collected during the FLAME campaigns.  All concentrations are in units of µg/m³.  An entry of "0.00" does not necessarily mean that particular species was absent, merely that it was not measured in the sample.*

| Sample Name | Fuel Description | Levoglucosan | Mannosan | Galactosan | Galactose | Glucose | Mannose | OC | EC | K⁺ |
|---|---|---|---|---|---|---|---|---|---|---|
| Burn 2-4 | Cellulose filter | 31.22 | 0.63 | 0.14 | 0.00 | 0.24 | 0.03 | 57.96 | 0.00 | 0.51 |
| Burn 5-7 | Cellulose filter (K doped 1) | 35.15 | 4.36 | 0.15 | 0.00 | 0.65 | 0.03 | 117.68 | 0.00 | 12.82 |
| Burn 8-10 | Cellulose filter (K doped 2) | 26.10 | 3.23 | 0.46 | 0.00 | 0.35 | 0.00 | 226.75 | 0.00 | 21.82 |
| Burn 11-13 | Cellulose Powder | 23.15 | 0.35 | 0.09 | 0.00 | 0.17 | 0.00 | 53.31 | 0.00 | 0.26 |
| Burn 14-16 | Montana Grass (dry) | 8.73 | 0.62 | 0.74 | 0.00 | 0.00 | 0.00 | 219.77 | 10.89 | 29.34 |
| Burn 17-19 | Montana Grass (fresh) | 4.77 | 0.52 | 0.51 | 0.00 | 0.11 | 0.00 | 225.44 | 0.00 | 58.51 |
| Burn 21-23 | Rice Straw | 33.02 | 0.60 | 3.43 | 0.00 | 0.16 | 0.00 | 363.69 | 0.00 | 36.29 |
| Burn 24-26 | Ponderosa Pine (PP) Duff | 8.41 | 4.37 | 2.27 | 0.02 | 0.05 | 0.03 | 110.24 | 1.40 | 0.37 |
| Burn 27-29 | PP Needle Litter | 21.05 | 14.15 | 6.17 | 0.04 | 0.12 | 0.05 | 312.11 | 6.11 | 1.20 |
| Burn 30-32 | PP Needle Litter | 41.52 | 40.15 | 14.98 | 0.05 | 0.17 | 0.08 | 678.81 | 0.82 | 1.91 |
| Burn 33-35 | PP Needle Litter | 23.48 | 17.62 | 6.23 | 0.04 | 0.11 | 0.05 | 285.23 | 6.39 | 1.35 |
| Burn 36-38 | PP Needle Litter | 25.15 | 18.22 | 8.13 | 0.03 | 0.10 | 0.03 | 335.40 | 1.55 | 1.12 |
| Burn 39-41 | PP Needle Litter | 25.74 | 18.13 | 8.11 | 0.03 | 0.06 | 0.00 | 364.61 | 2.69 | 0.93 |
| Burn 43-45 | PP Branches (dead; sm) | 5.41 | 1.26 | 1.09 | 0.00 | 0.05 | 0.03 | 69.92 | 57.11 | 0.61 |
| Burn 46-48 | PP Branches (dead; lg) | 6.35 | 1.80 | 1.41 | 0.00 | 0.04 | 0.02 | 49.86 | 38.05 | 0.57 |
| Burn 49-51 | PP Branches (fresh; sm) | 8.73 | 2.10 | 1.44 | 0.02 | 0.06 | 0.00 | 100.60 | 0.76 | 1.66 |
| Burn 52-54 | PP Needles (fresh) | 11.80 | 11.12 | 5.04 | 0.03 | 0.18 | 0.05 | 334.00 | 0.97 | 2.04 |
| Burn 55-57 | PP Branches (fresh; lg) | 7.80 | 1.84 | 1.06 | 0.00 | 0.04 | 0.00 | 87.58 | 0.44 | 0.78 |
| Burn 58-60 | Lodgepole Pine (LP) Needle Litter | 13.40 | 12.32 | 6.03 | 0.02 | 0.08 | 0.03 | 160.83 | 9.75 | 0.45 |
| Burn 61-63 | LP Needles (fresh) | 12.70 | 8.97 | 4.88 | 0.05 | 0.26 | 0.06 | 240.20 | 1.14 | 5.53 |
| Burn 64-66 | LP Needles (dead; sm) | 9.74 | 2.68 | 1.34 | 0.00 | 0.06 | 0.04 | 52.39 | 54.60 | 0.70 |
| Burn 67-69 | LP Needle Duff | 9.87 | 5.86 | 2.25 | 0.02 | 0.06 | 0.03 | 73.55 | 0.00 | 0.31 |
| Burn 70 | Rice Straw | 12.02 | 0.85 | 1.00 | 0.00 | 0.13 | 0.11 | 182.01 | 10.04 | 25.26 |

| Sample Name | Fuel Description | Levoglucosan | Mannosan | Galactosan | Galactose | Glucose | Mannose | OC | EC | K⁺ |
|---|---|---|---|---|---|---|---|---|---|---|
| Burn 71 | Rice Straw | 25.69 | 0.76 | 1.77 | 0.00 | 0.17 | 0.13 | 290.97 | 0.00 | 21.09 |
| Burn 72 | Rice Straw | 25.05 | 0.81 | 1.84 | 0.00 | 0.16 | 0.14 | 321.74 | 0.00 | 38.58 |
| Burn 73-75 | Palmetto Leaf (dry) | 3.35 | 0.34 | 0.39 | 0.06 | 0.09 | 0.06 | 86.69 | 27.72 | 126.30 |
| Burn 76-78 | Chamise Foliage | 20.32 | 0.81 | 2.89 | 0.05 | 0.19 | 0.05 | 320.15 | 5.18 | 46.36 |
| Burn 79-81 | Chamise Branches | 6.81 | 0.97 | 0.61 | 0.03 | 0.06 | 0.02 | 64.90 | 0.00 | 1.67 |
| Burn 82-84 | Chamise Foliage (fresh) | 21.98 | 0.93 | 3.48 | 0.06 | 0.20 | 0.00 | 380.53 | 0.00 | 35.37 |
| Burn 85-87 | Chamise Branches (fresh) | 6.19 | 1.00 | 0.60 | 0.03 | 0.06 | 0.02 | 60.22 | 0.17 | 2.36 |
| Burn 88-90 | Manzanita Leaves (fresh) | 14.49 | 0.30 | 3.15 | 0.03 | 0.13 | 0.02 | 294.83 | 0.00 | 7.28 |
| Burn 91-93 | Manzanita Branches (fresh) | 24.03 | 3.72 | 4.25 | 0.06 | 0.16 | 0.04 | 213.46 | 0.00 | 6.21 |
| Burn 94-96 | Manzanita Leaves (dry) | 15.08 | 0.28 | 5.16 | 0.03 | 0.17 | 0.02 | 476.74 | 2.16 | 6.90 |
| Burn 98-100 | Chamise Br. and Leaves (dry) | 2.66 | 0.24 | 0.42 | 0.00 | 0.05 | 0.00 | 73.42 | 35.16 | 29.85 |
| Test burn 1 | PP Needles | 986.45 | 0.00 | 47.67 | 27.05 | 15.35 | 0.08 | 0.30 | 0.11 | 4.60 |
| Test burn 2 | Ethanol | 0.00 | 0.00 | 0.00 | 0.00 | 0.00 | 0.00 | 0.00 | 0.00 | 0.00 |
| Test burn 3 | Propane Torch | 0.00 | 0.00 | 0.00 | 0.00 | 0.00 | 0.00 | 0.00 | 0.00 | 0.00 |
| Test burn 4 | PP Needles | 1017.13 | 0.74 | 37.55 | 18.25 | 10.62 | 0.00 | 0.19 | 0.09 | 5.75 |
| Burn 1 | Palmetto | 361.24 | 23.02 | 28.83 | 1.73 | 1.80 | 0.00 | 0.17 | 0.08 | 18.81 |
| Burn 2 | Palmetto (inland) | 417.91 | 63.66 | 19.31 | 1.37 | 1.50 | 0.00 | 0.14 | 0.00 | 22.66 |
| Burn 3 | Palmetto (coastal) | 323.26 | 38.27 | 24.00 | 1.39 | 1.03 | 0.00 | 0.18 | 0.08 | 37.89 |
| Burn 4 | Gallberry | 370.70 | 425.20 | 13.52 | 0.62 | 1.13 | 0.00 | 0.17 | 0.00 | 57.08 |
| Burn 5 | Longleaf Pine (LLP) Needles | 345.94 | 14.67 | 25.01 | 14.25 | 5.19 | 0.04 | 0.13 | 0.05 | 7.19 |
| Burn 6 | Oak Leaves | 394.18 | 14.99 | 24.57 | 1.98 | 4.53 | 0.00 | 0.17 | 0.00 | 24.80 |
| Burn 7 | Hickory Leaves | 290.35 | 12.38 | 10.83 | 1.14 | 2.21 | 0.00 | 0.18 | 0.00 | 27.22 |
| Burn 8 | Wiregrass | 118.48 | 11.59 | 20.36 | 0.52 | 0.41 | 0.00 | 0.12 | 0.00 | 2.25 |
| Burn 9 | Titi | 126.61 | 43.37 | 6.40 | 0.62 | 0.55 | 0.00 | 0.13 | 0.09 | 26.84 |
| Burn 10 | Phragmites | 224.08 | 4.29 | 16.85 | 0.92 | 1.59 | 0.00 | 0.33 | 0.14 | 4.44 |
| Burn 11 | Wax Myrtle | 320.92 | 12.29 | 18.92 | 1.34 | 2.16 | 0.10 | 0.16 | 0.08 | 41.27 |
| Burn 12 | Kudzu | 711.31 | 0.00 | 18.04 | 7.57 | 1.72 | 0.00 | 0.23 | 0.00 | 16.04 |
| Burn 13 | Palmetto & Gallberry | 500.02 | 0.00 | 36.17 | 2.87 | 3.61 | 0.21 | 0.28 | 0.00 | 17.48 |
| Burn 14 | LLP & Wiregrass | 137.62 | 0.54 | 18.45 | 4.19 | 1.79 | 0.08 | 0.11 | 0.00 | 2.54 |
| Burn 15 | Oak & Hickory Leaves | 334.19 | 0.00 | 17.17 | 1.23 | 3.06 | 0.20 | 0.22 | 0.00 | 15.43 |

| Sample Name | Fuel Description | Levoglucosan | Mannosan | Galactosan | Galactose | Glucose | Mannose | OC | EC | K⁺ |
|---|---|---|---|---|---|---|---|---|---|---|
| Burn 16 | PP Needles (25g) | 81.56 | 2.82 | 2.88 | 0.88 | 0.50 | 0.00 | 0.00 | 0.00 | 0.00 |
| Burn 17 | PP Needles (250g) | 1964.09 | 2.51 | 123.53 | 61.84 | 27.11 | 0.15 | 0.43 | 0.01 | 4.27 |
| Burn 18 | PP Needles (2460g) | 2562.04 | 253.07 | 81.51 | 59.45 | 35.25 | 0.08 | 0.29 | 0.01 | 41.72 |
| Burn 19 | PP Needles (80g) | 633.43 | 0.00 | 58.00 | 17.90 | 7.44 | 0.00 | 0.35 | 0.04 | 2.85 |
| Burn 20 | PP Needles (500g) | 1651.18 | 47.70 | 119.13 | 55.63 | 24.12 | 0.16 | 0.36 | 0.00 | 6.95 |
| Burn 21 | Black Spruce (dried) | 309.40 | 26.87 | 25.53 | 8.32 | 2.89 | 0.06 | 0.12 | 0.00 | 4.66 |
| Burn 22 | Black Spruce (fresh) | 359.43 | 3.67 | 28.32 | 6.72 | 2.80 | 0.09 | 0.19 | 0.00 | 4.37 |
| Burn 23 | Fir Needles (fresh) | 631.78 | 0.00 | 30.84 | 8.94 | 7.44 | 0.05 | 0.69 | 0.10 | 2.95 |
| Burn 24 | Fir Branches (fresh) | 97.56 | 6.44 | 2.82 | 0.86 | 0.76 | 0.00 | 0.00 | 0.00 | 0.00 |
| Burn 25 | Fir Needles & Branches (dry) | 131.44 | 0.00 | 6.34 | 1.90 | 1.87 | 0.03 | 0.06 | 0.03 | 0.79 |
| Burn 26 | Fir Needles & Branches (fresh) | 675.45 | 2.95 | 45.64 | 9.32 | 7.85 | 0.09 | 0.84 | 0.12 | 9.50 |
| Burn 27 | Fir Needles (dry) | 180.22 | 0.01 | 4.76 | 1.64 | 1.24 | 0.04 | 0.08 | 0.04 | 0.70 |
| Burn 28 | Fir Branches (dry) | 172.83 | 0.00 | 12.51 | 2.96 | 3.34 | 0.00 | 0.12 | 0.00 | 1.78 |
| Burn 29 | Manzanita | 315.27 | 21.06 | 27.54 | 1.13 | 2.27 | 0.00 | 0.20 | 0.00 | 26.02 |
| Burn 30 | Ceanothus | 184.15 | 29.06 | 9.95 | 0.68 | 0.75 | 0.00 | 0.20 | 0.00 | 75.65 |
| Burn 31 | PP Sticks (sm.) | 66.82 | 125.37 | 5.38 | 1.13 | 0.32 | 0.00 | 0.11 | 0.00 | 3.29 |
| Burn 32 | PP Sticks (med.) | 82.19 | 72.88 | 5.16 | 1.29 | 0.43 | 0.00 | 0.08 | 0.00 | 1.16 |
| Burn 33 | PP Sticks (lg.) | 61.40 | 32.59 | 2.16 | 0.86 | 0.28 | 0.00 | 0.07 | 0.00 | 0.90 |
| Burn 34 | Sage (polluted env.) | 308.32 | 5.27 | 4.57 | 1.23 | 0.77 | 0.00 | 0.00 | 0.00 | 26.20 |
| Burn 35 | Sage (washed) | 398.76 | 29.52 | 4.02 | 1.33 | 0.78 | 0.00 | 0.00 | 0.00 | 98.39 |
| Burn 36 | Chamise | 189.76 | 49.16 | 8.16 | 0.79 | 0.84 | 0.00 | 0.17 | 0.00 | 56.77 |
| Burn 37 | Chamise (washed) | 181.59 | 32.39 | 7.49 | 0.70 | 0.80 | 0.00 | 0.19 | 0.00 | 31.23 |
| Burn 38 | PP Needles- flaming | 595.24 | 598.02 | 27.13 | 6.94 | 4.10 | 0.00 | 0.00 | 0.00 | 20.29 |
| Burn 77-78 | PP Needles- flaming- feeding | 376.49 | 255.31 | 27.09 | 6.19 | 2.99 | 0.00 | 0.61 | 0.00 | 13.83 |
| Burn 39 | PP Needles- smoldering | 1956.55 | 0.00 | 101.26 | 55.38 | 23.97 | 0.00 | 0.29 | 0.18 | 2.39 |
| Burn 82 | PP Needles- smoldering- feeding | 692.04 | 0.00 | 27.50 | 5.66 | 3.47 | 0.00 | 0.42 | 0.00 | 0.00 |
| Burn 40 | Rice Straw (Taiwan)- flaming | 3407.09 | 0.00 | 201.23 | 13.59 | 17.04 | 1.17 | 1.86 | 1.34 | 1292.18 |
| Burn 41 | Rice Straw (Taiwan)- smoldering | 81.24 | 0.00 | 0.02 | 0.50 | 0.42 | 0.00 | 0.00 | 0.00 | 26.11 |
| Burn 42 | PP Needles- heading | 995.35 | 49.44 | 67.20 | 36.09 | 15.00 | 0.11 | 0.29 | 0.12 | 8.31 |
| Burn 43 | PP Needles- backing | 140.97 | 79.24 | 10.02 | 2.12 | 1.25 | 0.00 | 0.15 | 0.00 | 13.32 |

| Sample Name | Fuel Description | Levoglucosan | Mannosan | Galactosan | Galactose | Glucose | Mannose | OC | EC | K⁺ |
|---|---|---|---|---|---|---|---|---|---|---|
| Burn 44 | Sage- heading | 721.58 | 24.19 | 31.19 | 6.53 | 4.52 | 0.12 | 0.38 | 0.00 | 130.97 |
| Burn 45 | Sage- backing | 413.96 | 33.44 | 18.82 | 2.78 | 1.88 | 0.00 | 0.19 | 0.11 | 124.30 |
| Burn 46 | Sage ($(NH_4)_2SO_4$ coated) | 393.93 | 19.73 | 10.28 | 2.10 | 1.48 | 0.00 | 0.22 | 0.00 | 105.04 |
| Burn 47 | Chamise ($(NH_4)_2SO_4$ coated) | 193.90 | 90.39 | 7.29 | 1.04 | 0.99 | 0.00 | 0.00 | 0.00 | 57.06 |
| Burn 48 | Sage (KCl coated) | 419.29 | 14.42 | 13.24 | 2.43 | 1.79 | 0.00 | 0.21 | 0.00 | 117.04 |
| Burn 49 | Chamise (KCl coated) | 138.61 | 73.53 | 4.71 | 0.85 | 0.80 | 0.00 | 0.00 | 0.00 | 26.22 |
| Burn 50 | Sage (clean env.) | 690.01 | 19.73 | 28.33 | 6.51 | 4.59 | 0.11 | 0.28 | 0.11 | 96.33 |
| Burn 51 | Rice Straw | 550.67 | 0.00 | 28.76 | 1.53 | 2.30 | 0.12 | 0.25 | 0.11 | 39.49 |
| Burn 52 | Turkey Oak Leaves & Branches | 1124.38 | 50.07 | 52.87 | 3.60 | 12.48 | 0.09 | 0.18 | 0.08 | 60.72 |
| Burn 54 | Black Needle Rush & Salt Marsh Grass | 684.55 | 11.08 | 57.59 | 3.07 | 7.49 | 0.00 | 0.36 | 0.00 | 151.08 |
| Burn 55 | Saw Grass | 462.45 | 57.45 | 18.88 | 1.64 | 1.81 | 0.00 | 0.17 | 0.00 | 301.93 |
| Burn 56 | Alaskan Tundra Duff/Feathermoss/Duff | 182.14 | 0.00 | 23.71 | 17.79 | 10.46 | 0.04 | 0.07 | 0.04 | 1.09 |
| Burn 57 | U.S. Charcoal | 27.22 | 0.24 | 2.36 | 0.47 | 0.17 | 0.00 | 0.05 | 0.00 | 0.00 |
| Burn 58 | Asian Charcoal | 19.33 | 0.01 | 0.16 | 0.16 | 0.18 | 0.00 | 0.03 | 0.00 | 0.35 |
| Burn A-A | PP Pine Complex | 10.48 | 5.58 | 1.54 | 0.02 | 0.07 | 0.02 | 143.42 | 8.39 | 0.61 |
| Burn B-A | Chamise Complex | 1.61 | 0.12 | 0.15 | 0.00 | 0.02 | 0.00 | 31.60 | 64.11 | 20.82 |
| Burn C-A | PP Pine Complex | 19.41 | 23.20 | 9.66 | 0.03 | 0.18 | 0.05 | 541.06 | 45.38 | 0.71 |
| Burn D-A1 | Chamise Complex | 3.59 | 0.36 | 0.51 | 0.00 | 0.00 | 0.00 | 90.21 | 44.75 | 4.64 |
| Burn D-A2 | Chamise Complex | 2.72 | 0.36 | 0.40 | 0.00 | 0.00 | 0.00 | 73.79 | 91.06 | DNR |
| Burn E-A | Rice Straw | 7.44 | 0.15 | 0.40 | 0.00 | 0.04 | 0.00 | 74.59 | 1.63 | 25.66 |
| Burn F-A | PP Pine Duff | 11.94 | 11.97 | 4.49 | 0.02 | 0.05 | 0.02 | 195.98 | 1.12 | 0.70 |
| Burn G-A | Alaska Duff | 14.46 | 14.64 | 8.04 | 0.03 | 0.08 | 0.03 | 166.45 | 0.00 | 1.12 |
| Burn H-A | Manzanita | 4.74 | 0.38 | 0.38 | 0.00 | 0.02 | 0.01 | 59.14 | 47.70 | 15.46 |
| Burn I-A | Juniper Brush/Sticks | 0.78 | 0.23 | 0.16 | 0.00 | 0.02 | 0.00 | 52.70 | 182.06 | 14.56 |
| Burn J-A | Juniper/Rabbitbrush/Sage mix | 2.10 | 0.40 | 0.21 | 0.02 | 0.04 | 0.00 | 53.01 | 111.70 | 58.52 |
| Burn K-A | Lignin | 1.90 | 0.24 | 0.15 | 0.00 | 0.02 | 0.00 | 124.80 | 35.75 | 0.38 |
| Burn L-A | LP Needles/Branches | 15.72 | 11.28 | 4.53 | 0.02 | 0.05 | 0.02 | 212.63 | 14.33 | 0.58 |
| Burn M-A | Puerto Rico Fern | 10.13 | 9.17 | 1.46 | 0.01 | 0.06 | 0.02 | 144.63 | 8.34 | 7.46 |
| Burn N-A | Chamise (dry) | 1.97 | 0.34 | 0.19 | 0.00 | 0.03 | 0.00 | 44.66 | 61.98 | 26.92 |

| Sample Name | Fuel Description | Levoglucosan | Mannosan | Galactosan | Galactose | Glucose | Mannose | OC | EC | K⁺ |
|---|---|---|---|---|---|---|---|---|---|---|
| Burn O-A | Wax Myrtle | 7.07 | 1.59 | 1.23 | 0.01 | 0.06 | 0.00 | 126.79 | 16.60 | 24.93 |
| Burn P-A | Southern Pine Needles | 10.53 | 6.42 | 1.34 | 0.00 | 0.05 | 0.02 | 107.42 | 7.29 | 1.07 |
| Burn Q-A | Puerto Rico Dry Wood/Sticks | 7.30 | 0.62 | 0.26 | 0.00 | 0.04 | 0.00 | 56.79 | 5.88 | 1.47 |
| Burn R-A | Palmetto | 5.03 | 0.48 | 0.27 | 0.00 | 0.04 | 0.00 | 75.17 | 16.75 | 14.02 |
| Burn S-A | Ceanothus | 7.64 | 0.34 | 0.65 | 0.01 | 0.07 | 0.00 | 147.69 | 5.75 | 20.10 |
| Burn 112 | PP Needles | 519.13 | 21.64 | 17.37 | 15.24 | 7.22 | 0.02 | 0.13 | 0.03 | 1.87 |
| Burn 113 | LLP Needles & Wiregrass | 189.75 | 8.84 | 12.50 | 10.10 | 2.75 | 0.01 | 0.05 | 0.01 | 8.39 |
| Burn 114 | Black Needle Rush | 438.83 | 42.23 | 16.62 | 3.61 | 3.84 | 0.02 | 0.15 | 0.01 | 41.10 |
| Burn 115 | Hickory & Oak Leaves | 115.03 | 10.52 | 4.96 | 0.51 | 0.84 | 0.01 | 0.03 | 0.00 | 15.21 |
| Burn 116 | Fir Needles & Branches (fresh) | 57.03 | 27.46 | 2.53 | 0.51 | 0.30 | 0.07 | 0.04 | 0.02 | 6.84 |
| Burn 117 | Fir Needles & Branches (dry) | 98.58 | 0.59 | 3.69 | 1.00 | 0.83 | 0.02 | 0.03 | 0.02 | 0.46 |
| Burn 118 | Palmetto Leaves (coastal) | 25.78 | 34.53 | 0.62 | 0.12 | 0.09 | 0.00 | 0.02 | 0.00 | 6.85 |
| Burn 119 | Palmetto Leaves | 40.55 | 13.49 | 2.35 | 0.18 | 0.11 | 0.00 | 0.02 | 0.00 | 4.86 |
| Burn119ov | Burn 119 continued overnight | 8.29 | 2.51 | 0.17 | 0.04 | 0.02 | 0.00 | 0.00 | 0.00 | 0.84 |
| Burn 120 | Rice Straw | 33.34 | 0.89 | 1.97 | 0.16 | 0.15 | 0.00 | 0.02 | 0.00 | 6.84 |
| Burn 121 | Alaskan Duff Core | 126.42 | 0.86 | 12.59 | 11.60 | 7.07 | 0.04 | 0.09 | 0.03 | 2.20 |
| Burn 122 | Rhododendron | 68.38 | 6.88 | 6.89 | 0.57 | 0.55 | 0.01 | 0.05 | 0.02 | 3.94 |
| Burn 123 | Black Spruce | 77.29 | 24.11 | 5.64 | 1.35 | 0.42 | 0.02 | 0.05 | 0.02 | 1.05 |
| Burn 124 | Fir Needles & Branches (dry; 50g) | 86.66 | 0.00 | 2.23 | 0.61 | 0.36 | 0.00 | 0.04 | 0.02 | 1.96 |
| Burn 125 | Alaskan Duff Core (40g) | 95.89 | 0.00 | 14.67 | 6.32 | 2.11 | 0.03 | 0.07 | 0.03 | 0.00 |
| Burn 126 | Wiregrass | 39.75 | 2.62 | 7.98 | 0.36 | 0.21 | 0.00 | 0.07 | 0.06 | 0.84 |
| Burn 127 | Chamise | 43.60 | 43.98 | 1.60 | 0.22 | 0.17 | 0.00 | 0.03 | 0.02 | 19.86 |
| Burn 128 | Black Needlerush | 83.57 | 3.27 | 6.66 | 0.51 | 0.50 | 0.02 | 0.07 | 0.07 | 12.21 |
| Burn 129a | Sage- Undiluted | 205.96 | 124.54 | 8.72 | 1.12 | 0.45 | 0.00 | 0.05 | 0.00 | 132.56 |
| Burn 129b | Sage- Dilution #1 | 73.28 | 26.32 | 2.97 | 0.39 | 0.22 | 0.00 | 0.07 | 0.00 | 41.50 |
| Burn 129c | Sage- Dilution #2 | 33.99 | 9.54 | 1.08 | 0.18 | 0.10 | 0.00 | 0.04 | 0.00 | 15.27 |
| Burn 130a | LLP Needles- Undiluted | 722.59 | 15.38 | 30.59 | 27.29 | 14.28 | 0.06 | 0.22 | 0.06 | 7.31 |
| Burn 130b | LLP Needles- Dilution #1 | 152.78 | 0.00 | 15.05 | 6.09 | 1.61 | 0.47 | 0.09 | 0.05 | 1.25 |
| Burn 130c | LLP Needles- Dilution #2 | 88.64 | 0.00 | 7.88 | 2.27 | 0.46 | 0.00 | 0.08 | 0.05 | 0.81 |
| Burn 130d | LLP Needles- Dilution #3 | 7.81 | 0.06 | 0.37 | 0.08 | 0.01 | 0.00 | 0.01 | 0.00 | 0.09 |

| Sample Name | Fuel Description | Levoglucosan | Mannosan | Galactosan | Galactose | Glucose | Mannose | OC | EC | K⁺ |
|---|---|---|---|---|---|---|---|---|---|---|
| Burn 131 | Gallberry | 52.43 | 51.89 | 1.53 | 0.08 | 0.13 | 0.00 | 0.03 | 0.00 | 8.69 |
| Burn 132 | China Sugar Cane | 32.56 | 3.82 | 0.62 | 0.11 | 0.08 | 0.00 | 0.03 | 0.01 | 7.37 |
| Burn 133 | White Spruce | 55.07 | 0.00 | 7.31 | 1.35 | 0.43 | 0.02 | 0.07 | 0.02 | 3.14 |

**Table C.2** *Species concentrations from URG filters collected during the FLAME campaigns. All concentrations are in units of µg/m³. An entry of "0.00" does not necessarily mean that particular species was absent, merely that it was not measured in the sample.*

| Sample Name | Fuel Description | Backup NH₃ (cell. filter) | Nylon Filters | | | | | | | | |
|---|---|---|---|---|---|---|---|---|---|---|---|
| | | | $Na^+$ | $NH_4^+$ | $K^+$ | $Mg^{2+}$ | $Ca^{2+}$ | $Cl^-$ | $NO_2^-$ | $NO_3^-$ | $SO_4^{2-}$ |
| Burn1 | Ponderosa Pine (PP) Needles | 0.56 | 9.41 | 8.59 | 2.88 | 5.58 | 12.38 | 7.92 | 0.00 | 6.48 | 4.23 |
| Burn2ABC | Cellulose | 0.62 | 4.82 | 0.00 | 0.91 | 2.08 | 5.27 | 3.94 | 0.37 | 1.76 | 1.50 |
| Burn3ABC | Cellulose filter (K doped 1) | 0.23 | 2.54 | 0.58 | 5.69 | 1.49 | 1.40 | 1.94 | 0.19 | 1.32 | 0.94 |
| Burn4ABC | Cellulose filter (K doped 2) | 0.09 | 2.46 | 0.50 | 2.56 | 0.53 | 2.89 | 1.06 | 0.00 | 0.00 | 0.93 |
| Burn5ABC | Cellulose Powder | 0.26 | 1.75 | 0.47 | 0.34 | 1.76 | 2.45 | 0.92 | 0.48 | 1.13 | 0.71 |
| Burn6ABC | Dry Montana Grass | 0.70 | 6.29 | 1.58 | 20.43 | 0.00 | 8.11 | 33.86 | 1.21 | 4.90 | 5.66 |
| Burn7ABC | Wet Montana Grass | 0.55 | 2.02 | 0.86 | 29.08 | 0.00 | 0.00 | 26.15 | 0.64 | 1.88 | 3.65 |
| Burn8ABC | Rice Straw | 3.05 | 4.47 | 6.18 | 25.99 | 0.75 | 8.39 | 64.23 | 0.00 | 4.34 | 3.71 |
| Burn9ABC | PP Duff | 0.37 | 1.20 | 0.28 | 0.48 | 0.76 | 3.33 | 2.16 | 0.00 | 0.00 | 0.73 |
| Burn10ABC | PP Needle Litter | 0.56 | 1.51 | 0.44 | 0.99 | 1.56 | 1.53 | 3.77 | 0.00 | 1.80 | 1.17 |
| Burn11ABC | PP Needle Litter | 0.38 | 2.72 | 0.48 | 1.32 | 1.52 | 2.66 | 2.26 | 0.00 | 2.29 | 1.65 |
| Burn12ABC | PP Needle Litter | 1.06 | 1.92 | 0.51 | 1.07 | 3.01 | 2.61 | 2.79 | 0.00 | 2.25 | 1.42 |
| Burn13ABC | PP Needle Litter | 0.49 | 2.35 | 0.32 | 0.65 | 0.75 | 2.03 | 3.02 | 0.00 | 0.00 | 1.03 |
| Burn14ABC | PP Needle Litter | 0.42 | 2.76 | 0.45 | 0.76 | 1.29 | 2.05 | 4.03 | 0.00 | 2.06 | 1.29 |
| Burn15ABC | PP Branches (dead; sm.) | 0.00 | 5.07 | 0.00 | 0.00 | 1.46 | 5.15 | 1.44 | 0.00 | 0.00 | 0.57 |
| Burn16ABC | PP Branches (dead; lg.) | 0.15 | 2.28 | 0.29 | 0.00 | 0.66 | 1.87 | 1.72 | 0.00 | 1.22 | 0.96 |
| Burn17ABC | PP Branches (fresh; sm.) | 0.06 | 2.75 | 0.00 | 1.04 | 0.01 | 2.15 | 3.95 | 0.35 | 1.56 | 1.06 |
| Burn18ABC | PP Needles (fresh) | 0.34 | 1.03 | 0.24 | 1.36 | 0.00 | 0.00 | 1.82 | 0.00 | 0.88 | 0.95 |
| Burn19ABC | PP Branches (fresh; lg.) | 0.06 | 1.91 | 0.52 | 0.73 | 0.33 | 2.33 | 4.42 | 0.00 | 0.00 | 0.00 |
| Burn20ABC | Lodgepole Pine (LP) Needle Litter | 0.59 | 1.50 | 0.47 | 0.71 | 0.48 | 2.32 | 1.49 | 0.00 | 0.00 | 1.11 |
| Burn21ABC | LP Needles (fresh) | 0.74 | 1.21 | 0.31 | 2.83 | 0.00 | 1.65 | 1.32 | 0.00 | 0.99 | 1.22 |
| Burn23ABC | LP Branches (dead; sm.) | 0.29 | 2.57 | 0.62 | 0.85 | 1.92 | 3.86 | 3.08 | 0.00 | 2.25 | 1.20 |

| Sample Name | Fuel Description | Backup NH$_3$ | Na$^+$ | NH$_4$$^+$ | K$^+$ | Mg$^{2+}$ | Ca$^{2+}$ | Cl$^-$ | NO$_2$$^-$ | NO$_3$$^-$ | SO$_4$$^{2-}$ |
|---|---|---|---|---|---|---|---|---|---|---|---|
| Burn24ABC | LP Duff | 0.27 | 1.74 | 0.29 | 0.41 | 0.00 | 2.33 | 2.24 | 0.00 | 0.00 | 0.84 |
| Burn25ABC | Rice Straw | 2.20 | 5.32 | 6.25 | 18.59 | 0.00 | 0.00 | 47.46 | 0.00 | 2.93 | 3.35 |
| Burn26ABC | Palmetto Foliage | 4.90 | 14.59 | 14.19 | 79.24 | 0.00 | 0.00 | 132.82 | 0.00 | 3.24 | 18.37 |
| Burn27ABC | Chamise Foliage (dead) | 0.17 | 6.26 | 1.00 | 27.53 | 5.57 | 3.66 | 14.32 | 0.99 | 3.26 | 12.30 |
| Burn28ABC | Chamise Branches | 0.23 | 2.52 | 0.38 | 1.11 | 0.38 | 1.29 | 2.14 | 0.00 | 1.58 | 1.65 |
| Burn29A | Background | 0.06 | 1.50 | 0.44 | 0.53 | 1.59 | 1.82 | 1.74 | 0.00 | 1.26 | 1.04 |
| Burn30ABC | Chamise Foliage (fresh) | 0.22 | 5.06 | 0.89 | 23.59 | 0.00 | 0.00 | 7.83 | 1.09 | 3.28 | 10.47 |
| Burn31ABC | Chamise Branches (fresh) | 0.48 | 2.89 | 0.46 | 1.57 | 1.68 | 2.12 | 1.25 | 0.40 | 1.47 | 0.98 |
| Burn32ABC | Manzanita Leaves (fresh) | 0.63 | 2.81 | 0.68 | 4.48 | 0.82 | 1.32 | 1.60 | 0.00 | 0.00 | 1.59 |
| Burn33ABC | Manzanita Branches (fresh) | 0.50 | 6.57 | 1.08 | 3.52 | 1.28 | 3.00 | 3.81 | 0.56 | 2.18 | 1.93 |
| Burn34ABC | Manzanita Leaves (dry) | 0.98 | 1.55 | 0.39 | 3.49 | 0.90 | 1.68 | 2.36 | 0.00 | 1.34 | 1.56 |
| Burn35ABC | Chamise Branches and Leaves (dry) | 0.93 | 5.88 | 0.60 | 14.94 | 0.00 | 2.90 | 7.23 | 1.44 | 2.47 | 8.44 |
| Test burn 1 | PP Needles | 8.22 | 8.48 | 7.40 | 9.25 | 4.63 | 5.87 | 6.30 | 0.00 | 0.00 | 0.00 |
| Test burn 2 | Ethanol | 21.15 | 36.10 | 19.28 | 37.48 | 19.44 | 21.23 | 15.06 | 0.00 | 0.00 | 0.00 |
| Test burn 3 | Propane Torch | 32.78 | 21.93 | 10.55 | 22.94 | 11.50 | 11.37 | 8.01 | 13.81 | 0.00 | 0.00 |
| Test burn 4 | PP Needles | 4.87 | 6.42 | 3.80 | 10.08 | 3.84 | 4.59 | 7.42 | 0.00 | 0.00 | 0.00 |
| Burn 1 | Palmetto | 14.85 | 9.52 | 11.53 | 16.91 | 0.00 | 4.87 | 59.93 | 0.00 | 0.00 | 0.00 |
| Burn 2 | Palmetto (inland) | 9.38 | 15.95 | 10.87 | 18.24 | 4.21 | 5.21 | 79.28 | 0.00 | 7.89 | 11.50 |
| Burn 3 | Palmetto (coastal) | 7.02 | 14.26 | 15.64 | 26.22 | 4.66 | 5.42 | 73.57 | 0.00 | 8.73 | 18.56 |
| Burn 4 | Gallberry | 1.84 | 8.62 | 7.15 | 31.97 | 4.45 | 3.92 | 8.22 | 8.50 | 0.00 | 23.73 |
| Burn 5 | Longleaf Pine (LLP) Needles | 3.40 | 4.34 | 2.75 | 6.13 | 1.48 | 1.80 | 16.38 | 0.00 | 2.84 | 0.00 |
| Burn 6 | Oak Leaves | 2.61 | 10.48 | 7.99 | 20.14 | 5.07 | 5.07 | 8.40 | 0.00 | 0.00 | 14.86 |
| Burn 7 | Hickory Leaves | 2.71 | 10.04 | 8.30 | 18.90 | 5.14 | 5.16 | 9.34 | 10.01 | 0.00 | 0.00 |
| Burn 8 | Wiregrass | 2.41 | 5.89 | 2.91 | 6.58 | 3.26 | 3.62 | 6.30 | 0.00 | 0.00 | 0.00 |
| Burn 9 | Titi | 5.93 | 6.89 | 3.63 | 19.93 | 3.73 | 3.59 | 7.34 | 6.00 | 0.00 | 14.75 |
| Burn 10 | Phragmites | 6.44 | 11.11 | 7.34 | 12.33 | 5.91 | 5.87 | 28.92 | 0.00 | 0.00 | 0.00 |
| Burn 11 | Wax Myrtle | 4.24 | 10.93 | 7.10 | 26.31 | 3.13 | 3.11 | 30.35 | 5.50 | 0.00 | 14.09 |
| Burn 12 | Kudzu | 3.58 | 10.48 | 5.60 | 16.96 | 5.26 | 5.40 | 6.28 | 0.00 | 0.00 | 15.84 |
| Burn 13 | Palmetto & Gallberry | 7.41 | 4.11 | 5.99 | 12.77 | 2.29 | 3.20 | 40.71 | 0.00 | 4.30 | 5.13 |
| Burn 14 | LLP & Wiregrass | 2.55 | 2.27 | 1.39 | 3.33 | 1.12 | 1.40 | 9.08 | 0.00 | 0.00 | 3.05 |

| Sample Name | Fuel Description | Backup NH$_3$ | Na$^+$ | NH$_4^+$ | K$^+$ | Mg$^{2+}$ | Ca$^{2+}$ | Cl$^-$ | NO$_2^-$ | NO$_3^-$ | SO$_4^{2-}$ |
|---|---|---|---|---|---|---|---|---|---|---|---|
| Burn 15 | Oak & Hickory Leaves | 3.97 | 8.64 | 8.02 | 16.69 | 4.54 | 4.77 | 8.68 | 0.00 | 0.00 | 14.37 |
| Burn 16 | PP Needles (25g) | 9.64 | 11.94 | 5.58 | 11.78 | 6.09 | 6.24 | 3.78 | 0.00 | 0.00 | 0.00 |
| Burn 17 | PP Needles (250g) | 7.05 | 10.03 | 5.45 | 12.94 | 5.62 | 8.01 | 9.66 | 0.00 | 0.00 | 0.00 |
| Burn 18 | PP Needles (2460g) | 13.93 | 5.54 | 3.40 | 27.51 | 3.28 | 4.30 | 40.87 | 0.00 | 4.98 | 12.92 |
| Burn 19 | PP Needles (80g) | 4.94 | 12.20 | 5.35 | 12.06 | 6.22 | 8.41 | 6.35 | 0.00 | 0.00 | 0.00 |
| Burn 20 | PP Needles (500g) | 8.60 | 10.08 | 6.36 | 15.65 | 5.73 | 9.00 | 10.58 | 0.00 | 0.00 | 21.20 |
| Burn 21 | Black Spruce (dried) | 6.12 | 4.54 | 2.15 | 9.23 | 2.21 | 2.56 | 5.77 | 0.00 | 0.00 | 0.00 |
| Burn 22 | Black Spruce (fresh) | 5.91 | 6.19 | 5.24 | 8.09 | 3.27 | 3.55 | 6.50 | 0.00 | 0.00 | 0.00 |
| Burn 23 | Fir Needles (fresh) | 2.57 | 2.50 | 2.86 | 3.98 | 1.52 | 1.73 | 1.42 | 0.00 | 2.67 | 3.76 |
| Burn 24 | Fir Branches (fresh) | 5.40 | 11.43 | 5.27 | 11.95 | 5.94 | 6.59 | 4.00 | 0.00 | 0.00 | 0.00 |
| Burn 25 | Fir Needles & Branches (dry) | 0.96 | 2.01 | 0.92 | 2.36 | 1.16 | 1.41 | 1.04 | 0.00 | 0.00 | 0.00 |
| Burn 26 | Fir Needles & Branches (fresh) | 2.65 | 4.45 | 0.00 | 9.34 | 2.77 | 3.13 | 2.84 | 0.00 | 5.13 | 9.00 |
| Burn 27 | Fir Needles (dry) | 1.23 | 3.15 | 1.53 | 3.24 | 1.85 | 1.92 | 0.92 | 0.00 | 3.42 | 0.00 |
| Burn 28 | Fir Branches (dry) | 3.25 | 6.37 | 3.19 | 7.54 | 3.81 | 4.03 | 2.98 | 0.00 | 0.00 | 0.00 |
| Burn 29 | Manzanita | 5.17 | 5.53 | 5.77 | 18.67 | 3.66 | 3.50 | 7.73 | 4.78 | 0.00 | 12.36 |
| Burn 30 | Ceanothus | 4.20 | 7.91 | 4.68 | 43.18 | 0.00 | 3.91 | 23.15 | 13.56 | 0.00 | 21.87 |
| Burn 31 | PP Sticks (sm.) | 3.83 | 5.00 | 2.44 | 6.71 | 2.93 | 2.90 | 2.43 | 0.00 | 0.00 | 0.00 |
| Burn 32 | PP Sticks (med.) | 4.40 | 7.40 | 5.01 | 7.68 | 3.72 | 3.69 | 3.16 | 6.15 | 0.00 | 0.00 |
| Burn 33 | PP Sticks (lg.) | 2.08 | 4.13 | 1.73 | 4.24 | 2.01 | 2.16 | 2.32 | 0.00 | 4.24 | 3.44 |
| Burn 34 | Sage (polluted env.) | 11.06 | 13.48 | 5.42 | 24.32 | 6.58 | 6.36 | 39.34 | 0.00 | 0.00 | 0.00 |
| Burn 35 | Sage (washed) | 8.10 | 22.17 | 8.29 | 68.62 | 9.45 | 9.67 | 78.94 | 11.67 | 0.00 | 0.00 |
| Burn 36 | Chamise | 4.10 | 9.08 | 3.58 | 36.37 | 0.00 | 3.85 | 17.43 | 8.58 | 8.17 | 19.98 |
| Burn 37 | Chamise- washed | 1.76 | 20.56 | 0.18 | 26.96 | 0.00 | 1.55 | 14.58 | 10.43 | 0.00 | 7.61 |
| Burn 38 | PP Needles- flaming | 3.94 | 61.37 | 0.06 | 38.20 | 0.00 | 5.03 | 26.90 | 26.38 | 0.00 | 7.25 |
| Burn 39 | PP Needles- smoldering | 4.57 | 21.55 | 0.09 | 6.05 | 0.00 | 2.15 | 7.95 | 0.00 | 0.00 | 0.00 |
| Burn 40 | Rice Straw (Taiwan)- flaming | 59.32 | 138.09 | 101.35 | 787.95 | 0.00 | 24.43 | 1157.00 | 92.73 | 0.00 | 200.01 |
| Burn 41 | Rice Straw (Taiwan)- smoldering | 1.26 | 42.11 | 0.26 | 45.64 | 0.00 | 2.96 | 27.01 | 17.88 | 0.00 | 11.88 |
| Burn 42 | PP Needles- heading | 4.76 | 15.60 | 0.10 | 15.09 | 0.00 | 2.17 | 12.89 | 8.83 | 0.00 | 6.28 |

| Sample Name | Fuel Description | Backup NH₃ | Na⁺ | NH₄⁺ | K⁺ | Mg²⁺ | Ca²⁺ | Cl⁻ | NO₂⁻ | NO₃⁻ | SO₄²⁻ |
|---|---|---|---|---|---|---|---|---|---|---|---|
| Burn 43 | PP Needles- backing | 1.76 | 20.80 | 0.18 | 11.11 | 0.00 | 1.36 | 12.33 | 0.00 | 0.00 | 3.20 |
| Burn 44 | Sage- heading | 1.90 | 12.75 | 0.14 | 85.24 | 0.00 | 1.02 | 29.56 | 14.19 | 19.07 | 18.71 |
| Burn 45 | Sage- backing | 1.91 | 15.59 | 0.27 | 98.06 | 0.00 | 1.23 | 36.23 | 14.89 | 0.00 | 24.94 |
| Burn 46 | Sage ((NH₄)₂SO₄ coated) | 2.48 | 21.17 | 0.25 | 61.20 | 0.00 | 3.10 | 36.49 | 14.47 | 0.00 | 15.41 |
| Burn 47 | Chamise ((NH₄)₂SO₄ coated) | 2.71 | 35.54 | 0.00 | 51.89 | 0.00 | 3.20 | 27.12 | 24.82 | 0.00 | 16.77 |
| Burn 48 | Sage (KCl coated) | 8.95 | 19.45 | 0.10 | 60.53 | 0.00 | 1.67 | 38.62 | 14.68 | 0.00 | 16.75 |
| Burn 49 | Chamise (KCl coated) | 1.37 | 37.25 | 0.02 | 28.94 | 0.00 | 3.65 | 23.17 | 0.00 | 0.00 | 0.00 |
| Burn 50 | Sage (clean env.) | 2.31 | 15.53 | 0.20 | 76.18 | 0.00 | 1.05 | 29.82 | 9.36 | 19.79 | 17.73 |
| Burn 51 | Rice Straw | 5.08 | 15.77 | 3.24 | 41.15 | 0.00 | 2.53 | 48.96 | 0.00 | 26.90 | 12.21 |
| Burn 52 | Turkey Oak Leaves & Branches | 2.88 | 12.88 | 0.31 | 35.01 | 0.00 | 1.43 | 11.28 | 0.00 | 0.00 | 7.93 |
| Burn 54 | Black Needle Rush & Salt Marsh Grass | 6.86 | 76.89 | 3.90 | 119.17 | 0.00 | 2.42 | 176.92 | 0.00 | 0.00 | 18.16 |
| Burn 55 | Saw Grass | 7.31 | 33.96 | 0.81 | 235.42 | 0.00 | 2.57 | 194.12 | 0.00 | 0.00 | 17.62 |
| Burn 56 | Alaskan Tundra Duff/Feathermoss/Duff | 1.07 | 8.24 | 0.02 | 3.11 | 0.00 | 0.86 | 3.32 | 0.00 | 0.00 | 0.00 |
| Burn 57 | U.S. Charcoal | 0.60 | 3.56 | 0.03 | 1.51 | 0.00 | 0.69 | 2.00 | 0.00 | 0.00 | 0.00 |
| Burn 58 | Asian Charcoal | 0.51 | 7.86 | 0.16 | 1.91 | 0.00 | 0.57 | 4.41 | 0.00 | 0.00 | 0.00 |
| Burn37A | PP Complex | 3.77 | 0.83 | 0.00 | 0.00 | 0.00 | 0.57 | 1.99 | 0.00 | 0.00 | 0.50 |
| Burn37B | Chamise Complex | 1.92 | 1.98 | 0.56 | 30.98 | 0.00 | 0.00 | 12.13 | 0.26 | 1.73 | 11.19 |
| Burn37C | PP Complex | 11.97 | 1.26 | 0.81 | 0.70 | 0.00 | 0.96 | 2.82 | 0.28 | 2.36 | 1.39 |
| Burn37D | Chamise Complex | 4.07 | 2.79 | 0.00 | 18.20 | 0.00 | 0.00 | 8.35 | 0.00 | 2.55 | 8.52 |
| Burn38A | Rice Straw | 17.27 | 1.31 | 16.41 | 17.83 | 0.00 | 0.69 | 52.67 | 0.00 | 1.18 | 2.22 |
| Burn38B | PP Duff | 5.70 | 0.99 | 0.57 | 0.58 | 0.35 | 0.80 | 1.35 | 0.18 | 1.31 | 1.22 |
| Burn38C | Alaska Duff | 2.92 | 1.29 | 0.58 | 0.65 | 0.36 | 0.80 | 1.34 | 0.00 | 0.00 | 1.06 |
| Burn38D | Manzanita | 2.59 | 1.31 | 0.00 | 10.60 | 0.00 | 0.00 | 4.35 | 0.00 | 0.78 | 5.78 |
| Burn39A | Juniper | 3.76 | 0.80 | 0.23 | 10.23 | 0.00 | 0.00 | 5.77 | 0.00 | 0.96 | 3.99 |
| Burn39B | Juniper/Rabbitbrush/Sage | 1.23 | 1.85 | 0.46 | 40.02 | 0.00 | 0.00 | 17.03 | 0.35 | 1.31 | 10.57 |
| Burn39D | Lignin | 3.97 | 1.31 | 0.52 | 0.37 | 0.00 | 0.61 | 1.95 | 0.18 | 0.92 | 0.92 |
| Burn39E | LP Needles/Branches | 3.14 | 0.91 | 0.70 | 0.00 | 0.00 | 0.72 | 0.21 | 2.32 | 0.00 | 1.00 |
| Burn40A | Puerto Rico Fern (dry) | 6.38 | 0.76 | 0.83 | 3.22 | 0.00 | 0.00 | 0.38 | 12.81 | 1.40 | 2.27 |
| Burn40B | Chamise (dry) | 2.49 | 0.86 | 0.00 | 14.02 | 0.00 | 0.00 | 7.54 | 0.00 | 0.95 | 9.69 |

| Sample Name | Fuel Description | Backup NH₃ | Na⁺ | NH₄⁺ | K⁺ | Mg²⁺ | Ca²⁺ | Cl⁻ | NO₂⁻ | NO₃⁻ | SO₄²⁻ |
|---|---|---|---|---|---|---|---|---|---|---|---|
| Burn40D | Wax Myrtle | 8.64 | 6.91 | 0.58 | 13.96 | 0.00 | 0.54 | 27.10 | 0.21 | 1.34 | 4.10 |
| Burn40E | Southern Pine Needles | 4.32 | 0.57 | 0.54 | 0.51 | 0.00 | 0.56 | 2.02 | 0.00 | 1.09 | 0.77 |
| Burn41A | Puerto Rico Wood | 1.78 | 1.04 | 0.00 | 0.53 | 0.00 | 0.51 | 1.11 | 0.00 | 0.00 | 1.10 |
| Burn41B | Palmetto | N/A | N/A | N/A | N/A | N/A | N/A | N/A | N/A | N/A | N/A |
| Burn41C | Ceanothus | 5.16 | 0.73 | 0.00 | 8.63 | 0.00 | 0.53 | 8.07 | 0.00 | 1.03 | 4.64 |
| Test burn 1 | PP Needles | 2.45 | 2.35 | 0.51 | 3.23 | 0.08 | 0.70 | 5.03 | 0.00 | 4.02 | 2.18 |
| Burn 113 | LLP Needles & Wiregrass | 2.34 | 2.47 | 3.06 | 8.00 | 0.00 | 0.42 | 18.11 | 0.00 | 3.08 | 1.93 |
| Burn 114 | Black Needle Rush | 3.94 | 68.02 | 11.10 | 58.55 | 0.00 | 0.58 | 232.19* | 0.00 | 4.16 | 17.82 |
| Burn 115 | Hickory & Oak Leaves | 0.42 | 1.83 | 0.21 | 10.39 | 0.00 | 0.33 | 3.05 | 0.00 | 3.37 | 6.51 |
| Burn 116 | Fir Needles & Branches (fresh) | 0.20 | 1.91 | 0.04 | 5.91 | 0.00 | 0.17 | 1.74 | 0.00 | 3.30 | 3.33 |
| Burn 117 | Fir Needles & Branches (dry) | 0.60 | 1.83 | 0.19 | 1.40 | 0.00 | 0.39 | 1.14 | 1.63 | 3.91 | 1.00 |
| Burn 118 | Palmetto Leaves (coastal) | 2.98 | 3.64 | 6.04 | 5.21 | 0.00 | 0.38 | 30.51 | 0.00 | 0.00 | 3.96 |
| Burn 119 | Palmetto Leaves | 3.51 | 1.10 | 5.07 | 3.80 | 0.00 | 0.36 | 23.54 | 1.34 | 3.22 | 1.50 |
| Burn119ov | Burn 119 continued overnight | 0.40 | 0.39 | 0.14 | 0.65 | 0.00 | 0.07 | 1.31 | 0.00 | 0.00 | 0.51 |
| Burn 120 | Rice Straw | 2.72 | 1.00 | 5.97 | 4.08 | 0.00 | 0.49 | 22.35 | 0.00 | 0.59 | 1.91 |
| Burn 121 | Alaskan Duff Core | 0.75 | 0.88 | 0.89 | 1.71 | 0.15 | 0.39 | 0.61 | 0.00 | 1.38 | 1.09 |
| Burn 122 | Rhododendron | 0.64 | 0.91 | 0.81 | 2.50 | 0.12 | 0.33 | 2.53 | 0.00 | 0.79 | 1.45 |
| Burn 123 | Black Spruce | 0.63 | 0.96 | 0.75 | 1.32 | 0.11 | 0.31 | 0.62 | 0.00 | 0.82 | 1.07 |
| Burn 124 | Fir Needles & Branches (dry; 50g) | 0.89 | 1.23 | 0.93 | 1.83 | 0.13 | 0.32 | 0.16 | 0.00 | 0.00 | 0.00 |
| Burn 125 | Alaskan Duff Core (40g) | 0.98 | 1.23 | 0.97 | 1.29 | 0.15 | 0.36 | 0.26 | 0.00 | 0.00 | 0.00 |
| Burn 126 | Wiregrass | 0.45 | 1.27 | 1.00 | 1.79 | 0.16 | 0.37 | 1.77 | 0.00 | 0.76 | 0.99 |
| Burn 127 | Chamise | 0.25 | 1.32 | 1.03 | 9.64 | 0.13 | 0.33 | 6.22 | 0.78 | 0.99 | 5.60 |
| Burn 128 | Black Needlerush | 0.41 | 2.76 | 1.31 | 5.50 | 0.16 | 0.43 | 12.91 | 0.33 | 1.37 | 2.09 |
| Burn 129a | Sage- Undiluted | 0.48 | 1.79 | 1.65 | 93.56 | 0.00 | 0.00 | 51.34 | 1.51 | 1.33 | 21.05 |
| Burn 129b | Sage- Dilution #1 | 0.27 | 2.36 | 1.82 | 18.26 | 0.17 | 0.46 | 12.99 | 0.00 | 0.00 | 6.38 |
| Burn 129c | Sage- Dilution #2 | 0.15 | 1.23 | 0.91 | 7.19 | 0.12 | 0.29 | 4.92 | 0.58 | 1.04 | 3.90 |
| Burn 130a | LLP Needles- Undiluted | 1.46 | 2.98 | 4.53 | 5.94 | 0.28 | 0.77 | 26.97 | 0.00 | 1.36 | 2.92 |
| Burn 130b | LLP Needles- Dilution #1 | 2.32 | 2.76 | 2.09 | 3.66 | 0.32 | 1.05 | 2.74 | 0.00 | 1.39 | 0.00 |

| Sample Name | Fuel Description | Backup $NH_3$ | $Na^+$ | $NH_4^+$ | $K^+$ | $Mg^{2+}$ | $Ca^{2+}$ | $Cl^-$ | $NO_2^-$ | $NO_3^-$ | $SO_4^{2-}$ |
|---|---|---|---|---|---|---|---|---|---|---|---|
| Burn 130c | LLP Needles- Dilution #2 | 1.03 | 2.48 | 1.84 | 2.90 | 0.27 | 0.66 | 0.75 | 1.07 | 1.25 | 0.00 |
| Burn 130d | LLP Needles- Dilution #3 | 0.13 | 0.10 | 0.12 | 0.18 | 0.03 | 0.05 | 0.06 | 0.00 | 0.07 | 0.17 |
| Burn 131 | Gallberry | 0.86 | 1.24 | 0.90 | 4.10 | 0.11 | 0.23 | 0.79 | 0.58 | 0.51 | 3.22 |
| Burn 132 | China Sugar Cane | 0.52 | 1.21 | 1.80 | 3.74 | 0.18 | 0.41 | 9.11 | 0.00 | 0.00 | 1.28 |
| Burn 133 | White Spruce | 0.44 | 1.20 | 1.33 | 2.49 | 0.15 | 0.34 | 4.88 | 0.66 | 0.00 | 0.00 |

*Peak area outside calibration range for this species; high uncertainty.

# Appendix D.  Data from IMPROVE Samples

**Table D.1** *Carbohydrate and K$^+$ concentrations for the IMPROVE sites.  Levoglucosan concentrations are in units of µgC/m$^3$; Other carbohydrates and K$^+$ are in units of µg/m$^3$.*

| Sampling Site | Sample Start | Levo. | Mannosan | Galactosan | Galactose | Glucose | Mannose | K$^+$ |
|---|---|---|---|---|---|---|---|---|
| HANC | 6/29/2005 | 0.02 | 0.00 | 0.00 | 0.00 | 0.00 | 0.00 | 0.30 |
| HANC | 7/6/2005 | 0.01 | 0.00 | 0.00 | 0.00 | 0.00 | 0.00 | 0.08 |
| HANC | 7/13/2005 | 0.03 | 0.00 | 0.00 | 0.00 | 0.01 | 0.00 | 0.13 |
| HANC | 7/20/2005 | 0.02 | 0.00 | 0.00 | 0.00 | 0.01 | 0.00 | 0.12 |
| HANC | 7/27/2005 | 0.01 | 0.00 | 0.00 | 0.00 | 0.01 | 0.00 | 0.02 |
| HANC | 8/3/2005 | 0.01 | 0.00 | 0.00 | 0.00 | 0.01 | 0.00 | 0.01 |
| HANC | 8/10/2005 | 0.01 | 0.01 | 0.00 | 0.00 | 0.01 | 0.00 | 0.02 |
| HANC | 8/17/2005 | 0.01 | 0.00 | 0.00 | 0.00 | 0.01 | 0.00 | 0.01 |
| MORA | 6/2/2004 | 0.01 | 0.01 | 0.00 | 0.00 | 0.00 | 0.00 | 0.04 |
| MORA | 6/9/2004 | 0.01 | 0.00 | 0.00 | 0.00 | 0.01 | 0.00 | 0.02 |
| MORA | 6/16/2004 | 0.01 | 0.01 | 0.00 | 0.00 | 0.07 | 0.00 | 0.04 |
| MORA | 6/23/2004 | 0.01 | 0.00 | 0.00 | 0.00 | 0.02 | 0.00 | 0.03 |
| MORA | 6/30/2004 | 0.01 | 0.00 | 0.00 | 0.00 | 0.01 | 0.00 | 0.27 |
| MORA | 7/14/2004 | 0.01 | 0.00 | 0.00 | 0.00 | 0.01 | 0.00 | 0.04 |
| MORA | 7/21/2004 | 0.01 | 0.00 | 0.00 | 0.00 | 0.01 | 0.00 | 0.13 |
| MORA | 7/28/2004 | 0.02 | 0.00 | 0.00 | 0.00 | 0.01 | 0.00 | 0.05 |
| MORA | 8/3/2004 | 0.01 | 0.00 | 0.00 | 0.00 | 0.01 | 0.00 | 0.02 |
| MORA | 8/10/2004 | 0.01 | 0.00 | 0.00 | 0.00 | 0.01 | 0.00 | 0.03 |
| MORA | 8/17/2004 | 0.01 | 0.00 | 0.00 | 0.00 | 0.01 | 0.00 | 0.01 |
| MORA | 8/24/2004 | 0.01 | 0.00 | 0.00 | 0.00 | 0.01 | 0.00 | 0.02 |
| MORA | 12/1/2004 | 0.03 | 0.00 | 0.00 | 0.00 | 0.00 | 0.00 | 0.01 |
| MORA | 12/8/2004 | 0.02 | 0.01 | 0.00 | 0.00 | 0.00 | 0.00 | 0.01 |
| MORA | 12/15/2004 | 0.05 | 0.02 | 0.00 | 0.00 | 0.00 | 0.00 | 0.02 |
| MORA | 12/22/2004 | 0.06 | 0.02 | 0.01 | 0.00 | 0.00 | 0.00 | 0.02 |
| MORA | 12/29/2004 | 0.05 | 0.01 | 0.00 | 0.00 | 0.00 | 0.00 | 0.01 |
| MORA | 1/5/2005 | 0.04 | 0.01 | 0.00 | 0.00 | 0.00 | 0.00 | 0.02 |
| MORA | 1/12/2005 | 0.01 | 0.00 | 0.00 | 0.00 | 0.00 | 0.00 | 0.01 |
| MORA | 1/19/2005 | 0.02 | 0.01 | 0.00 | 0.00 | 0.01 | 0.00 | 0.01 |
| MORA | 1/26/2005 | 0.03 | 0.01 | 0.00 | 0.00 | 0.00 | 0.00 | 0.01 |
| MORA | 2/2/2005 | 0.04 | 0.01 | 0.00 | 0.00 | 0.00 | 0.00 | 0.02 |
| MORA | 2/9/2005 | 0.05 | 0.01 | 0.00 | 0.00 | 0.00 | 0.00 | 0.02 |
| MORA | 2/16/2005 | 0.13 | 0.04 | 0.01 | 0.00 | 0.00 | 0.00 | 0.04 |
| MORA | 2/23/2005 | 0.05 | 0.02 | 0.00 | 0.00 | 0.01 | 0.00 | 0.03 |
| PHOE I | 6/22/2005 | 0.01 | 0.00 | 0.00 | 0.00 | 0.01 | 0.00 | 0.29 |
| PHOE I | 7/6/2005 | 0.01 | 0.00 | 0.00 | 0.00 | 0.02 | 0.00 | 0.24 |
| PHOE I | 7/12/2005 | 0.01 | 0.01 | 0.00 | 0.00 | 0.01 | 0.00 | 0.24 |
| PHOE I | 7/20/2005 | 0.01 | 0.01 | 0.00 | 0.00 | 0.02 | 0.00 | 0.13 |
| PHOE I | 7/27/2005 | 0.00 | 0.01 | 0.00 | 0.00 | 0.01 | 0.00 | 0.05 |
| PHOE I | 8/3/2005 | 0.00 | 0.01 | 0.00 | 0.00 | 0.01 | 0.00 | 0.03 |
| PHOE I | 8/10/2005 | 0.00 | 0.00 | 0.00 | 0.00 | 0.02 | 0.00 | 0.04 |

| Sampling Site | Sample Start | Levo. | Mannosan | Galactosan | Galactose | Glucose | Mannose | K+ |
|---|---|---|---|---|---|---|---|---|
| PHOE I | 8/17/2005 | 0.00 | 0.00 | 0.00 | 0.00 | 0.02 | 0.00 | 0.10 |
| PHOE I | 8/24/2005 | 0.00 | 0.00 | 0.00 | 0.00 | 0.01 | 0.00 | 0.09 |
| PHOE I | 11/30/2005 | 0.08 | 0.01 | 0.00 | 0.00 | 0.01 | 0.00 | 0.11 |
| PHOE I | 12/7/2005 | 0.20 | 0.05 | 0.01 | 0.00 | 0.02 | 0.00 | 0.26 |
| PHOE I | 12/14/2005 | 0.12 | 0.03 | 0.00 | 0.00 | 0.01 | 0.00 | 0.22 |
| PHOE I | 12/21/2005 | 0.14 | 0.03 | 0.00 | 0.00 | 0.02 | 0.00 | 0.21 |
| PHOE I | 12/28/2005 | 0.14 | 0.03 | 0.00 | 0.00 | 0.02 | 0.00 | 0.22 |
| PHOE I | 1/4/2006 | 0.06 | 0.01 | 0.00 | 0.00 | 0.03 | 0.00 | 0.17 |
| PHOE I | 1/11/2006 | 0.07 | 0.01 | 0.00 | 0.00 | 0.05 | 0.00 | 0.14 |
| PHOE I | 1/18/2006 | 0.06 | 0.01 | 0.00 | 0.00 | 0.02 | 0.00 | 0.23 |
| PHOE I | 1/25/2006 | 0.05 | 0.01 | 0.00 | 0.00 | 0.02 | 0.00 | 0.26 |
| PHOE I | 2/1/2006 | 0.04 | 0.01 | 0.00 | 0.00 | 0.03 | 0.00 | 0.41 |
| PHOE I | 2/8/2006 | 0.05 | 0.01 | 0.00 | 0.00 | 0.03 | 0.00 | 0.16 |
| PHOE I | 2/15/2006 | 0.04 | 0.01 | 0.00 | 0.00 | 0.03 | 0.00 | 0.27 |
| PHOE I | 2/22/2006 | 0.03 | 0.01 | 0.00 | 0.00 | 0.03 | 0.00 | 0.27 |
| PUSO | 6/2/2004 | 0.01 | 0.01 | 0.00 | 0.00 | 0.03 | 0.00 | 0.06 |
| PUSO | 6/9/2004 | 0.01 | 0.01 | 0.00 | 0.00 | 0.01 | 0.00 | 0.05 |
| PUSO | 6/16/2004 | 0.01 | 0.01 | 0.00 | 0.00 | 0.02 | 0.00 | 0.09 |
| PUSO | 6/23/2004 | 0.01 | 0.00 | 0.00 | 0.00 | 0.01 | 0.00 | 0.06 |
| PUSO | 6/30/2004 | 0.01 | 0.00 | 0.00 | 0.00 | 0.00 | 0.00 | 0.48 |
| PUSO | 7/7/2004 | 0.01 | 0.01 | 0.00 | 0.00 | 0.01 | 0.00 | 0.06 |
| PUSO | 7/14/2004 | 0.01 | 0.01 | 0.00 | 0.00 | 0.01 | 0.00 | 0.06 |
| PUSO | 7/21/2004 | 0.01 | 0.00 | 0.00 | 0.00 | 0.00 | 0.00 | 0.07 |
| PUSO | 7/28/2004 | 0.01 | 0.00 | 0.00 | 0.00 | 0.00 | 0.00 | 0.09 |
| PUSO | 8/4/2004 | 0.01 | 0.01 | 0.00 | 0.00 | 0.00 | 0.00 | 0.05 |
| PUSO | 8/11/2004 | 0.01 | 0.00 | 0.00 | 0.00 | 0.00 | 0.00 | 0.09 |
| PUSO | 8/18/2004 | 0.00 | 0.00 | 0.00 | 0.00 | 0.00 | 0.00 | 0.04 |
| PUSO | 8/25/2004 | 0.00 | 0.00 | 0.00 | 0.00 | 0.00 | 0.00 | 0.04 |
| PUSO | 12/1/2004 | 0.05 | 0.01 | 0.00 | 0.00 | 0.00 | 0.00 | 0.06 |
| PUSO | 12/8/2004 | 0.03 | 0.01 | 0.00 | 0.00 | 0.00 | 0.00 | 0.03 |
| PUSO | 12/15/2004 | 0.06 | 0.02 | 0.01 | 0.00 | 0.00 | 0.00 | 0.09 |
| PUSO | 12/22/2004 | 0.07 | 0.03 | 0.01 | 0.00 | 0.01 | 0.00 | 0.08 |
| PUSO | 12/29/2004 | 0.07 | 0.03 | 0.01 | 0.00 | 0.00 | 0.00 | 0.12 |
| PUSO | 1/5/2005 | 0.06 | 0.02 | 0.01 | 0.00 | 0.00 | 0.00 | 0.33 |
| PUSO | 1/12/2005 | 0.04 | 0.01 | 0.00 | 0.00 | 0.00 | 0.00 | 0.04 |
| PUSO | 1/19/2005 | 0.04 | 0.01 | 0.00 | 0.00 | 0.00 | 0.00 | 0.07 |
| PUSO | 1/26/2005 | 0.05 | 0.01 | 0.00 | 0.00 | 0.00 | 0.00 | 0.08 |
| PUSO | 2/16/2005 | 0.16 | 0.05 | 0.02 | 0.00 | 0.02 | 0.00 | 0.32 |
| PUSO | 2/23/2005 | 0.05 | 0.02 | 0.01 | 0.00 | 0.03 | 0.00 | 0.27 |
| ROMO | 6/28/2005 | 0.02 | 0.01 | 0.00 | 0.00 | 0.02 | 0.00 | 0.08 |
| ROMO | 7/5/2005 | 0.03 | 0.00 | 0.00 | 0.00 | 0.06 | 0.00 | 0.12 |
| ROMO | 7/12/2005 | 0.03 | 0.02 | 0.00 | 0.00 | 0.03 | 0.00 | 0.10 |
| ROMO | 7/19/2005 | 0.02 | 0.01 | 0.00 | 0.00 | 0.03 | 0.00 | 0.20 |
| ROMO | 7/27/2005 | 0.03 | 0.01 | 0.00 | 0.00 | 0.03 | 0.00 | 0.04 |
| ROMO | 8/3/2005 | 0.08 | 0.01 | 0.00 | 0.00 | 0.02 | 0.00 | 0.03 |
| ROMO | 8/9/2005 | 0.05 | 0.01 | 0.00 | 0.00 | 0.01 | 0.00 | 0.05 |

| Sampling Site | Sample Start | Levo. | Mannosan | Galactosan | Galactose | Glucose | Mannose | K⁺ |
|---|---|---|---|---|---|---|---|---|

| Sampling Site | Sample Start | Levo. | Mannosan | Galactosan | Galactose | Glucose | Mannose | $K^+$ |
|---|---|---|---|---|---|---|---|---|
| ROMO | 8/16/2005 | 0.03 | 0.01 | 0.00 | 0.00 | 0.01 | 0.00 | 0.03 |
| SAGO | 6/28/2005 | 0.00 | 0.00 | 0.00 | 0.00 | 0.02 | 0.00 | 0.04 |
| SAGO | 7/5/2005 | 0.02 | 0.00 | 0.00 | 0.00 | 0.02 | 0.00 | 0.06 |
| SAGO | 7/12/2005 | 0.00 | 0.00 | 0.00 | 0.00 | 0.03 | 0.00 | 0.05 |
| SAGO | 7/19/2005 | 0.00 | 0.00 | 0.00 | 0.00 | 0.02 | 0.00 | 0.06 |
| SAGO | 7/26/2005 | 0.00 | 0.01 | 0.00 | 0.00 | 0.02 | 0.00 | 0.04 |
| SAGO | 8/3/2005 | 0.01. | 0.01 | 0.00 | 0.00 | 0.04 | 0.00 | 0.04 |
| SAGO | 8/9/2005 | 0.00 | 0.00 | 0.00 | 0.00 | 0.01 | 0.00 | 0.01 |
| TONT | 6/29/2005 | 0.01 | 0.00 | 0.00 | 0.00 | 0.01 | 0.00 | 0.25 |
| TONT | 7/6/2005 | 0.00 | 0.00 | 0.00 | 0.00 | 0.01 | 0.00 | 0.09 |
| TONT | 7/13/2005 | 0.01 | 0.00 | 0.00 | 0.00 | 0.01 | 0.00 | 0.14 |
| TONT | 7/20/2005 | 0.03 | 0.01 | 0.00 | 0.00 | 0.03 | 0.00 | 0.15 |
| TONT | 7/27/2005 | 0.01 | 0.01 | 0.00 | 0.00 | 0.03 | 0.00 | 0.03 |
| TONT | 8/3/2005 | 0.01 | 0.02 | 0.00 | 0.00 | 0.02 | 0.00 | 0.02 |
| TONT | 8/10/2005 | 0.01 | 0.01 | 0.00 | 0.00 | 0.02 | 0.00 | 0.02 |
| TONT | 8/17/2005 | 0.01 | 0.01 | 0.00 | 0.00 | 0.02 | 0.00 | 0.05 |
| TONT | 11/30/2005 | 0.00 | 0.00 | 0.00 | 0.00 | 0.00 | 0.00 | 0.05 |
| TONT | 12/7/2005 | 0.01 | 0.00 | 0.00 | 0.00 | 0.00 | 0.00 | 0.04 |
| TONT | 12/14/2005 | 0.02 | 0.00 | 0.00 | 0.00 | 0.00 | 0.00 | 0.04 |
| TONT | 12/21/2005 | 0.00 | 0.00 | 0.00 | 0.00 | 0.00 | 0.00 | 0.03 |
| TONT | 12/28/2005 | 0.00 | 0.00 | 0.00 | 0.00 | 0.00 | 0.00 | 0.05 |
| TONT | 1/4/2006 | 0.00 | 0.00 | 0.00 | 0.00 | 0.00 | 0.00 | 0.04 |
| TONT | 1/11/2006 | 0.00 | 0.00 | 0.00 | 0.00 | 0.00 | 0.00 | 0.05 |
| TONT | 1/18/2006 | 0.00 | 0.00 | 0.00 | 0.00 | 0.00 | 0.00 | 0.03 |
| TONT | 1/25/2006 | 0.00 | 0.00 | 0.00 | 0.00 | 0.00 | 0.00 | 0.05 |
| TONT | 2/1/2006 | 0.00 | 0.00 | 0.00 | 0.00 | 0.00 | 0.00 | 0.04 |
| TONT | 2/8/2006 | 0.00 | 0.00 | 0.00 | 0.00 | 0.00 | 0.00 | 0.03 |
| TONT | 2/15/2006 | 0.00 | 0.00 | 0.00 | 0.00 | 0.00 | 0.00 | 0.06 |
| TONT | 2/22/2006 | 0.00 | 0.00 | 0.00 | 0.00 | 0.00 | 0.00 | 0.04 |

**Table D.2** *Carbon concentrations for the IMPROVE sites. All concentrations are in units of μgC/m³. Biomass C was calculated using region-based source profiles.*

| Sampling Site | Sample Start | OC | EC | TC (OC+EC) | Biomass C | Fossil C | Cont. C | ¹⁴C TC |
|---|---|---|---|---|---|---|---|---|
| HANC | 6/29/2005 | 4.23 | 0.67 | 4.90 | 1.31 | -0.01 | 4.09 | 4.08 |
| HANC | 7/6/2005 | 1.92 | 0.19 | 2.11 | 0.70 | 0.09 | 1.76 | 1.85 |
| HANC | 7/13/2005 | 3.53 | 0.00 | 3.53 | 1.83 | 0.24 | 5.17 | 5.41 |
| HANC | 7/20/2005 | 2.11 | 0.00 | 2.11 | 0.90 | 0.01 | 2.86 | 2.87 |
| HANC | 7/27/2005 | 1.37 | 0.00 | 1.37 | 0.46 | 0.06 | 1.12 | 1.18 |
| HANC | 8/3/2005 | 0.98 | 0.00 | 0.98 | 0.54 | 0.03 | 0.91 | 0.94 |
| HANC | 8/10/2005 | 1.67 | 0.05 | 1.72 | 0.62 | 0.00 | 1.81 | 1.81 |
| HANC | 8/17/2005 | 0.78 | 0.06 | 0.84 | 0.36 | 0.08 | 0.92 | 1.00 |
| MORA | 6/2/2004 | 2.98 | 0.00 | 2.98 | 0.30 | 0.65 | 1.51 | 2.16 |
| MORA | 6/9/2004 | 1.01 | 0.02 | 1.03 | 0.26 | 0.08 | 0.48 | 0.56 |
| MORA | 6/16/2004 | 2.28 | 0.00 | 2.28 | 0.57 | 0.48 | 2.36 | 2.84 |

| Sampling Site | Sample Start | OC | EC | TC (OC+EC) | Biomass C | Fossil C | Cont. C | $^{14}$C TC |
|---|---|---|---|---|---|---|---|---|
| MORA | 6/23/2004 | 1.32 | 0.00 | 1.32 | 0.45 | 0.22 | 1.41 | 1.63 |
| MORA | 6/30/2004 | 1.93 | 0.14 | 2.07 | 0.50 | 0.35 | 1.52 | 1.87 |
| MORA | 7/14/2004 | 2.14 | 0.00 | 2.14 | 0.52 | 0.58 | 2.23 | 2.81 |
| MORA | 7/21/2004 | 2.51 | 0.00 | 2.51 | 0.46 | 0.64 | 2.36 | 3.00 |
| MORA | 7/28/2004 | 2.72 | 0.00 | 2.72 | 0.67 | 0.63 | 3.38 | 4.01 |
| MORA | 8/3/2004 | 1.02 | 0.00 | 1.02 | 0.35 | 0.20 | 1.02 | 1.22 |
| MORA | 8/10/2004 | 2.39 | 0.00 | 2.39 | 0.44 | 1.25 | 3.15 | 4.40 |
| MORA | 8/17/2004 | 1.17 | 0.00 | 1.17 | 0.30 | 0.41 | 1.34 | 1.75 |
| MORA | 8/24/2004 | 0.97 | 0.00 | 0.97 | 0.39 | 0.04 | 1.23 | 1.27 |
| MORA | 12/1/2004 | 0.83 | 0.01 | 0.84 | 0.26 | 0.02 | 0.77 | 0.79 |
| MORA | 12/8/2004 | 0.83 | 0.03 | 0.86 | 0.16 | -0.02 | 0.96 | 0.94 |
| MORA | 12/15/2004 | 1.01 | 0.10 | 1.11 | 0.41 | 0.06 | 1.08 | 1.14 |
| MORA | 12/22/2004 | 1.36 | 0.23 | 1.59 | 0.49 | 0.08 | 1.65 | 1.73 |
| MORA | 12/29/2004 | 0.75 | 0.00 | 0.75 | 0.36 | 0.00 | 0.99 | 0.99 |
| MORA | 1/5/2005 | 0.80 | 0.05 | 0.84 | 0.32 | -0.01 | 0.79 | 0.78 |
| MORA | 1/12/2005 | 0.53 | 0.03 | 0.56 | 0.08 | N/A | N/A | N/A |
| MORA | 1/19/2005 | 0.69 | 0.00 | 0.69 | 0.18 | 0.03 | 0.58 | 0.61 |
| MORA | 1/26/2005 | 0.92 | 0.00 | 0.92 | 0.24 | 0.02 | 0.97 | 0.99 |
| MORA | 2/2/2005 | 0.93 | 0.00 | 0.93 | 0.34 | 0.00 | 0.98 | 0.98 |
| MORA | 2/9/2005 | 0.91 | 0.00 | 0.91 | 0.35 | 0.05 | 1.13 | 1.18 |
| MORA | 2/16/2005 | 1.49 | 0.00 | 1.49 | 1.02 | 0.29 | 2.80 | 3.09 |
| MORA | 2/23/2005 | 1.14 | 0.00 | 1.14 | 0.38 | 0.20 | 1.83 | 2.03 |
| PHOE I | 6/22/2005 | 4.47 | 1.08 | 5.55 | 0.54 | 2.04 | 2.99 | 5.03 |
| PHOE I | 7/6/2005 | 5.94 | 1.25 | 7.20 | 0.33 | 2.24 | 2.58 | 4.82 |
| PHOE I | 7/12/2005 | 5.39 | 0.76 | 6.15 | 0.33 | 2.31 | 4.26 | 6.57 |
| PHOE I | 7/20/2005 | 5.39 | 0.48 | 5.87 | 0.45 | 0.87 | 1.94 | 2.81 |
| PHOE I | 7/27/2005 | 2.61 | 0.29 | 2.90 | 0.22 | 1.24 | 1.62 | 2.86 |
| PHOE I | 8/3/2005 | 1.98 | 0.50 | 2.47 | 0.13 | 2.18 | 1.82 | 4.00 |
| PHOE I | 8/10/2005 | 1.49 | 0.00 | 1.49 | 0.19 | 1.64 | 1.56 | 3.20 |
| PHOE I | 8/17/2005 | 1.95 | 0.00 | 1.95 | 0.19 | 2.15 | 2.02 | 4.17 |
| PHOE I | 8/24/2005 | 2.53 | 0.00 | 2.53 | 0.18 | 2.50 | 2.59 | 5.09 |
| PHOE I | 11/30/2005 | 5.52 | 2.42 | 7.94 | 0.46 | 3.39 | 3.35 | 6.74 |
| PHOE I | 12/7/2005 | 8.70 | 0.10 | 8.80 | 1.14 | 6.45 | 7.07 | ### |
| PHOE I | 12/14/2005 | 2.68 | 0.00 | 2.68 | 0.68 | 4.12 | 4.16 | 8.28 |
| PHOE I | 12/21/2005 | 12.33 | 0.43 | 12.77 | 0.81 | 8.48 | 7.28 | ### |
| PHOE I | 12/28/2005 | 4.08 | 0.00 | 4.08 | 0.83 | 5.53 | 6.54 | ### |
| PHOE I | 1/4/2006 | 7.07 | 0.06 | 7.13 | 0.33 | 6.32 | 5.80 | ### |
| PHOE I | 1/11/2006 | 10.26 | 0.00 | 10.26 | 0.38 | 6.57 | 5.38 | ### |
| PHOE I | 1/18/2006 | 3.88 | 0.00 | 3.88 | 0.32 | 5.15 | 5.31 | ### |
| PHOE I | 1/25/2006 | 3.79 | 0.00 | 3.79 | 0.29 | 5.59 | 5.25 | ### |
| PHOE I | 2/1/2006 | 4.41 | 0.00 | 4.41 | 0.23 | 4.86 | 4.55 | 9.41 |
| PHOE I | 2/8/2006 | 6.14 | 0.00 | 6.14 | 0.30 | 5.13 | 5.59 | ### |
| PHOE I | 2/15/2006 | 6.04 | 0.00 | 6.04 | 0.24 | 4.27 | 4.23 | 8.50 |
| PHOE I | 2/22/2006 | 7.33 | 0.00 | 7.33 | 0.17 | 5.35 | 4.38 | 9.73 |
| PUSO | 6/2/2004 | 2.11 | 0.00 | 2.11 | 0.48 | 1.21 | 1.54 | 2.75 |
| PUSO | 6/9/2004 | 1.27 | 0.11 | 1.38 | 0.52 | 0.94 | 1.37 | 2.31 |

D-4

| Sampling Site | Sample Start | OC | EC | TC (OC+EC) | Biomass C | Fossil C | Cont. C | $^{14}$C TC |
|---|---|---|---|---|---|---|---|---|
| PUSO | 6/16/2004 | 3.19 | 1.36 | 4.55 | 0.53 | 2.51 | 3.55 | 6.06 |
| PUSO | 6/23/2004 | 1.60 | 0.00 | 1.60 | 0.27 | 1.43 | 1.89 | 3.32 |
| PUSO | 6/30/2004 | 1.71 | 0.44 | 2.15 | 0.28 | 1.30 | 1.55 | 2.85 |
| PUSO | 7/7/2004 | 1.80 | 0.45 | 2.25 | 0.43 | 1.55 | 1.98 | 3.53 |
| PUSO | 7/14/2004 | 1.96 | 0.00 | 1.96 | 0.30 | 1.71 | 2.10 | 3.81 |
| PUSO | 7/21/2004 | 2.52 | 0.05 | 2.56 | 0.23 | 2.65 | 3.17 | 5.82 |
| PUSO | 7/28/2004 | 3.13 | 0.00 | 3.13 | 0.26 | 2.89 | 3.01 | 5.90 |
| PUSO | 8/4/2004 | 1.97 | 0.86 | 2.83 | 0.24 | 2.33 | 1.76 | 4.09 |
| PUSO | 8/11/2004 | 1.84 | 0.00 | 1.84 | 0.20 | 3.75 | 2.76 | 6.51 |
| PUSO | 8/18/2004 | 1.42 | 0.00 | 1.42 | 0.08 | 2.20 | 1.21 | 3.41 |
| PUSO | 8/25/2004 | 1.29 | 0.09 | 1.38 | 0.07 | 1.79 | 0.96 | 2.75 |
| PUSO | 12/1/2004 | 1.30 | 0.00 | 1.30 | 0.37 | 1.84 | 2.20 | 4.04 |
| PUSO | 12/8/2004 | 1.06 | 0.00 | 1.06 | 0.22 | 1.38 | 1.34 | 2.72 |
| PUSO | 12/15/2004 | 1.31 | 0.00 | 1.31 | 0.46 | 3.47 | 2.86 | 6.33 |
| PUSO | 12/22/2004 | 2.84 | 0.71 | 3.55 | 0.57 | 1.86 | 3.01 | 4.87 |
| PUSO | 12/29/2004 | 1.81 | 0.02 | 1.83 | 0.57 | 2.08 | 3.74 | 5.82 |
| PUSO | 1/5/2005 | 2.07 | 0.01 | 2.08 | 0.50 | 2.31 | 3.39 | 5.70 |
| PUSO | 1/12/2005 | 1.17 | 0.00 | 1.17 | 0.32 | 1.28 | 1.70 | 2.98 |
| PUSO | 1/19/2005 | 3.47 | 0.17 | 3.64 | 0.29 | 3.47 | 2.55 | 6.02 |
| PUSO | 1/26/2005 | 3.64 | 0.30 | 3.94 | 0.38 | 3.59 | 2.70 | 6.29 |
| PUSO | 2/16/2005 | 3.84 | 0.00 | 3.84 | 1.25 | 2.34 | 3.69 | 6.03 |
| PUSO | 2/23/2005 | 3.37 | 0.00 | 3.37 | 0.38 | 4.35 | 4.00 | 8.35 |
| ROMO | 6/28/2005 | 3.50 | 0.00 | 3.50 | 1.04 | 0.22 | 1.71 | 1.93 |
| ROMO | 7/5/2005 | 4.21 | 0.00 | 4.21 | 2.01 | 0.21 | 2.47 | 2.68 |
| ROMO | 7/12/2005 | 4.38 | 0.00 | 4.38 | 1.97 | 0.47 | 3.06 | 3.53 |
| ROMO | 7/19/2005 | 4.56 | 0.00 | 4.56 | 1.29 | 0.29 | 2.60 | 2.89 |
| ROMO | 7/27/2005 | 3.14 | 0.00 | 3.14 | 2.15 | 0.31 | 1.74 | 2.05 |
| ROMO | 8/3/2005 | 2.78 | 0.14 | 2.93 | 4.88 | 0.20 | 1.68 | 1.88 |
| ROMO | 8/9/2005 | 2.86 | 0.00 | 2.86 | 3.39 | 0.21 | 1.58 | 1.79 |
| ROMO | 8/16/2005 | 2.33 | 0.00 | 2.33 | 1.70 | 0.18 | 1.02 | 1.20 |
| SAGO | 6/28/2005 | 2.42 | 0.12 | 2.54 | 0.18 | -0.40 | 3.47 | 3.07 |
| SAGO | 7/5/2005 | 2.09 | 0.00 | 2.09 | 0.83 | -1.89 | 6.24 | 4.35 |
| SAGO | 7/12/2005 | 1.98 | 0.00 | 1.98 | 0.15 | -0.06 | 3.41 | 3.35 |
| SAGO | 7/19/2005 | 2.31 | 0.02 | 2.33 | 0.27 | -0.05 | 3.10 | 3.05 |
| SAGO | 7/26/2005 | 2.07 | 0.00 | 2.07 | 0.22 | 0.54 | 2.79 | 3.33 |
| SAGO | 8/3/2005 | 1.98 | 0.00 | 1.98 | 0.27 | 0.24 | 2.48 | 2.72 |
| SAGO | 8/9/2005 | 1.04 | 0.10 | 1.14 | 0.05 | -10.22 | 13.51 | 3.29 |
| TONT | 6/29/2005 | 0.91 | 0.46 | 1.37 | 0.50 | 0.63 | 2.14 | 2.77 |
| TONT | 7/6/2005 | 2.42 | 0.13 | 2.55 | 0.14 | 0.55 | 1.80 | 2.35 |
| TONT | 7/13/2005 | 3.80 | 0.24 | 4.04 | 0.54 | 0.38 | 3.03 | 3.41 |
| TONT | 7/20/2005 | 4.91 | 0.76 | 5.67 | 1.40 | 0.16 | 4.04 | 4.20 |
| TONT | 7/27/2005 | 1.65 | 0.03 | 1.68 | 0.64 | 0.11 | 1.52 | 1.63 |
| TONT | 8/3/2005 | 1.54 | 0.00 | 1.54 | 0.46 | 0.23 | 1.09 | 1.32 |
| TONT | 8/10/2005 | 1.41 | 0.00 | 1.41 | 0.33 | 0.19 | 1.02 | 1.21 |
| TONT | 8/17/2005 | 1.68 | 0.00 | 1.68 | 0.60 | 0.19 | 1.26 | 1.45 |
| TONT | 11/30/2005 | 1.19 | 0.11 | 1.31 | 0.02 | 0.29 | 0.79 | 1.08 |

| Sampling Site | Sample Start | OC | EC | TC (OC+EC) | Biomass C | Fossil C | Cont. C | $^{14}$C TC |
|---|---|---|---|---|---|---|---|---|
| TONT | 12/7/2005 | 1.34 | 0.00 | 1.34 | 0.05 | 0.35 | 1.13 | 1.48 |
| TONT | 12/14/2005 | 1.46 | 0.11 | 1.57 | 0.13 | 0.14 | 1.15 | 1.29 |
| TONT | 12/21/2005 | 1.06 | 0.00 | 1.06 | 0.02 | 0.20 | 0.63 | 0.83 |
| TONT | 12/28/2005 | 1.01 | 0.00 | 1.01 | 0.02 | 0.30 | 0.51 | 0.81 |
| TONT | 1/4/2006 | 0.99 | 0.00 | 0.99 | 0.01 | 0.25 | 0.65 | 0.90 |
| TONT | 1/11/2006 | 1.49 | 0.00 | 1.49 | 0.03 | 0.46 | 0.99 | 1.45 |
| TONT | 1/18/2006 | 1.17 | 0.00 | 1.17 | 0.03 | 0.31 | 0.78 | 1.09 |
| TONT | 1/25/2006 | 1.53 | 0.00 | 1.53 | 0.01 | 0.41 | 0.99 | 1.40 |
| TONT | 2/1/2006 | 1.21 | 0.00 | 1.21 | 0.01 | 0.46 | 0.80 | 1.26 |
| TONT | 2/8/2006 | 1.19 | 0.01 | 1.20 | 0.02 | 0.32 | 0.75 | 1.07 |
| TONT | 2/15/2006 | 1.50 | 0.00 | 1.50 | 0.01 | 0.42 | 0.86 | 1.28 |
| TONT | 2/22/2006 | 1.27 | 0.00 | 1.27 | 0.01 | 0.56 | 0.81 | 1.37 |